Renewable diesel fuels and emission control strategies

Implications for occupational exposure, human health, and the environment

Gren, Louise

2022

Document Version:
Publisher's PDF, also known as Version of record

Renewable diesel fuels and emission control strategies

Implications for occupational exposure, human health, and the environment

LOUISE GREN
ERGONOMICS AND AEROSOL TECHNOLOGY | LTH | LUND UNIVERSITY

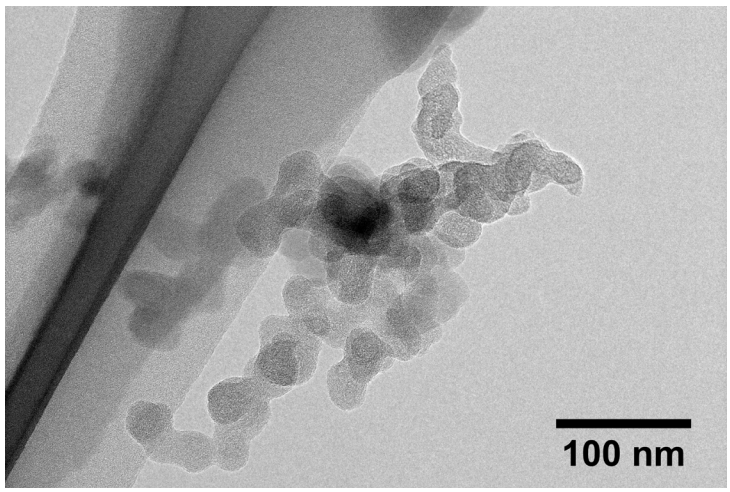

Transmission electron microscopy image of an HVO exhaust particle from the exposure study in Paper 4.

Printed by Media-Tryck, Lund 2021 NORDIC SWAN ECOLABEL 3041 0903

Faculty of Engineering
Department of Design Sciences
Ergonomics and Aerosol Technology

ISBN 978-91-8039-127-6
ISSN 1650-9773
Publication 71

Renewable diesel fuels and emission control strategies

Renewable diesel fuels and emission control strategies

Implications for occupational exposure, human health, and the environment

Louise Gren

LUND UNIVERSITY

DOCTORAL DISSERTATION

by due permission of the Faculty of Engineering, Lund University, Sweden.
To be defended at Stora Hörsalen, IKDC, Lund.
Date: 11th of February 2021. Time: 9.15 a.m.

Faculty opponent
Prof. Leonidas Ntziachristos
Department of Mechanical Engineering
Aristotle University Thessaloniki, Greece

Organization	Document name
LUND UNIVERSITY	**Doctoral dissertation**
Department of Design Sciences Ergonomics and Aerosol Technology	**Date of issue** **11 February 2022**
Author: Louise Gren	Sponsoring organization

Renewable diesel fuels and emission control strategies: Implications for occupational exposure, human health, and the environment

Combustion of fossil diesel is a major environmental problem for both the climate and human health. Renewable diesel fuels have been developed and introduced to the market to reduce the net CO_2 emissions. Emission control strategies, such as aftertreatment systems, have been implemented to reduce the health hazardous particulate matter (PM) and nitrogen oxides (NO_x) emissions. The overall aim of this thesis was to understand the effect of introducing renewable diesel fuels and emission abatement techniques on health relevant exhaust emissions.

Laboratory studies were performed to assess the primary and secondary emissions from a heavy-duty diesel engine fueled by the renewable diesel fuels HVO (hydrotreated vegetable oil) and RME (rapeseed methyl ester). The emissions were characterized by detailed particle and gas measurements. We also evaluated the effect of using an aftertreatment system consisting of a diesel oxidation catalyst (DOC) and a diesel particle filter (DPF) on the exhaust emissions. The occupational exposure to diesel exhaust from vehicles in a Swedish modern underground mine was quantified and evaluated in relation to the vehicles' level of emission reduction technology. The underground ambient concentrations were quantified, and real-world emission factors were calculated. The short-term health effects of HVO exhaust from modern non-road vehicles (2019), with or without the PM fraction, were investigated in a controlled human exposure chamber study.

Replacing fossil diesel with HVO and RME significantly reduced the PM emissions, especially the soot emissions (measured as elemental carbon [EC] and equivalent black carbon [eBC]). The fuel change also reduced the hydrocarbon and carbon monoxide emissions, particularly from RME. The significantly reduced hydrocarbon emissions from RME also reduced the secondary aerosol formation, and thus potentially reducing the total atmospheric particle mass burden. Aftertreatment systems containing both a DOC and DPF were very efficient in removing the particle concentrations in the laboratory studies for all fuels. However, as long as a large portion of the vehicle fleet does not have any PM removal systems, the usage of HVO and RME will have a positive impact on overall PM reductions.

The average occupational exposure concentration of EC was 7 µg m^{-3} in the underground mine. This is much lower than the future EU occupational exposure limit (OEL) for diesel exhaust (50 µg EC m^{-3}, from 2026 underground). However, epidemiological studies suggest health-based limits closer to 1 µg m^{-3}, which indicates that we should aim to further reduce the exposure. The measured EC exposures ware reduced in areas where vehicles had DPFs.

Short-term exposure to HVO exhaust below the EU OELs did not cause severe pulmonary function changes in healthy subjects. However, the subjects experienced an increase in self-rated mild irritation symptoms, and a mild decrease in nasal patency after both the particle-laden and the particle-free HVO exposure. This may indicate irritative effects from exposure to HVO exhaust from modern non-road vehicles below future OELs.

Air pollution from combustion sources (not only from vehicles) is a global problem that will be present for years to come. Due to the many adverse effects linked to aerosol air pollution, measures need to be taken to reduce the particle exposures in environmental and occupational settings. The future occupational exposure limit of 50 µg EC m^{-3} is still much higher than proposed health-based limits. For combustion vehicles, the most efficient way to reduce EC emissions is by using aftertreatment systems focused on removing the PM, such as DPFs. Resources need to be focused on ensuring that such systems are in place and working effectively in all combustion vehicles. This is especially the case in highly exposed areas such as in cities and enclosed work environments.

Key words HVO, RME, DOC, DPF, emission factors, heavy-duty engine, non-road engine, chamber exposure, aerosol, occupational exposure limits, emission standards

Classification system and/or index terms (if any)

Supplementary bibliographical information		**Language** English
ISSN and key title 1650-9773 Publication 71		ISBN 978-91-8039-127-6 (print) ISBN 978-91-8039-128-3 (pdf)
Recipient's notes	**Number of pages** 99	Price
	Security classification	

Signature 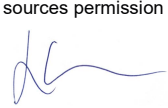 Date 2022-01-18

Renewable diesel fuels and emission control strategies

Implications for occupational exposure, human health, and the environment

Louise Gren

LUND
UNIVERSITY

Cover photos by Louise Gren
Back cover by Louise Gren

Ergonomics and Aerosol Technology
Department of Design Sciences
Faculty of Engineering
Lund University

ISBN 978-91-8039-127-6 (print)
ISBN 978-91-8039-128-3 (pdf)

Printed in Sweden by Media-Tryck, Lund University
Lund 2021

Table of Contents

Abstract

Combustion of fossil diesel is a major environmental problem for both the climate and human health. Renewable diesel fuels have been developed and introduced to the market to reduce the net CO_2 emissions. Emission control strategies, such as aftertreatment systems, have been implemented to reduce the health hazardous particulate matter (PM) and nitrogen oxides (NO_x) emissions. The overall aim of this thesis was to understand the effect of introducing renewable diesel fuels and emission abatement techniques on health relevant exhaust emissions.

Laboratory studies were performed to assess the primary and secondary emissions from a heavy-duty diesel engine fueled by the renewable diesel fuels HVO (hydrotreated vegetable oil) and RME (rapeseed methyl ester). The emissions were characterized by detailed particle and gas measurements. We also evaluated the effect of using an aftertreatment system consisting of a diesel oxidation catalyst (DOC) and a diesel particle filter (DPF) on the exhaust emissions. The occupational exposure to diesel exhaust from vehicles in a Swedish modern underground mine was quantified and evaluated in relation to the vehicles' level of emission reduction technology. The underground ambient concentrations were quantified, and real-world emission factors were calculated. The short-term health effects of HVO exhaust from modern non-road vehicles (2019), with or without the PM fraction, were investigated in a controlled human exposure chamber study.

Replacing fossil diesel with HVO and RME significantly reduced the PM emissions, especially the soot emissions (measured as elemental carbon [EC] and equivalent black carbon [eBC]). The fuel change also reduced the hydrocarbon and carbon monoxide emissions, particularly from RME. The significantly reduced hydrocarbon emissions from RME also reduced the secondary aerosol formation, and thus potentially reducing the total atmospheric particle mass burden. Aftertreatment systems containing both a DOC and DPF were very efficient in removing the particle concentrations in the laboratory studies for all fuels. However, as long as a large portion of the vehicle fleet does not have any PM removal systems, the usage of HVO and RME will have a positive impact on overall PM reductions.

The average occupational exposure concentration of EC was 7 $\mu g\ m^{-3}$ in the underground mine. This is much lower than the future EU occupational exposure limit (OEL) for diesel exhaust (50 μg EC m^{-3}, from 2026 underground). However, epidemiological studies suggest health-based limits closer to 1 $\mu g\ m^{-3}$, which indicates that we should aim to further reduce the exposure. The measured EC exposures ware reduced in areas where vehicles had DPFs.

Short-term exposure to HVO exhaust below the EU OELs did not cause severe pulmonary function changes in healthy subjects. However, the subjects experienced an increase in self-rated mild irritation symptoms, and a mild decrease in nasal

patency after both the particle-laden and the particle-free HVO exposure. This may indicate irritative effects from exposure to HVO exhaust from modern non-road vehicles below future OELs.

Air pollution from combustion sources (not only from vehicles) is a global problem that will be present for years to come. Due to the many adverse effects linked to aerosol air pollution, measures need to be taken to reduce the particle exposures in environmental and occupational settings. The future occupational exposure limit of 50 µg EC m^{-3} is still much higher than proposed health-based limits. For combustion vehicles, the most efficient way to reduce EC emissions is by using aftertreatment systems focused on removing the PM, such as DPFs. Resources need to be focused on ensuring that such systems are in place and working effectively in all combustion vehicles. This is especially the case in highly exposed areas such as in cities and enclosed work environments.

Populärvetenskaplig sammanfattning

Luftföroreningar utomhus är ett globalt hälsoproblem som varje år orsakar 4-9 miljoner fall av för tidig död enligt WHO. I Sverige var motsvarande siffra 7600 fall år 2015, och uppskattades kosta samhället 56 miljarder kronor per år. Avgaser från dieselfordon bidrar till stor del till dessa luftföroreningar. Avgaserna innehåller föroreningar i gasfas, som koldioxid, kolmonoxid och organiska gaser, men även väldigt små partiklar. Partiklarna har en diameter som är hundra gånger mindre än ett hårstrås diameter, och består till stor del av svart sot. Avgaser från dieselfordon orsakar cancer vid långvarig exponering och en ökad risk för luftvägssjukdomar och hjärt- och kärlsjukdomar. De svarta små sotpartiklarna som släpps ut vid förbränningen av diesel anses ha en nyckelroll i dessa hälsoeffekter. Avgaserna har också en påverkan på vår miljö och atmosfär. Koldioxiden som släpps ut när vi kör fordon på fossila bränslen såsom diesel bidrar till växthuseffekten. Sotpartiklarna bidrar med en kortlivad värmande effekt i vår atmosfär.

Både hälsa och miljö tjänar på minskade utsläpp från fossil diesel och ett byte till förnybara alternativ. På senare år har utvecklingen gjort att förnybara dieselbränslen går att använda i dieselfordon. I Sverige används framförallt HVO (’hydrotreated vegetable oil’) och FAME (’fatty acid methyl ester’). HVO är gjort på restprodukter från mat- och avfallsindustrin, medan FAME tillverkas av vegetabiliska oljor som utvinns från jordbruksgrödor (t.ex. raps). På grund av reduktionsplikten som kräver att klimatpåverkan från bränslen måste minskas, så används HVO och FAME som inblandning i fossil diesel på många tankstationer (upp till 50 % HVO, och 7 % FAME). I takt med att reduktionsplikten ökar kommer även mängden inblandning av förnybara drivmedel öka. Dessutom kör många diesellastbilar i Sverige på ren HVO.

Mängden avgaser som får släppas ut från fordon är reglerade och blir mer och mer strikta. I praktiken betyder det att alla nya dieselfordon måste ha någon typ av efterbehandlingssystem som tar bort hälsoskadliga ämnen i avgassystemet. Efterbehandlingssystemen består ofta av olika enheter som tar bort specifika föroreningar. Ofta har de enheter som filtrerar kolmonoxid, organiska ämnen, sotpartiklar, och kväveoxider. Äldre fordon har inte lika bra efterbehandlingsystem, eller inga alls. Det betyder att de kan släppa ut höga koncentrationer av dieselavgaser som vi nu vet är hälsoskadliga.

I arbetet som lett fram till denna avhandling har vi studerat avgaser från motorer i laboratorium och från dieselfordon på arbetsplatser. Studierna har syftat till att; 1) undersöka hur HVO samt FAME gjort på raps (RME) påverkar avgasutsläppen jämfört med fossil diesel, 2) hur olika efterbehandlingssystem påverkar avgaserna, 3) hur exponeringen på arbetsplatser som använder moderna dieselfordon ser ut, samt 4) hur avgaserna från förnybara dieselbränslen kan påverka människors hälsa.

I två studier har vi undersökt hur avgaserna från ett fordon utan efterbehandlingsystem förändras när man byter ut fossil diesel mot ren HVO eller RME. Att använda HVO eller RME resulterade i en generell minskning av hälsoskadliga partiklar och gaser. Framför allt minskades sotpartikelutsläppen med ungefär hälften för HVO och RME. Andra forskare som undersökt detta har fått liknande resultat. Det innebär att för fordon som saknar efterbehandlingssystem, är det positivt både för hälsa och miljö att tanka HVO eller RME istället för fossil diesel.

De flesta nya dieselfordonen i Europa och USA har någon form av efterbehandlingsystem. Hur påverkas då utsläppen från ett sådant fordon om vi använder fossil eller förnybar diesel? Enheterna som tar bort partiklar kallas dieselpartikelfilter (DPF) och är ofta väldigt effektiva på att filtrera bort sotpartiklar i labbmätningar. Vi såg en klar sotpartikelminskning med drygt 99 % när vi körde en modern lastbilsmotor i laboratorium, både om vi använde traditionell diesel, HVO eller RME. Däremot är det inte alltid säkert att efterbehandlingssystemen fungerar lika effektivt efter en tids användning, eller när de körs i verkligheten. Därför är det viktigt att mäta hur mycket avgaser fordon släpper ut när de används i verkligheten och hur det påverkar de personer som är i närheten, t.ex. på olika arbetsplatser.

En arbetsplats där det används tunga dieselfordon är i underjordiska gruvor. Arbetsmiljön i gruvor innehåller ofta trånga utrymmen med begränsad ventilation. Förr, när dieselfordon släppte ut mer hälsoskadliga avgaser blev många exponerade för höga halter av avgaser. Detta ledde till ökad risk för lungcancer. För att skydda arbetarna finns det föreskrifter om till exempel hygieniska gränsvärden, som reglerar hur hög koncentration som de får exponeras för när de är på sin arbetsplats. På senare år har dessa gränsvärden sänkts, i takt med att fordonen fått hårdare krav på sig att släppa ut mindre hälsoskadliga avgaser. Vi undersökte hur exponeringen för dieselavgaser såg ut i en svensk järnmalmsgruva under jord. Arbetarna fick bära små detektorer som mätte olika avgaskoncentrationer (gaser, partiklar och cancerogena ämnen) medan de jobbade. Våra resultat visade att de anställdas exponering för sotpartiklar och kväveoxider minskat generellt sedan en äldre studie från början av 2000-talet. Koncentrationerna låg för det mesta under det hygieniska gränsvärdet för kvävedioxid och även under det kommande hygieniska gränsvärdet för sotpartiklar. Däremot såg vi att enstaka arbetare var exponerade för högre koncentrationer än vad gränsvärdena tillåter. De som arbetade i de något äldre fordonen (från 2012-2015) hade högre exponering än de som arbetade med de som var nyare (från 2019). Nya fordon har bättre, eller åtminstone någon typ av efterbehandlingssystem.

Från våra och andra forskares studier, så vet vi nu att mängden sotpartiklar minskar när vi använder HVO istället för diesel. Vi vet också att emissionerna minskar om vi använder fordon med ett efterbehandlingsystem som filtrerar bort sotpartiklarna

(DPF). För att studera om HVO avgaser ger negativa hälsoeffekter, och om hälsoeffekterna beror på sotpartiklarna eller ämnena i gasfas, studerade vi detta med en kontrollerad exponeringsstudie. Vi undersökte hälsopåverkan genom att under tre timmar exponera en grupp friska volontärer för utspädda HVO avgaskoncentrationer som motsvarade en arbetsdags exponering. Alla exponerades även för en session med ren luft som användes som jämförelse. Vi använde ett fordon utan efterbehandlingssystem och ett fordon med ett efterbehandlingsystem som tog bort sotpartiklarna, för att jämföra om det gav olika hälsopåverkan. Vi kunde se att exponering för både sotpartiklar och gaser gjorde att fler av personerna kände någon typ av irritationssymtom, t.ex. irritation i ögon och svalg. Antal personer som gjorde det efter den partikelfria exponeringen var lägre, men fortfarande fler jämfört med exponering av ren luft. Utöver det såg vi att båda HVO-exponeringarna skapade en lätt svullnad i näsan/nästäppa. Detta är inget som påverkar lungfunktionen på kort sikt, men långvarig exponering av irriterande ämnen, kan leda till obstruktiva lungsjukdomar såsom astma. Effekterna vi såg från HVO-exponeringen var generellt milda. Men med tanke på att de milda effekterna var liknande de som tidigare setts från fossil dieselexponering, kan vi inte utesluta att HVO skulle kunna ge liknande långtidseffekter som fossil dieselexponering.

Våra studier visar att det finns en klar hälso- och miljövinst i att byta ut fossil diesel mot förnybara dieselbränslen. Däremot bör HVO-avgaser betraktas som lika hälsovådligt som dieselavgaser. Att använda fordon med efterbehandlingssystem, framför allt dieselpartikelfilter, krävs för att minska utsläppen av sotpartiklar ännu mer. Utsläppskrav och hygieniska gränsvärden bör fortsätta sänkas för att se till att avgaskoncentrationerna blir lägre i vår arbetsplats- och omgivningsluft.

Bilden är tagen i en underjordsgruva där arbetsplatsmätningar utfördes. Underjordslastaren på bilden används för att transportera järnmalm. Vi utförde aerosolmätningar i omgivningsluften och i förarnas andningsszon.

Papers included in this thesis

Paper 1

Gren, L., Malmborg, V.B., Jacobsen, N.R., Shukla, P.C., Bendtsen, K.M., Eriksson, A. C., Essig, Y.J., Krais, A.M., Loeschner, K., Shamun, S., Strandberg, B., Tunér, M., Vogel, U., Pagels, J. (2020). **Effect of renewable fuels and intake O_2 concentration on diesel engine emission characteristics and reactive oxygen species (ROS) formation**. *Atmosphere*, 11(6). https://doi.org/10.3390/atmos11060641

Paper 2

Gren, L., Malmborg, V.B., Falk, J., Markula, L., Novakovic, M., Shamun, S., Eriksson, A.C., Kristensen, T. B., Svenningsson, B., Tunér, M., Karjalainen, P., Pagels, J. (2021). **Effects of renewable fuel and exhaust aftertreatment on primary and secondary emissions from a modern heavy-duty diesel engine.** *Journal of Aerosol Science*, 156, 105781. https://doi.org/10.1016/j.jaerosci.2021.105781

Paper 3

Gren L., Krais A.M., Assarsson E., Broberg K., Engfeldt M., Lindh C., Strandberg, B., Pagels J., Hedmer, M. **Underground emissions and miners' personal exposure to diesel and renewable diesel exhaust.** *Submitted to a scientific journal and under review.*

Paper 4

Gren L., Dierschke, K., Mattsson, F., Assarsson, E., Krais A.M., Kåredal, M., Lovén, K., Löndahl, J., Pagels, Strandberg, B., Tunér, M., Xu Y., Wollmer, P., Albin, M., Nielsen, J., Gudmundsson, A., Wierzbicka, A. **Lung function and self-rated symptoms in healthy volunteers after exposure to hydrotreated vegetable oil (HVO) exhaust with and without particles**. *Accepted for publication in Particle and Fibre Toxicology.*

Author's contributions to the papers included in this thesis

Paper 1: I actively participated in planning and designing the experiment and setup. I conducted the aerosol experiments together with co-authors (except the AMS). I performed the particle collection and extraction, TEM, and initial ROS analysis. I analyzed and interpreted the data in collaboration with the co-authors. I wrote the main part of the original draft of the paper and review replies during the peer review process with assistance from the co-authors.

Paper 2: I participated in planning and conducting the experiments of the primary emissions. I analyzed the data from the SMPS, aethalometer and gas-phase emissions, performed the mass size distribution and emission factor calculations, compiled and interpreted the data, and wrote most of the original draft of the paper and the review replies.

Paper 3: I actively participated in planning the field measurements at the mine and was responsible for planning and conducting the stationary aerosol measurements. I analyzed and interpreted the data from the aerosol measurements. I wrote the original draft of the paper.

Paper 4: I actively participated in planning the experiments and was responsible for the aerosol generation and measurements during the exposures. I had a major role in designing the aerosol generation (i.e., type of vehicles and fuels) by planning and conducting pilot studies. I analyzed and interpreted the aerosol data, applied lung deposition models, and interpreted the respiratory measurements together with medical doctors. I planned and initiated splitting the data into different publications within this interdisciplinary study. I had a major role in coordinating the paper and wrote the original draft of the paper and the review replies.

Peer-reviewed publications not included in this thesis

Namazi, L., **Gren, L.,** Nilsson, M., Garbrecht, M., Thelander, C., Zamani, R.R., & Dick, K.A. (2018). **Realization of Wurtzite GaSb using InAs Nanowire Templates**. *Advanced Functional Materials*, 28(28). https://doi.org/10.1002/adfm.201800512

Shukla, P.C., Shamun, S., **Gren, L**., Malmborg, V., Pagels, J., & Tuner, M. (2018). **Investigation of particle number emission characteristics in a heavy-duty compression ignition engine fueled with hydrotreated vegetable oil (HVO)**. *SAE Technical Papers*, 2018-April. https://doi.org/10.4271/2018-01-0909

Malmborg, V.B., Eriksson, A. C., Török, S., Zhang, Y., Kling, K., Martinsson, J., Fortner, E.C., **Gren, L.,** Kook, S., Onasch, T.B., Bengtsson, P.-E., & Pagels, J. (2019). **Relating aerosol mass spectra to composition and nanostructure of soot particles**. *Carbon*, 142. https://doi.org/10.1016/j.carbon.2018.10.072

Perović, D., Van Hees, P., Madsen, D., Malmborg, V., **Gren, L.,** Pagels, J., Rios, O., & La Mendola, S. (2020). **Identification and characterization of design fires and particle emissions to be used in performance-based fire design of nuclear facilities**. *Fire and Materials*, October 2019, 1–17. https://doi.org/10.1002/fam.2881

Bendtsen, K., **Gren, L.,** Malmborg, V., Shukla, P., Tunér, M., Essig, Y., Krais, A., Clausen, P., Berthing, T., Loeschner, K., Jacobsen, N., Wolff, H., Pagels, J., & Vogel, U. (2020**). Particle characterization and toxicity in C57BL/6 mice following instillation of five different diesel exhaust particles designed to differ in physicochemical properties**. *Particle and Fibre Toxicology*, 17. https://doi.org/10.21203/rs.3.rs-18458/v1

Malmborg, V., Eriksson, A., **Gren, L**., Török, S., Shamun, S., Novakovic, M., Zhang, Y., Kook, S., Tunér, M., Bengtsson, P.-E., & Pagels, J. (2021). **Characteristics of BrC and BC emissions from controlled diffusion flame and diesel engine combustion**. *Aerosol Science and Technology*, 0(0), 1–19. https://doi.org/10.1080/02786826.2021.1896674

Krais, A.M., Essig, J. Y., **Gren, L**., Vogs, C., Assarsson, E., Dierschke, K., Nielsen, J., Strandberg, B., Pagels, J., Broberg, K., Lindh, C. H., Gudmundsson, A., & Wierzbicka, A. (2021). **Biomarkers after controlled inhalation exposure to exhaust from hydrogenated vegetable oil (HVO)**. *International Journal of Environmental Research and Public Health*, 18(12), 6492. https://doi.org/10.3390/ijerph18126492

Scholten, R. H., Essig, Y. J., Roursgaard, M., Jensen, A., Krais, A. M., **Gren, L**., ... & Møller, P. (2021). **Inhalation of hydrogenated vegetable oil combustion exhaust and genotoxicity responses in humans**. *Archives of Toxicology*, 1-10.

Falk, J., Korhonen, K., Malmborg, V.B., **Gren, L.,** Eriksson, A.C., Karjalainen, P., ... & Kristensen, T.B. (2021). **Immersion freezing ability of freshly emitted soot with various physico-chemical characteristics**. *Atmosphere*, 12(9), 1173.

List of abbreviations and acronyms

APM	aerosol particle mass analyzer
CO	carbon monoxide
CO_2	carbon dioxide
DOC	diesel oxidation catalyst
DPF	diesel particulate filter
eBC	equivalent black carbon
EC	elemental carbon
EGR	exhaust gas recirculation
EU	European union
FAME	fatty acid methyl ester
GM	geometric mean
HC	hydrocarbons
HVCI	high-volume cascade impactor
HVO	hydrotreated vegetable oil
IARC	international agency for research on cancer
LTC	low temperature combustion
MPPD	multiple-path particle dosimetry
MSS	micro soot sensor
NFA	Danish national research centre for the working environment
NIOSH	U.S. national institute for occupational safety and health
NO	nitric oxide
NO_2	nitrogen dioxide
NO_x	nitrogen oxides
OA	organic aerosol
OC	organic carbon
OEL	occupational exposure limit
OFR	oxidation flow reactor

PAH	polycyclic aromatic hydrocarbon
PAM	potential aerosol mass chamber
PBZ	personal breathing zone
PFAD	palm fatty acid distillate
PM	particulate matter
PN	particle number
PNIF	peak nasal inspiratory flow
POA	primary organic aerosol
RME	rapeseed methyl ester
ROS	reactive oxygen species
SCR	selective catalytic reduction
SMPS	scanning mobility particle sizer
SOA	secondary organic aerosol
SSA	specific surface area
SVOC	semi-volatile organic compound
TEM	transmission electron microscopy
VAS	visual analogue scale
VOC	volatile organic compound

Introduction

Combustion of fossil fuels is a major environmental problem for both the climate and human health. The major combustion product is CO_2, which is a long-lived greenhouse gas [1]. The combustion-related particle emissions have short-lived climate effects, both warming and cooling depending on the composition [1]. Nitrate and sulphate are secondary particle emissions, formed in the atmosphere from emitted gases. They reflect sun radiation and have a cooling effect, while the primary emissions of absorbing black carbon (BC) has a warming effect [2]. These particles are included in the particulate matter smaller than 2.5 μm ($PM_{2.5}$), which is a major contributor to the total outdoor air pollution. This pollution has been estimated to cause between 4 and 9 million premature deaths annually [3]. In Sweden, the outdoor air pollution exposures of $PM_{2.5}$ and nitrogen oxides (NO_x) have been estimated to cause 7,600 premature deaths per year [4]. The World Health Organization (WHO) updated their global air quality guidelines in 2021, where the recommended annual mean of $PM_{2.5}$ was reduced from 10 to 5 μg m^{-3}, and nitrogen dioxide (NO_2) was reduced from 30 to 10 μg m^{-3} [3].

Renewable diesel fuels have been developed and implemented to reduce the climate impact from diesel vehicles, mainly by reducing the net CO_2 emissions. In addition, they generally reduce the PM emissions compared to diesel [5,6]. The reduced mass emissions may also have co-benefits for reducing the negative health effects from diesel vehicles. However, other particle properties such as the physical surface area and chemical composition are reported to be of equal or greater importance for health effects [7]. How these characteristics change depending on the fuel, and its impact on the particles' biologically relevant characteristics, are important for evaluating the risks or co-benefits of the renewable fuels.

In addition to CO_2 and the particulate fraction, diesel engine exhaust emissions generally also NO_x and a complex mixture of gaseous hydrocarbons (HC) [8]. The particulate emissions from diesel engines are often characterized by small particles around 100 nm. Such small particles are able to penetrate and deposit deep in the lungs upon inhalation, and the following health effects depend on the particle characteristics. The particles' chemical composition and physical characteristics depend strongly on the combustion conditions and the type of fuel [9]. How particle characteristics with health relevance, for example reactive oxygen species (ROS) formation, relate to the combustion conditions and type of fuel are less known. ROS formation is a measure of oxidative stress, which can initiate inflammation

processes in the body that have been linked to multiple diseases [10,11]. Particle-induced ROS have also been connected to oxidative DNA damage and genotoxicity [12].

Since 2012, diesel engine exhaust has been classified as carcinogenic to humans (group 1 [13]), and is also related to lung and cardiovascular diseases. The diesel exhaust emissions as well as the occupational exposure levels allowed have since then become more stringent. The newer diesel vehicles in the EU and the U.S. are now required to reduce exhaust emissions to a great extent, which in practice requires most vehicles to have sophisticated emission control strategies. For example, the vehicles can be equipped with emission reduction units such as a diesel oxidation catalyst (DOC) that removes the organic components and CO, a diesel particulate filter (DPF) that reduces the PM and particle number concentration, and a NO_x removal system such as selective catalytic reduction units (SCR). The aftertreatment systems have varying degrees of removal efficiencies, and the units can be used alone and in combination to reduce emissions according to the legislation. However, in many parts of the world, the regulations are much less stringent than in the EU or the U.S., or even absent. In addition, older vehicles without any emission abatement techniques will be in use for several years to come. This means that diesel exhaust emissions will continue to affect ambient and workplace air. Knowing how the use of renewable diesel fuels change these emissions is of great importance in order to understand the potential effects they can have on climate and health.

Occupational exposure to diesel exhaust is a known occupational health risk, and has historically been high especially in underground working environments (up to 660 µg EC m^{-3} [14]). The EU's occupational exposure limits have become more stringent recently, with the implementation of a new limit value of diesel exhaust PM (measured as elemental carbon, EC) of 50 µg m^{-3} from 2023 (effective underground from 2026). However, such exposure levels throughout a life time still pose a considerable risk, and it is suggested that health-based limits should be closer to 1 µg m^{-3} [15,16]. It is thus of great importance to monitor occupational exposure and to evaluate measures for reducing exposure to diesel exhaust.

Aims

The overall aim of the research presented in this thesis was to:

Determine the effect of introducing renewable diesel fuels and emission abatement techniques on health-relevant exhaust emissions and occupational exposures.

The specific aims were to:

- Assess the effect of renewable diesel fuels and emission abatement techniques on emissions and exhaust particle characteristics in laboratory studies (Papers 1 and 2).
- Quantify real-world underground emissions and occupational exposure to diesel exhaust, with multiple exposure markers, in relation to the level of emission abatement technology used in a modern underground mine (Paper 3).
- Assess the toxicity of exhaust particles and exhaust emissions from renewable fuels and their potential health effects (Papers 1 and 4).

Background

Renewable diesel fuels

Renewable diesel fuels have been developed and implemented to decrease the negative environmental impact from diesel vehicles. During combustion of fossil diesel, a large amount of fossil CO_2 is emitted, which is a long-lived greenhouse gas that contributes to the warming of the atmosphere [1]. Particulate matter (PM) is also formed from incomplete combustion, which is harmful to both the environment and human health [3]. The total amount of delivered renewable diesel fuels in Sweden, blends and in pure form (B100), have increased from 2.5% in 2011, to 20.1% in 2020. The increase is due to the Swedish greenhouse gas reduction mandate which requires fuel suppliers to add in renewable fuels to diesel (and gasoline) to reduce their greenhouse gas emissions. The required reduction in emissions is increasing yearly since 2017, and thus increasing the amount of renewable fuels blended into the fossil fuels [17]. The increase in renewable fraction in the Swedish MK1 diesel is shown in Fig. 1a, and the evolution of the delivered amount of pure renewable diesel fuels in Fig. 1b.

The most common types of renewable diesel fuels used in Sweden, are hydrotreated vegetable oil (HVO) and fatty acid methyl esters (FAME). The Swedish Energy Agency estimates that FAME and HVO fuels used in full substitution reduce fossil CO_2 emissions by 59% and 86%, respectively, compared to fossil diesel [18]. Previous studies have also shown that both FAME [19,20] and HVO [6,21] can reduce soot and PM mass emissions compared to fossil diesel, and thus potentially reduce the radiative forcing due to light absorption from BC.

FAME fuels are produced by transesterification of vegetable oils or animal fats, and the commonly used feedstock consists of feed crops such as rapeseed, corn and soy. Of the FAME fuels used in Sweden, 85-90% originate from rapeseeds and are commonly called rapeseed methyl ester (RME) [22,23]. The FAME fuels have an oxygen content of about 10%, which affects the combustion and performance of the engine. HVO is mainly derived from waste products (oil or fats) by hydrodeoxygenation [24]. In Sweden the most common sources of HVO have been palm fatty acid distillate (PFAD) and slaughterhouse waste [22,23]. The sustainability of such feedstock is questionable, as well as the sustainability issues regarding the use of edible crops and/or using farmlands for production of biofuels.

However, transitioning to using renewable diesel fuels instead of fossil fuels in existing diesel vehicles generally has a positive impact on the environment. Issues related to the sustainability of the renewable fuels are further discussed in the *Sustainability* section of the *Results and Discussion* chapter.

HVO consists of paraffinic hydrocarbons (alkanes) and is chemically similar to fossil diesel but with a negligible aromatic content and generally a higher cetane number [21,24,25]. The chemical composition of HVO has a low dependence on feedstock and can generally replace fossil diesel in diesel engines without engine modifications. While renewable diesel fuels are a proposed solution to decrease regulated emissions (such as PM) in ambient air and at workplaces, less is known about the health effects of the renewable diesel emissions and non-regulated emissions with a high health impact, such as for example specific polycyclic aromatic hydrocarbons (PAHs).

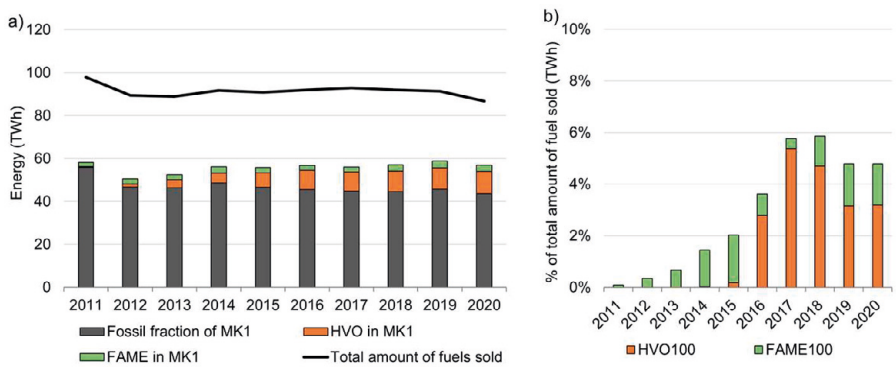

Figure 1. a) The renewable and fossil components in Swedish MK1 diesel, compared to the total amount of vehicle fuels (liquid and gas) delivered in Sweden (in TWh). The renewable diesel fuels used in Sweden are hydrotreated vegatable oil (HVO) and fatty acid methyl ester (FAME) fuels. In 2020, MK1 diesel contributed to 66% of the total amount of fuels (in TWh), and the renewable fraction of MK1 diesel was 23.3%. The volume % (not shown here) of renewable fuels in MK1 diesel in 2020 was 24.4% HVO and 5.5% FAME. **b)** The fraction (per TWh) pure renewable diesel fuels (B100) in Sweden. The amount of HVO100 was 3.2% in 2020. The total amount of all HVO and FAME in Sweden have increased from 2.5% in 2011 to 20.1% in 2020. The figures are produced by data obtained from the Swedish Energy Agency [23].

Diesel engine exhaust emissions

Diesel engine exhaust emissions are composed of a particulate fraction and of major gas-phase species such as CO_2, carbon monoxide (CO), nitrogen oxides (NO_x), and a complex mixture of volatile organic compounds (VOCs) including gaseous hydrocarbons (HC) and polycyclic aromatic hydrocarbons (PAHs) [8]. The particulate emissions from diesel engines are often characterized by a bimodal particle size distribution, with nucleation mode particles (often <20 nm) dominating

the number concentration, and soot mode particles (often around 100 nm) dominating the total emitted mass [8,9]. The soot mode particles are generally composed of 1) a solid carbonaceous fraction, in the literature referred to as soot, EC or eBC, 2) a liquid organic fraction containing particulate PAHs, and 3) an ash fraction containing trace metals. The gas-to-particle partitioning of semi-volatile organic compounds (SVOCs) for example PAHs depends on the dilution factor and temperature.

Nucleation mode particles

The particle number size distribution of the nucleation mode depends on the dilution strategy, while the soot mode is generally less affected by the dilution strategy [26]. Liquid nucleation mode particles are formed as volatile and semi-volatile gas-phase compounds in the exhaust are transformed to the particle phase by condensation. This is determined by the compound's vapor pressure, the dilution ratio, concentration, temperature, relative humidity, and residence time. Dilution strategies that favors supersaturation ratios of semi-volatile compounds, increases the nucleation potential [27]. In addition, depending on fuel composition and engine operation, the nucleation can either be hydrocarbon dominated (low loads) or sulphur driven (higher load, higher fuel sulphur content) [28]. Real-world nucleation mode formation from vehicle exhaust has been found to be the highest at low temperature and high relative humidity [28].

The nucleation mode particles have a different chemical composition compared to the larger soot particles, and are dominated by lubrication oil and metal oxides [8,29–31]. Since the nucleation mode particles are not included in any exhaust emission legislation (the EU PN legislation considers solid PN>23 nm), these particles may not be well reduced in modern engines and might also be of health concern in modern technology vehicles, which needs to be investigated [32].

Soot formation

Soot is a by-product formed during incomplete combustion. The hydrocarbon molecules in diesel oil break down into smaller gas-phase carbon units that act as soot precursors. Depending on the temperature and oxygen availability in the combustion cylinder, these soot precursors will form larger carbon units such as PAHs. These PAHs or hydrocarbons grow and cluster to form incipient soot particles (1-6 nm) [33,34]. The incipient soot particles evolve by coalescence and condensation of PAHs to form larger primary soot particles of 10-30 nm. The primary soot particles evolve by dehydrogenation to become more graphitized, and can agglomerate and aggregate to form larger structures >50 nm. These soot aggregates are characterized by a high specific surface area ($m^2\ g^{-1}$). Soot is often discussed in relation to its light absorbing properties and its degree of maturity. The spectrum ranges from poorly absorbing incipient soot particles, to highly absorbing graphitized soot particles or aggregates [35]. The soot particles mature, that is,

become more light absorbing and graphitized, as the temperature increase during the combustion [36]. The soot oxidizes in the later step of the soot evolution [37]. The completeness of the combustion in the diesel engine depends on oxygen availability, time, and temperature, which can be modified with exhaust gas recirculation (EGR) and fuel injection parameters, for example. During combustion with higher in-cylinder oxygen availability (i.e., higher temperature), the the soot would become more graphitized, carbonaceous compounds would oxidize to CO_2, and the soot mass emission would decrease.

Soot terminology

Soot mass is measured by its characteristics and can vary depending on what is measured [35]. For its environmental impact, the soot's light absorbing properties in the near-IR or IR spectral regions are measured, and called equivalent black carbon (eBC). For exposure assessments, soot is measured thermo-optically as elemental carbon (EC) [38,39]. Soot with high eBC and EC content is also referred to as "mature carbon" which is carbon that has been oxidized in the combustion process and became more graphitized. Frequently, the organic fraction of the diesel exhaust PM is discussed when the soot properties are determined. The organic carbon (OC), contrary to EC, consists of carbonaceous particles chemically bonded to other elements such as hydrogen, oxygen, and nitrogen. This is generally measured thermo-optically in the same assay as EC is determined, but as the mass that desorbs in an inert atmosphere under heating [40,41].

Impact of renewable fuels

Previous studies show that both FAME [19] and HVO [6] can reduce particulate mass emissions compared to fossil-based diesel. When the mass emissions were reduced for FAME type fuels, increased nucleation mode particle number emissions have been observed instead [20]. Emission characteristics have also been found to depend on the feedstock from which the fuel was derived for FAME fuels [20,42,43]. This includes examples of altered primary particle size and changes to the internal nanostructure depending on FAME substitution level and oxygen content of the FAME [44,45]. HVO have instead been reported to generate soot particles similar in size, nanostructure, and soot oxidation characteristics as fossil diesel exhaust particles from older diesel engine technologies [46].

The physico-chemical composition of the exhaust emissions depends greatly on combustion conditions and fuel. How these parameters interact and change the emission characteristics are of great importance for the future development of emission reduction techniques and health assessments of exhaust emissions.

Emission reduction techniques

Exhaust gas recirculation (EGR) and low temperature combustion (LTC)

EGR is a well-known and commercially used internal combustion technique to reduce the NO_x emissions from engines [47]. The amount of recirculated exhaust determines the oxygen (O_2) concentration and flame temperature in the combustion cylinder (Fig. 2). The effects of EGR and fuel have been widely studied on regulated gas emissions such as NO_x, CO, and HC, as well as on engine performance and soot emissions. NO_x emissions decrease with increasing EGR (decreasing O_2 concentration) while HC, CO and soot emissions increase [48,49]. From a particle toxicity perspective, the chemical composition (for example PAH and metal emissions) and the physical properties of particle emissions induced by varying the EGR have been much less studied.

Very high levels of EGR and combustion close to stoichiometric conditions in compression ignition engines can be used for what is referred to as low temperature combustion (LTC) concepts. LTC summarizes combustion concepts where flame temperatures are drastically reduced, and premixing time increased, to simultaneously achieve very low NO_x and PM emissions from engines [50]. Emissions with health impacts such as aromatic compounds [51], including PAHs, may increase as the combustion temperature decreases. As this happens, there is a transition from mature soot to immature soot and eventually PAHs [52–54]. The altered particle characteristics may drastically change the health effects or behavior in different aftertreatment systems. Varying the EGR can thus be used to investigate fundamental soot formation and soot particle properties.

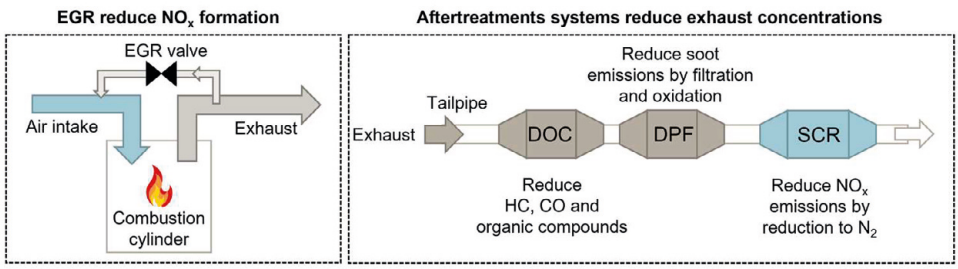

Figure 2. Conceptual illustration of emission control strategies. Exhaust gas recirculation (EGR) is an internal combustion technique to reduce the NO_x formation by lowering the available O_2 and combustion temperature, which is done by recirculating a fraction of the exhaust gas to the air intake. Aftertreatment systems in the exhaust pipe removes specific compounds in the exhaust. A common setup can be composed of a diesel oxidation catalyst (DOC), a diesel particulate filter (DPF) and a selective catalytic reduction (SCR) catalyst.

Exhaust aftertreatment systems

Exhaust aftertreatment systems (EATS) are designed to reduce exhaust emission concentrations in the tailpipe of a vehicle (Fig. 2). The EATS are usually composed

in such a manner that different compounds are treated in different steps or individual units. A common approach is to use a diesel oxidation catalyst (DOC) to remove hydrocarbons and CO, followed by a diesel particulate filter (DPF) for removing the PM, and a device to remove NO_x.

A DOC oxidizes CO to CO_2, and hydrocarbons to CO_2 and H_2O. It may also partially oxidize NO to NO_2. The catalyst coatings used are of noble metals, often platinum or palladium, and the conversion rate generally depends on the type of metal and its quality [55]. The removal efficiency generally increases with temperature (above the minimum temperature needed for the catalytic reaction), and typically hydrocarbon and CO emissions are reduced by 60-90% after a DOC [56].

The DPF removes the PM by either wall-flow or flow-through filtration and the filter deposits are removed by regeneration (oxidation of the carbonaceous PM)[55]. The wall-flow filter is a honeycomb structure, with porous walls with catalytic coating (for example silica carbide). Commonly, the expected PM removal efficiency is 95% or higher [55]. The flow-through filters have poorer filtration efficiency (up to 60%) and are thus not suitable for later emission standards (Euro 6) [57]. Regeneration of the DPF to remove the oxidizable filter deposits are either performed by passive or active regeneration. Passive regeneration is performed continuously, utilizing NO_2 from the exhaust and/or from the conversion of NO to NO_2 in the DOC to oxidize the soot. Active regeneration is instead performed by using oxygen, in timed "burn-off" events. The regeneration efficiency depends on the exhaust temperature, and in modern diesel vehicles the exhaust temperature needed is around 500-600°C [55,58].

There are different approaches to remove the NO_x emissions, either by in-cylinder techniques such as EGR or in the exhaust pipe with an aftertreatment unit. While EGR reduces the formation of NO_x to some extent, to comply with later emission standards an aftertreatment system for the NO_x removal is often needed [55]. In addition, EGR will increase the PM emissions as the NO_x emissions decrease, known as the PM-NO_x trade-off [59]. The NO_x removal unit is commonly a selective catalytic reduction (SCR) catalyst that uses gas-phase ammonia to covert NO_x to N_2 and H_2O [60]. The NO_x conversion efficiency depends on the type of catalytic compounds, temperature, NO/NO_2 ratio, etc., but generally a conversion rate of at least 50-70% can be expected [60,61].

The EATS are generally optimized for fossil diesel exhaust, and the use of renewable fuels may change their operation efficiency as the type of fuel may alter the physico-chemical exhaust properties (concentrations, chemical composition, particle reactivity, exhaust temperature, etc.). In addition, these systems are developed to reduce the primary aerosol emissions, while leaving the impact of the EATS on the secondary emissions unregulated and less well known.

Emission standards

Emission standards refer to the limit values of exhaust compounds regulated by nations and group of nations (like the EU). The emission standards (and names) vary depending on the type of vehicle and the engine being used, for example light-duty vehicles, heavy-duty vehicles, and non-road engines. For non-road engines, the emission standards also vary depending on the engine size (kW). Generally, the larger the non-road engine size, the more stringent the regulation. In addition, the emission standards (and names) vary depending on the region and are generally not fully harmonized. Generally, the higher the number of the emission standard (i.e., 1, 2, 3 or I, II, III, etc.), the more recent and more stringent the regulation it refers to. In the EU, the emission standards for light-duty vehicles are referred to as Euro 1-6, for heavy-duty vehicles Euro I-VI, and for non-road engines Euro Stage I-V (referred to Stage I-V from now on).

The newer diesel vehicles in the EU and the U.S. are now required to comply with stringent emission standards and thus reduce the exhaust emissions to a great extent. In practice this requires most vehicles to utilize sophisticated emission abatement techniques. However, in many parts of the world, the regulations are much less stringent or even missing. In addition, older vehicles without any emission reduction systems will be in use for several more years. Heavy-duty trucks in the EU have been under legislation which in practice requires them to utilize diesel particulate filters (DPF) since 2013 to remove the PM and PN, and selective catalytic reduction units (SCR) for removing the NO_x emissions. However, older vehicles are still in use. For example, in Sweden where this legislation applies, only 42% of all heavy-duty trucks had DPFs in 2019, and 72% had SCR [62]. This means that there are still many vehicles in operation that contribute to high emissions of PM. Utilizing renewable fuels in these vehicles without DPFs has the potential to decrease their negative impact on air pollution and health.

As the use of renewable fuels increases in both vehicles with and without aftertreatment systems, it is important to understand how this affects the primary emissions as well as the secondary emissions (transformation of primary emissions in the atmosphere) compared to fossil diesel. In addition, little is known if the improvements in legislation have improved the occupational exposure levels in previously high diesel exposure environments.

Secondary aerosol formation

The primary emissions from vehicles and other combustion sources are important sources of air pollution, but the secondary aerosol formation in the atmosphere also has a great impact on the total air pollution. Secondary organic aerosol (SOA) is a significant part of the ambient organic aerosol (OA) and often have seasonal

variations [63,64]. SOA is formed from the oxidation of gas-phase precursors emitted from both anthropogenic and biogenic OA sources.

Diesel exhaust is an important primary organic aerosol (POA) emitter as well as an SOA precursor and a source of photochemical smog, which all contribute to the total ambient PM. Secondary aerosol particles from the exhaust form in the atmosphere through different gas-particle conversion processes such as nucleation, condensation, and chemical reactions. SOA can be formed from volatile organic compounds (VOCs) when the gas phase of the exhaust is photo-oxidized in the atmosphere and forms particles. The gas phase of the exhaust is composed of both primary high volatility gas-phase emissions as well as evaporated compounds from the POA particulate phase. The particle-to-gas and gas-to-particle phase transfer of the POA depends on its volatility and dilution. Diesel exhaust POA is mainly semi-volatile and hence may be partially evaporated after atmospheric dilution and be able to contribute to the SOA formation [63,65].

Renewable diesel fuels have a different molecular composition compared to fossil diesel, which can affect the molecular composition of the exhaust emissions, and thus yield different SOA formation potentials. For example, the semi-volatile fraction from FAME fuels can be higher than for fossil diesel [66,67], which suggests an increased SOA formation potential per mass. The aromatic content of the fuel has also been identified as a compound that significantly increases the SOA potential [68]. Aromatic content is a key difference between the otherwise similar fossil diesel and HVO, as HVO is an aromatics free fuel. This difference would suggest a decreased SOA yield of HVO compared to diesel. Instead, in comparison to fossil diesel, similar SOA yields have been found for a FAME type fuel [69] and a HVO type fuel [70]. Continued research on how these types of renewable diesel and aftertreatment systems affect the SOA formation potential is of importance in order to model and predict future air pollution [70].

Health effects and occupational exposure to diesel exhaust

Lung deposition

The toxicity of diesel exhaust PM depends on the chemical composition and on the lung deposition upon inhalation. The deposited fraction depends on the size, shape and density of the aerosol particles, as well as on the individual's lung parameters and breathing pattern [71]. Due to the small mobility size of the exhaust particles (<100 nm), a high fraction is able to reach the alveolar region of the lung and deposit there rather than in the upper airways (Fig. 3). Deposited soluble particles are

dissolved and enter the blood stream but insoluble particles, such as soot, stay deposited until removed by clearance mechanisms. In the tracheobronchial region, inhaled particles are removed mechanically by mucuscilary clearance within a day [72]. The cilia in the tracheobronchial region move in sweeping rhythmic motions that cause the mucus, and the particles deposited, to move upwards to the epiglottis where they are swallowed [73]. In the alveolar region (where the gas exchange takes place) there is no cilia, and the clearance is performed by phagocytosis as macrophages engulf the particles and are transported to the lymph nodes or the blood flow [73]. However, this process can take up to months [72], and the inhaled solid particles may thus accumulate and have a long-term effect on the lungs.

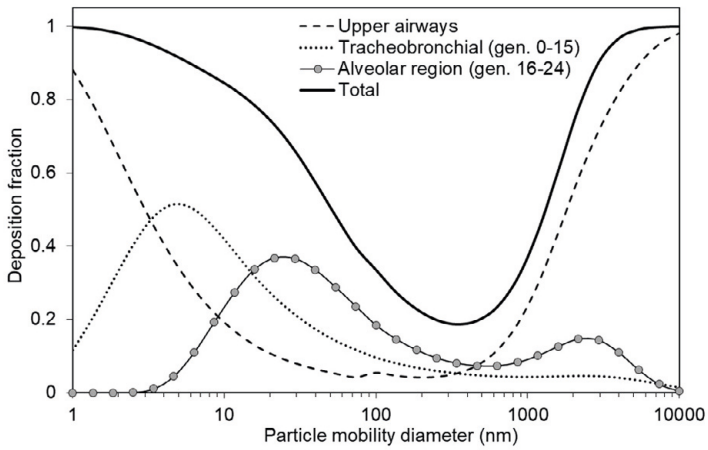

Figure 3. Estimated particle deposition in the different areas of the lung depending on particle mobility size. The estimation is based on the MPPD model, using the median lung parameters derived from the test subjects in Paper 4. The parameters used were: breathing frequency of 17.1 min^{-1}, tidal volume of 875 ml, and a forced residual capacity of 3204 ml.

Reactive oxygen species (ROS) formation

The mechanisms that drive the diesel exhaust toxicity are not yet fully understood. Exposure-induced pulmonary oxidative stress from generation of reactive oxygen species (ROS) is suggested to play a key role alongside inflammation and genotoxicity [74]. Oxidative stress is initiated when high levels of reactive oxygen species (ROS) overwhelm the antioxidant defenses within the cells. High levels of ROS in cells can trigger a cascade of events associated with inflammation and apoptosis [75] but also DNA damage, mutations, and a direction towards carcinogenesis. ROS from PM inhalation can either be related to the PM itself with particle-bound ROS, or from in-vivo interactions that cause the formation of ROS.

The ROS formation potential/and or oxidative potential of particles can be measured with multiple cell-free and intracellular assays, and the sensitivity to different PM

compounds varies depending on the assay used [76,77]. The particle-bound ROS formation is measured in cell-free assays. One commonly used assay is with the 2′,7′-dichlorofluorescin (DCFH) probe. The DCFH is a non-fluorescent molecule that becomes florescent by oxidation caused by particle-bound ROS. The intensity of the fluorescence is measured and related to the particle-bound ROS per PM mass.

Renewable diesel exhaust emissions have shown both higher [78,79] and lower [78,80,81] ROS formation potential compared to fossil diesel. These apparently contradictory results could be due to the difficulties in separating fuel and combustion induced variations in particle properties. It could also be related to the type of assay used and their varying sensitivity to PM components.

The chemical composition and physical characteristics of the diesel exhaust PM depends strongly on the combustion conditions and the type of fuel [9]. How particle characteristics with health relevance, for example the reactive oxygen species (ROS) formation, relate to the combustion conditions and fuels are less known.

Occupational exposure

Occupational exposure and lung cancer

Exposure to diesel exhaust is classified as causing lung cancer in humans based on, among others, epidemiological studies of occupational diesel exposure [13]. Long-term diesel exhaust exposure has also been linked to other health effects such as asthma [82] and cardiovascular disease [83]. Occupational diesel exposure tends to be higher in enclosed underground workplaces such as mines and underground construction, but also above ground in semi-enclosed environments such as mechanics shops, harbors and ferries [14,16]. The reported workplace diesel exhaust exposure concentrations, measured as elemental carbon (EC), ranged from <25 μg m^{-3} up to 660 μg m^{-3} in a review summarizing the occupational exposures from 10,000 measurements performed before 2009 [14].

Epidemiological studies have assessed the excess lifetime risk for lung cancer caused by diesel exposure. The excess lifetime risk describes the excess number of people who develop or die from a disease in an exposed population compared to a similar population without the exposure. A full working life (45 years) exposure to 25 μg EC m^{-3} was estimated to yield 689 excess deaths from lung cancer alone per 10,000 (6.9%) [16], and more recently, estimates of 300 excess deaths per 10,000 (3.0%) were reported for 50 μg EC m^{-3} [15]. Even though there are discrepancies and large uncertainties in such estimations, they still indicate that there is a considerable risk at low exposure concentrations and a high individual risk. There is no absolute number of what level of risk from occupational exposure is considered acceptable, but there are some national guidelines. For chemical substances classified as occupational carcinogens, the U.S. National Institute for Occupational

Safety and Health (NIOSH) considers that an acceptable risk is 1 excess cancer case per 10,000 workers (corresponding to an individual risk of 0.01%). Germany and the Netherlands similarly consider an acceptable risk to be 4/10,000 (0.04%) [84,85]. Based on epidemiological studies, exposure concentrations of 1 µg EC m^{-3} yield an individual risk of 0.17% [16] or 0.04% [15] which are closer to the acceptable levels. It should also be noted that these excess mortality levels estimated by the two studies [15,16] are for excess mortality due to lung cancer alone, and do not include other lung diseases or cardiovascular diseases. The EC exposure estimations in such studies can be estimated from job-exposure matrices [15,86]. Contributions to updated values of occupational exposure concentrations at modern workplaces will improve such estimations in the future.

Occupational exposure limits

After the evaluation of diesel exhaust carcinogenicity and its classification as carcinogenic to humans (group 1) by the WHO's International Agency for Research on Cancer (IARC) in 2012 [13], the development and use of emission abatement techniques have increased as the regulations have become more stringent. The current workplace exposure legislation in Sweden was updated in 2018 with reduced occupational exposure limits (OELs) of NO, NO_2 [87] and are summarized in Table 1. These limit values do not go into effect until 2023 for underground workplaces because the implementation of solutions reducing the exposure are deemed more challenging here than in workplaces above ground. The EU decided on a new occupational exposure metric of the particulate fraction from diesel exposure in 2019, measured as elemental carbon (EC). The 8-hour OEL will be 50 µg EC m^{-3} and be implemented in 2023 in the EU [88], including Sweden [89], at general workplaces and in 2026 also at underground workplaces. Denmark and the Netherlands have already implemented a more stringent EC limit of 10 µg m^{-3}, which is being enforced in Denmark as of 2021 [90], and in the Netherlands since 2020 [91].

It is important to investigate what impacts these more stringent OELs and emission standards have on occupational exposure, as well as if the emission levels can be reduced with the use of renewable fuels or a more modern vehicle fleet. As not all compounds are regulated, and the regulations can be more stringent for one compound than another, the exhaust composition (ratio between different exhaust components) is likely to change compared to "older" diesel exhaust. Landwehr et al. [92] reviewed the trouble with this in 2020 and found that there is no significant evidence that the health effect of newer engine technology (using DPFs for example) is lower, despite a significant reduction of the PM emissions. In addition, health effects have been associated with both whole and particle-filtered diesel exhaust, but the effects of individual exhaust components are not fully understood [93]. As of yet, there have only been a few studies – and only one with controlled exposures in humans [94] – of the health effects from diesel vehicles with and without

aftertreatment systems [93]. This highlights the need for future research on the health effects from modern diesel vehicles with different aftertreatment systems. In addition, in the few studies of the human health effects of biodiesel exposure, similar or even more health effects have been found compared to diesel [81,95]. Cell cultures and animal studies have found both increased and decrease toxic potency and the exposure is suggested to potentially induce similar effects as diesel exposure on oxidative stress, inflammation, and genotoxicity [96]. No controlled human exposure studies of HVO have previously been performed. Such studies are of importance as this is the type of renewable diesel fuel that is currently used the most in Sweden (both as blends and in 100% substitution) and have the potential to replace fossil diesel in existing diesel vehicles. In the future, the use of renewable diesel fuels may dominate in workplaces, which emphasize the need of exposure studies of these fuels.

Table 1. The current and future occupational exposure (8 hours) limit values in Sweden [87]. The short-term exposure limit values (15 minutes) are shown in ().

	Year	NO (mg/m^3)	NO_2 (mg/m^3)	EC ($\mu g/m^3$)
General workplaces	2018	2.5 (-)	0.96 (1.9)	-
	2023			50
Underground and tunnel work	2018	30 (60)	2 (10)	-
	2023	2.5 (-)	0.96 (1.9)	-
	2026			50

Methodology

Both laboratory and field measurements were performed in the research presented in this thesis. The two different environments yield different advantages and practical limitations. In the laboratory, more instruments and more advanced techniques are possible to use in combination with a higher degree of control of the emission source. In the field (an underground mine in this thesis) there is logistical and environmental challenges such as transport, operation stability and mobility of the instruments. The advantage is the potential to gain an understanding of emissions and exposures under real-world conditions that have direct implications for the workers who are exposed. By combining the intricate knowledge gained from the laboratory measurements, one can achieve a better understanding from fewer measurement techniques in the field. In this thesis research, the health effects have also been evaluated by performing a controlled human exposure study in a chamber. Such studies are preferred in order to investigate the effects of exposure with a high degree of control. However, this also poses challenges in terms of balancing ethical considerations and exposure relevance, and with the drawback that it is only possible to investigate short-term effects.

Study designs

An overview of the studied parameters in each paper is presented in Table 2.

The laboratory study in Paper 1 investigated the exhaust emissions from a heavy-duty diesel engine depending on fundamental combustion conditions and type of renewable diesel fuel (HVO, RME). The engine was operated at constant low load (≈25%) and the combustion conditions were varied by varying the available O_2 concentration in the combustion cylinder (by means of EGR), which relates to the combustion temperature. Three specific engine setpoints were chosen to study 1) low-temperature combustion particles (immature soot), 2) mature soot, and 3) highly oxidized soot. The particle-induced ROS production of these different types of soot was measured, which has implications for genotoxic effects and inflammation in-vivo. In addition, relatively large amounts (>50 mg) of fine particles (PM1) were collected to be used in toxicological studies.

The laboratory study presented in Paper 2 evaluated the effect of replacing fossil diesel with renewable diesel fuels (HVO, RME) in a modern engine, with and without external aftertreatment systems. The engine operation was chosen to reflect a modern engine under ahigh NO_x/low eBC operation condition, which was realized by using a low amount of EGR. The engine was operated at constant low load (≈25%). In addition, a no combustion case ('motoring') was tested by simulating engine braking. The effects on primary emissions and secondary emissions (simulated with photochemical aging) were investigated. A common arrangement of an aftertreatment system was chosen, and the measurement points were: 1) engine out (no aftertreatment), 2) after a DOC, and 3) after a DOC combined with a DPF. In addition, we used a dilution system mimicking atmospheric dilution to investigate "real-world" nucleation mode particle size distributions down to 1.4 nm.

The field study presented in Paper 3 investigated the underground emission characteristics (stationary ambient concentrations) and the occupational exposure to diesel exhaust in an underground mine. We applied and evaluated multiple exposure metrics for offline and direct reading analyses that monitored diesel exhaust. The study was designed to explore and characterize different exposures in relation to work tasks in the mine where diesel vehicles with different emission standards were in use. The ambient concentrations and personal exposures were evaluated in relation to the level of the emission standards and technical advancements of the vehicles used. In addition, urinary PAH metabolites were measured to evaluate the efficiency of simpler exposure metrics to assess personal exposure to diesel exhaust compared to measuring airborne concentrations. Effect biomarkers related to oxidative stress was also measured in urine to investigate potential health effects of the occupational exposure compared to the normal population.

In the Paper 4 laboratory study, the health effects from 3-hours exposure to renewable diesel (HVO) exhaust from modern non-road vehicles were investigated in comparison to filtered air exposure. This was achieved by choosing vehicles that are commonly found in workplaces and that were manufactured the same year as the exposure. The exposures were generated by operating the vehicles with varying idle and load settings. In addition, we evaluated the effect of 1) exposure to exhaust particles combined with NO_x, and 2) exposures to only NO_x, with filtered air exposure. This was achieved by choosing two vehicles where one had an aftertreatment system and the other one not. The health effects were evaluated by self-rated symptoms, nasal patency, and pulmonary function assessments.

Table 2. Overview of the study designs of the papers included in this thesis.

	Study design			Fuels and vehicle type			Emission control technique	
	Study type	**Varied parameters**	**Determined parameters**	**Fuel**	**Vehicles/Engine**	**Emission standard**	**In engine**	**Exhaust system**
Paper 1	Fundamental/Lab	Fuel Combustion temperature (EGR)	Detailed exhaust characteristics Particle-bound ROS formation	HVO RME Diesel	Modern heavy-duty engine	-	EGR 9-21% O_2	-
Paper 2	Applied/Lab	Fuel Aftertreatment system Aging	Detailed exhaust characteristics Emission factors Secondary aerosol formation	HVO RME Diesel	Modern heavy-duty engine	-	EGR 18% O_2	None DOC DOC+DPF
Paper 3	Occupational/field study	Emission standard Occupational environment (Fuel)	Emission factors Personal exposure Urinary metabolites	Diesel (HVO30)	Non-road vehicles (300kW, 2012-2015)	Stage IIIB Stage IV	Not specified	None SCR
				Diesel	Non-road vehicle (300kW, 2019) Heavy-duty trucks	Stage V Euro VI	Not specified	DPF+deNOx
				Diesel	Mixed light-duty, heavy-duty, nonroad.	Mixed	Not specified	Mixed*
Paper 4	Controlled chamber exposure	Emission standard	Exhaust characteristics Lung function Nasal obstruction Irritation symptoms	HVO	Non-road vehicle (23kW, 2019)	Stage IIIA	Not specified	None
					Non-road vehicle (55kW, 2019)	Stage V	Not specified	DOC+DPF

EGR: exhaust gas recirculation, ROS: reactive oxygen species, HVO: hydrotreated vegetable oil, RME: rapeseed methyl ester, DOC: diesel oxidation catalyst, DPF: diesel particulate filter, SCR: selective catalytic reduction, deNOx: NO_x reduciton unit (details not available).

Method for evaluating laboratory exhaust characteristics

In the Paper 1 study, a highly-controlled modern heavy-duty diesel engine in a laboratory was operated on 100% diesel, HVO, and RME (no blends). The amount of EGR was varied in order to change the available O_2 concentration and to investigate its fundamental impact on exhaust particle properties. Fossil diesel exhaust particles were collected at three levels of EGR (10%, 13%, and 17% intake O_2) to investigate the toxic effect depending on engine operation. At the medium level of EGR (13% intake O_2), particles were collected for all fuels (diesel, HVO, and RME) to investigate if the particle properties and toxic characteristics of the soot particles changed depending on fuel. The potentially toxic effect was evaluated by measuring the particle-bound ROS-formation potential (which is an indicator of oxidative stress). In a separate work not part of this PhD thesis, a mice installation study was carried out with the same particle samples by the National Research Centre for the Working Environment (NFA) in Denmark [97].

The dilution setup in the Paper 1 study (Fig. 4), which included ejector diluters and a dilution tunnel, was developed to enable dilution with a high flow rate as the particle collection was performed with a high-volume cascade impactor (HVCI, 1000 lpm). The PM <1µm was collected on Teflon filters with the HVCI, which sorts and collects particles by inertia at a high flow rate. The collected particles were extracted with methanol for ROS and toxicological analyses (details described in Paper 1).

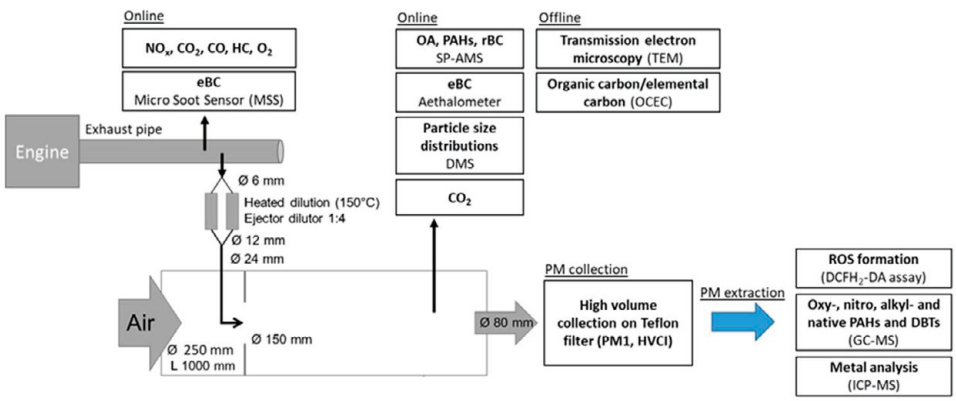

Figure 4. Setup used in the Paper 1 study showing the dilution system (particle dilution flow tunnel) and the measurements techniques.

In the Paper 2 study, a modern heavy-duty diesel engine was operated on 100% diesel, HVO, and RME, with and without an aftertreatment system. The aftertreatment system consisted of a DOC alone, and a DOC in combination with a DPF. A low level of EGR was used to decrease the NO_x emissions and slightly increase the PM emissions to evaluate the effect of the aftertreatment systems on the PM. To achieve atmospherically relevant dilution to investigate the fresh primary aerosol emissions, a partial flow dilution setup was used that was composed of a porous tube diluter and a small residence chamber (2.5 s, in order to stabilize the nucleation mode particles). Additional ejector diluters were used to further dilute the emissions [28,70] (Fig. 5).

Atmospheric ageing by photochemical oxidation was simulated in a Potential Aerosol Mass (PAM) oxidation flow reactor (OFR) to evaluate the effects of the different fuels and aftertreatments on the atmospheric particle loading. The reactor is a 13 l steel chamber with two Hg lamps with peak intensities at 185 and 254 nm. The UV light together with a humidifier generate ozone and hydroxyl radicals (OH) that oxidize the incoming aerosol. The flow determines the residence time (approx. 160 s using a flow rate of 5 lpm) in the chamber. A single OFR set point was employed in the experiments and the OH exposure represented 4.8±2.6 OH days assuming a 24 h average OH concentration of 1.5 x 10^6 molecules cm^{-3} [98].

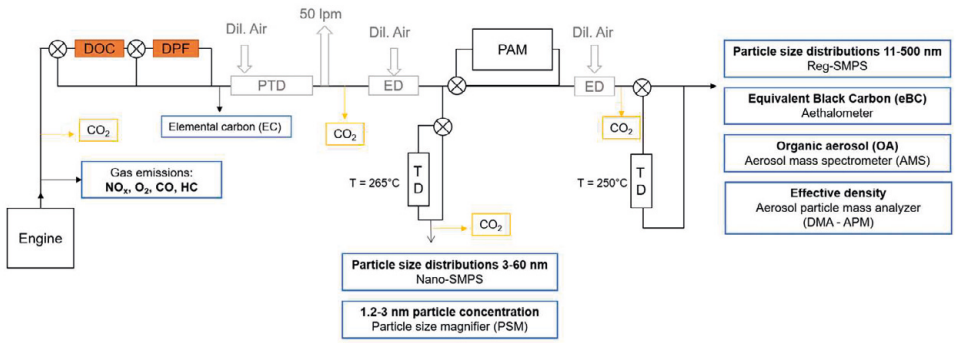

Figure 5. Experimental setup used in the Paper 2 study showing the dilution system and the measurement techniques. Sampling was carried out engine-out, after the DOC, and after the DOC+DPF. The dilution was performed with a porous tube diluter (PTD) and two ejector diluters (ED).

Method for studying occupational exposure

Paper 3 presents a field study we performed in an underground mine. A limited setup, consisting of selected instruments from the lab studies, was used in the "mobile lab" setup (Fig. 6a). The underground environment poses several challenges, nonetheless regarding safety and accessibility. Aerosol measurements in locations such as the mine are also challenging for several reasons, as many state-of-the-art aerosol instruments are sensitive to vibrations and require stable operating conditions, or require conditions not easily maintained outside a lab (stable pressure, vacuum, uninterrupted power), or cannot be transported.

The ambient concentrations were measured in two drifts with a different setup of heavy mining equipment and vehicles following different emission standards (Stage IIIB-IV vs. Stage V and Euro VI), and at a busy underground roadside. The measurements in different stationary locations were used to relate the emission levels in different areas depending on vehicle type, and to compare them to the personal exposures. Personal exposures to airborne diesel exhaust components were assessed by measurements in the breathing zone of 12 miners with small personal online and offline devices (Fig. 6b). In the breathing zone, we performed time-resolved eBC measurements, filter sampling for EC, and passive sampling for PAHs and NO_2 (details in Paper 3). The instruments and sampling methods for personal exposure were carried by the workers on a vest and needed to be small and light in order for them to perform their work tasks as usual.

Personal exposure was also assessed by biological sampling that consisted of collecting urine samples from a larger group of 27 miners. In 10 of these 27 miners, we had also performed airborne exposure measurements on the same day as the biological sampling to investigate the correlation between airborne exposure and urinary PAH metabolites and/or a specific set of effect biomarkers.

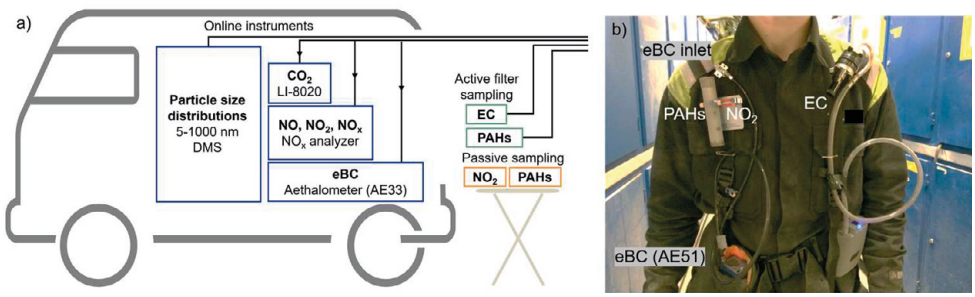

Figure 6. **a)** The stationary measurement setup for analyzing the underground ambient air. The online instruments were arranged inside a van, while the offline sampling (active and passive sampling) was set up outside. **b)** The instruments used for the personal breathing zone measurements mounted on a worker in the mine. The personal exposure of PAHs and NO_2 was measured with passive methods, and EC with active filter sampling. The same measurements were also performed in the stationary measurement setup, but the PAHs was additionally measured with active filter sampling and the NO_2 with a direct reading technique in the stationary setup.

Method for evaluating health effects − human exposure study

The effects of HVO exhaust exposure on lung function and self-rated symptoms were investigated in the Paper 4 study, and the setup is shown in Fig. 7. It is of great importance to create an exposure scenario that is realistic (including the type of fuel) in order to evaluate the potential health effects. In addition, to increase the credibility of our study, our aim was to use modern vehicles (delivered 2019) and not ones based on old technology. We also wanted to operate the vehicles in a realistic manner, which meant using load and not only idle. In addition to all this, we wanted to investigate the impact of the exhaust particles vs. that of the NO_x exposure. To find vehicles that could comply with these set requirements, we performed several minor pilot studies using a set of non-road vehicles commonly found in workplaces.

Two non-road vehicles of different engine sizes were chosen: a Stage IIIA (23 kW) and a Stage V (55.4 kW) wheel loader. Wheel loaders can often be found at different workplaces, such as minor road/park/city maintenance and construction sites. The Stage IIIA loader did not have any external aftertreatment system; the Stage V loader had a DOC and a DPF. Consequently, the Stage IIIA loader emitted all the common components of diesel engine exhaust (PM, organic gases, NO_x), while the Stage V loader's aftertreatment system efficiently removed PM and organic gases while leaving the NO_x emissions close to unchanged.

As we had chosen wheel loaders, the load could be applied while standing still by using the wheel loader bucket. The buckets were lifted and pushed to their upper position while gas was applied to simulate a load event. The loaders were operated in 15 min intervals by switching from load event to idle mode. This was done in order to operate the vehicles in a relevant manner (i.e. with load).

The exposure levels were chosen to comply with the current OELs of NO, NO_2 and future OELs of EC.

Nineteen healthy volunteers were exposed to HVO exhaust from the two different vehicles separately, with at least a one-week wash-out in between. They were also exposed to filtered air to act as a reference exposure. The exposure levels were below the OELs, and thus lower than most previous human chamber exposure studies of exhaust emissions. The result of the exposures would thus give information on the short-term health effects from one day of exposure at exposure levels that are considered acceptably safe for a whole working life by the EU and Swedish standards. Detailed aerosol characterization was performed with both online and offline techniques, and the lung deposited doses were estimated with the MPPD model. The health effects presented in Paper 4 were assessed with self-rated symptoms and measured respiratory system functions.

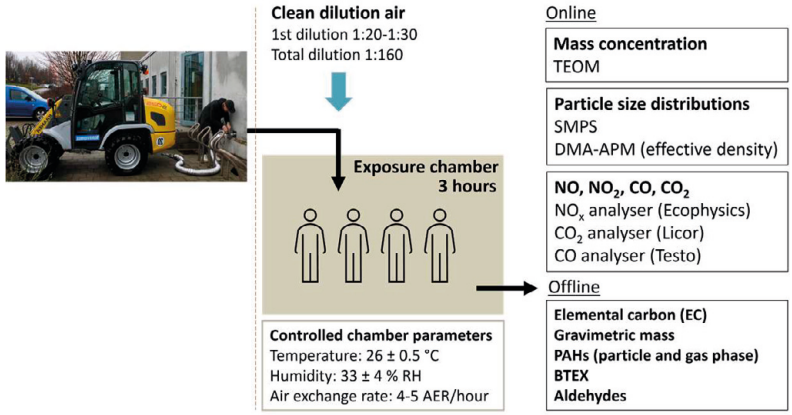

Figure 7. The experimental setup used for the human chamber exposure in the Paper 4 study. The HVO exhaust was diluted and led into the chamber where a maximum of four persons were sitting, and the exposure concentrations were continuously sampled and measured. The exposure scenarios were 1) HVO exhaust, 2) particle-free HVO exhaust, 3) filtered air.

Aerosol measurements

Particle number size distribution and concentration

Two techniques for particle number size distributions have been used: a scanning mobility particle sizer (SMPS), and a differential mobility spectrometer (DMS). An SMPS was used to measure particle size distributions of 10-430 nm (Paper 4), and an SMPS and a nano-SMPS were used to measure particle size distributions of 11-300 nm and 3-40 nm, respectively (Paper 2). In Papers 1 and 3 the DMS was used to measure the size distribution in the range 5-1000 nm.

The SMPSs consist of a differential mobility analyzer (DMA) and a condensation particle counter (CPC). The aerosol is charged by a bipolar charger and sorted by scanning the voltage. Particles with an electrical mobility corresponding to the given voltage are then counted by the CPC. The scanning of the voltage subsequently builds up a particle size distribution and the time resolution is a couple of minutes (~3 min). The DMS, on the other hand, measures the full size distribution at once as the particles of different sizes are detected simultaneously in a column of electrometer detectors. The DMS has a time resolution of down to 0.1 s but with a lower size resolution than the SMPS. Another difference is that the DMS uses a unipolar charger to charge the aerosol, and the DMS is thus more sensitive to particle shape/structure. This is corrected in the software by choosing an appropriate inversion matrix. For diesel exhaust, a matrix developed by the manufacturer which takes the aggregated structure of diesel soot into account was used. The SMPS is also more sensitive, while the DMS requires higher concentrations, making it optimal for measuring the exhaust but poorer in ambient measurements with lower concentrations.

Soot measurements

Mature soot can be measured as elemental carbon (EC) or equivalent black carbon (eBC) [35,38].

The eBC content of the aerosol was measured with a micro soot sensor (MSS, model 483, AVL), with a stationary aethalometer (AE33, Magee Scientific), and with portable aethalometers (AE51 and MA200 from AethLabs). The MSS is based on an in-situ photoacoustic technique and the aethalometer on a filter-based optical technique. The MSS was used in Paper 1 and aethalometers were used in Papers 2-4. The MSS operates well at higher concentrations (1 μg m^{-3} to 1 g m^{-3}), which is why it was used when the BC was measured in the exhaust in Paper 1. The detection range of the aethalometer (0.01 μg m^{-3} to 100 μg m^{-3}) makes it more suitable for ambient concentrations or measurements after dilution and was hence chosen for Papers 2, 3 and 4. The MSS and the aethalometers can have a time resolution of seconds.

The MSS measures particles that absorb IR-light at λ=808 nm. These particles will be heated due to the absorption and expand in size. The expansion causes a sound wave in the measurement cell that is detected and translated into an eBC concentration.

The aethalometer (AE33, MA200) uses a filter-based technique to measure the optical properties (i.e., the light attenuation) of the aerosol. The aerosol is deposited on a filter tape and LEDs with several wavelengths illuminate the sample, and the transmitted light is detected by a photodetector on the other side of the filter. The light attenuation of different wavelengths can be related to carbon with different optical properties. The eBC mass is calculated by the optical attenuation of the 880 nm light (AE33), and as other aerosol particles absorb significantly less in this region, all can be attributed to eBC [99]. The simpler portable aethalometer (AE51) only detects one wavelength (880 nm) on a filter strip that manually needs to be changed regularly to avoid filter over loading [100]. In addition, a post-processing filter loading correction (based on the measured attenuation) was performed on the eBC data from the AE51 in Paper 3 [100,101].

EC is measured with an offline technique where the aerosol is collected on quartz filters and analyzed with a thermal optical analyzer. Different protocols for the analysis can be used, but generally the sample is first heated in an inert He atmosphere where the organic carbon (OC) evolves and can be quantified, and thereafter in an oxidizing atmosphere where the EC fraction is oxidized and quantified. In Papers 1 and 2, the EUSAAR_2 protocol was used to include a detailed analysis of the OC evolvement [41], while the NIOSH 5040 protocol was used in the studies in Papers 3 and 4 because this is the recommended method for quantifying EC from diesel exhaust in occupational environments [102].

Mass-mobility relationship of soot agglomerates

The effective density of the exhaust particles was measured in the Paper 2 and 4 studies by using an aerosol particle mass analyzer (APM) in combination with a DMA. The effective density of an aerosol describes the particle mass in relation to its mobility size. Due to instrumental limitations, particles with low mass (i.e., $d_m <$ 50 nm) were not measured. The effective density was used in combination with the particle number size distribution from the SMPS in order to calculate the particle mass size distribution and total mass concentration.

The APM is composed of an inner and outer rotating rod, with the aerosol flow in the gap in between. A voltage is applied to the inner rod, and the aerosol particles are exposed to the electric field and the centrifugal force created by the rotating rods. When these two forces are balanced, the particles will be able to exit the rods and are counted by a CPC. The centrifugal force varies by mass and is independent of shape, and by varying the voltage, a mass distribution spectra of the aerosol is measured [103]. The DMA is used before the APM to create a quasi-monodisperse aerosol and hence, particles of a known mobility diameter size (d_p) enter the APM. The mean mass (m) can be used to calculate the effective density (ρ_{eff}) by assuming spherical particles following Eq. (1). The scan time of the APM for one particle mobility size was about 7 minutes.

$$\rho_{eff}(d_p) = \frac{6\,m}{\pi\,d_p^3} \qquad (1)$$

The effective density of soot agglomerates generally follows a power law function, where C" is a constant and D_{fm} the mass-mobility exponent [104]:

$$\rho_{eff} = C'' d_p^{D_{fm}-3} \qquad (2)$$

Transmission electron microscopy (TEM) and surface area

I assessed the morphology, primary particle size and surface area of the soot agglomerates by means of transmission electron microscopy (Papers 1 and 4). Exhaust particles were collected with an electrostatic precipitator on a carbon coated Cu-grid and imaged by means of TEM. The optical column in the TEM is operated under high vacuum and multiple electromagnetic lenses are used to focus the electron beam in the desired manner. The specimen is placed in the column and irradiated by a high-energy electron beam. The transmitted electrons are projected down and detected by a charged coupled device camera. The electron-matter interactions in the specimen are used to extract information such as morphology and structure (elastic scattering), and chemical composition (inelastic scattering).

The diameters of the clear primary particles without overlap at the edges of the soot agglomerates were measured in TEM images with high magnification (>20,000). A lognormal distribution was fitted to the primary particle size distribution, and the geometric mean was used as the mean primary particle size.

The specific surface area (SSA, $m^2\ g^{-1}$) was calculated with a slightly different approach in Papers 1 and 4 depending on the available data

In Paper 4, the SSA distribution was calculated using the model described by Rissler et al. [105], which is based on DMA-APM and TEM measurements. From the DMA-APM, the mass of individual agglomerates as a function of mobility particle size can be extracted if the effective density follows the soot power law function (Eq. 2). The surface area of individual agglomerates was then calculated by dividing the mass of the agglomerate by the primary particle mass and surface area (Eq. 3).

$$SA = \frac{6}{\rho_{pp} \times d_{pp}} \qquad (3)$$

The primary particle size (d_{pp}) is obtained from TEM images, and the inherent material density of soot (1.8 g cm^{-3}) used for the primary particle density (ρ_{pp}). From the surface area of individual agglomerates as a function of mobility particle size, the particle number distribution (from the SMPS) can be converted to a particle surface area distribution. This method accounts for the agglomerated soot structure and is described in more detail by Rissler et al. and Wierzbicka et al. [105,106].

In the Paper 1 study, a simplified version of the SA calculation was used. The SSA for each measured primary particle was estimated by using the primary particle diameter (d_{pp}) measured by TEM and an assumed inherent material density (ρ_{pp}) of 1.8 g cm^{-3} according to the Eq. 3. By assuming point contact between the primary particles in the agglomerates, we estimated that the primary particle SA was representative of the sample SA. A limitation is that this may overestimate the surface area compared to the BET surface area, for example. The primary particle SSA distribution was assumed to be lognormal, and the geometric mean was used as an estimate of the samples SA.

Gas measurements

The NO, NO_2 and NO_x were measured with chemiluminescence analyzers. In Papers 1 and 2, an AMA i60 (AVL) was used to measure the NO_x emissions and in Papers 3 and 4, the NO and NO_2 concentrations were measured with the CLD 700 AL (Ecophysics). The analyzers can have a time resolution of seconds. In Paper 3, the NO_2 was also measured with an offline passive sampling based on diffusion [107,108]. The PAHs in Paper 3 were also measured with a passive sampling method [109,110].

The CO and CO_2 were measured by non-dispersive infrared techniques. In Papers 1 and 2, the AMA i60 (AVL) was used to measure CO and CO_2 in the raw exhaust, and the CO_2 concentration in the diluted exhaust was measured with the LI-8020 (LI-COR). In Papers 3 and 4, the LI-8020 was used to measure the CO_2 concentration. CO and CO_2 were used to measure the dilution ratios and to estimate the emissions factors. The analyzers can have a time resolution of seconds.

Emission factors

Emission factors in g per kg fuel were calculated by following Eq. (4) [111]. In paper 2 these were converted into to g MJ^{-1}. The calculation was performed by assuming complete combustion, that is, all carbon in the fuel was converted to CO_2.

$$Emission\ factor\ (EF) = 10^3\ \frac{[Pollutant]}{\Delta[CO_2]\frac{MW_C}{MW_{CO_2}}}\ C_f \qquad (4)$$

where the background-corrected concentrations of Δ[Pollutant] and Δ[CO_2] were in μg m^{-3}. The carbon mass fraction (C_f) was analyzed for diesel and RME (Table 3) used in Paper 2, but not for HVO, which was assumed to be the same as for diesel.

In Paper 2, the emission factors per kg fuel were normalized to the energy content of the fuels and presented in g MJ^{-1}. This was done by dividing the factors by the lower heating values of the fuels (MJ kg $fuel^{-1}$) in Table 3.

The emission factors in Paper 3 (in g per kg fuel) were converted to g kWh^{-1} in this thesis to allow comparison with the vehicle emission standards. This was done by assuming an average fuel conversion efficiency of 35%. Together with the heating value content (kWh L^{-1}) and fuel density (Table 3), the EF was calculated:

$$EF\ (g\ kWh^{-1}) = \frac{EF\ (g\ kg\ fuel^{-1})}{heating\ value\ (kWh\ L^{-1})\ /\ fuel\ density(kg\ L^{-1}) \times 0.35} \qquad (5)$$

Table 3. Fuel characteristic values used for the emission factor calculations.

	C_f	Lower heating values (MJ kg^{-1})	Heating values (kWh L^{-1}) [a]	Fuel density (kg L^{-1})
Diesel	0.85	43.15	9.8	0.815 [a]
HVO	0.772	44.1 [112]	9.44	0.78 [b]
RME	0.772	37.3 [113]	9.17	0.88 [c]

[a] Values from official fuel statistics from the Swedish Energy Agency "Värmevärden från Energimyndighetens datalager (DW) 2017". [b] Density of Preem 100% HVO fuel following fuel standard SS-EN 15940. [c] Density of RME is defined to be 0.86-0.9 kg L-1 by fuel standard SS-EN 14214.

Pre-campaign soot measurement comparison and validation

A comparison of EC (offline sampling) and eBC measured with direct-reading stationary and personal monitoring instruments are shown in Table 4 and Fig. 8. The comparison was performed in preparation for the underground mine study (Paper 3). The aim was to compare the instruments that would be used to assess personal exposure to eBC with EC, and compare the controlled intercomparison with the performance of the measures and instruments in the harsh mining environment in the Paper 3 study. The intercomparison was carried out in the exposure chamber (22 m^3) with HVO exhaust generated with a small wheel loader (Stage IIIA). This type of exposure (similar concentrations and same exposure time) was later used in the Paper 4 study and called HVO_{PM+NOx} exposure.

eBC corrections and comparisons

The eBC data from the AE51 was filter load corrected by using the attenuation value [100]. The correction increased the eBC concentration on average by 64±10%. The high correction percentage is due to the high concentrations and lack of filter change, which caused the attenuation to rapidly increase over recommended levels (≈80, [100]) and measured at attenuation levels that were too high for about 2/3 of the time during the intercomparison. However, the variability between the three AE51 instruments after the attenuation correction was low and around ±10%. To minimize filter loading artifacts, the filters were changed frequently during the occupational exposure measurements in the Paper 3 study. The load correction was applied to the data set in the mine (Paper 3), where the attenuation was kept below the recommended maximum attenuation values. The correction increased the measured eBC concentrations by on average 27±16% in the mine. After this correction, the eBC_{AE51}/eBC_{AE33} ratio during the intercomparison was 0.74±0.06. Failing to perform the filter loading correction would hence further underestimate the eBC from AE51 compared to AE33.

Table 4. A summary of eBC and EC measurements during the intercomparison. The aerosol measured was generated from a Stage IIIA wheel loader used in the chamber study presented in Paper 4. The sessions were performed with similar concentrations and conditions as during the repeated exposures presented in Paper 4.

		Instrument		Conc. (µg m^{-3})	eBC/EC
Direct reading instruments	PM2.5	AE33	eBC	131	2.75
	PM1.6	AE51 (1)	eBC*	106	2.24
	PM1.6	AE51 (2)	eBC*	96	2.04
	PM1.6	AE51 (3)	eBC*	86	1.82
Offline sampling	PM1	Thermooptical method	TC	104	
			EC	47	
			OC	57	

*Load corrected eBC. On average the load correction increased the orignally measured eBC value (AE51) by 64±10%.

eBC and EC comparison

The eBC_{AE33}/EC offset during the intercomparison was 2.75 (Table 4) and was also similar in Paper 2 (2.8±0.6). Similar offsets have been found in semi-urban areas with AE33, 2.7-3.3 [114]. The eBC_{AE51}/EC factor during the intercomparison was 2.0±0.2, which was slightly lower than in the mine (GM: 2.9). Similar offset between eBC from the AE51 and EC has been reported for waste workers, 1.99 [115].

The comparisons showed that using real-time monitoring of eBC was a good proxy for EC, which is useful for identifying work tasks or areas with elevated risks of EC exposure, for example. However, eBC from AE51 or AE33 generally showed a factor 2-3 higher values than EC. The comparison also showed the importance of performing the filter loading correction for the AE51, and that the AE33 generally yield slightly higher eBC values.

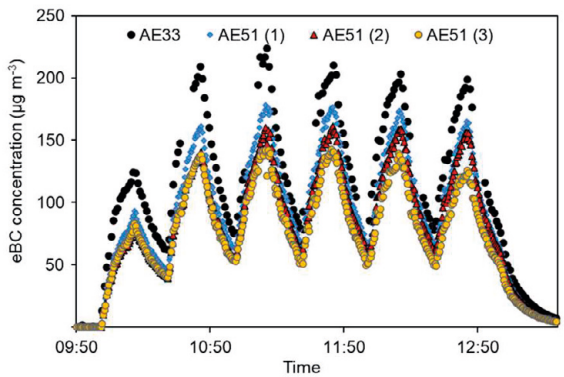

Figure 8. The laboratory intercomparison of the direct reading instruments used for measuring eBC. AE33 is the stationary instrument, and AE51 the smaller portable instruments used for personal exposure measurements. The instruments were measuring in parallel. The eBC from AE51 was corrected for filter loading artifacts by the method described in [100].

Measures of health effects and medical assessments

Reactive oxygen species (ROS)

The ability of the extracted PM to generate ROS was determined in Paper 1 by using the cells-free version of the 2′,7′ dichlorodihydrofluorescein diacetate ($DCFH_2$-DA). The $DCFH_2$-DA is a fluorescent probe that in its native state is non-fluorescent. It can be hydrolyzed to form 2′,7′ dichlorodihydrofluorescein ($DCFH_2$) that will form the florescent DCF molecule upon oxidation, which can be spectrofluorimetrically detected. In the assay used, the oxidation is caused by the particle-generated ROS.

In the Paper 1 study, exhaust particles were collected and extracted in order to perform ROS measurements. Each PM sample was prepared in triplicates of 8 PM concentration doses, ranging from 1.05 up to 101.25 μg/ml. The generated ROS caused the formation of DCF from $DCFH_2$ that was spectrofluorimetrically measured following 3h of incubation in the dark (37°C and 5% CO_2). Excitation and emission wavelengths were $\lambda_{ex} = 490$ nm and $\lambda_{em} = 520$ nm, respectively (Victor Wallac-2 1420; PerkinElmer). ROS forming PM will cause saturation of the probe at higher doses, which is seen as a plateau or a decrease of fluorescence at higher doses. The linear dose-response relationship (α) was hence calculated from the doses before this plateau and used to compare the ROS forming ability of the PM samples.

Self-rated irritation symptoms

The participants in the exposure study (Paper 4) reported self-rated symptoms scores on a visual analogue scale (VAS) before, during, and after each aerosol exposure. Symptoms from eyes, nose, throat, and chest/lower airways were reported.

Nasal patency assessment

An assessment of nasal patency was performed with measurements of Peak Nasal Inspiratory Flow (PNIF) using an inspiratory flow meter (In-check, Clement Clarke International Limited, England) (Paper 4). The inspiratory flow at was measured at three time points during the exposure and was compared to the baseline value measured before the exposure on the individual basis. A decrease in PNIF compared to the baseline value indicated an increased nasal obstruction [116].

Lung deposited dose

The estimated individual lung deposited doses presented in Paper 4 were calculated with the multiple-path particle dosimetry (MPPD) model using individually measured tidal volumes (Tremoflo, THORASYS, Thoracic Medical System Inc.) and breathing frequencies (Noxturnal). Details of the input parameters are presented in Paper 4.

Urinary metabolites and biomarkers

The urine samples presented in Paper 3 were analyzed for PAH metabolites and biomarkers as described in Krais et al. [117]. PAH metabolites of naphthalene (2-naphthol), fluorene (2,3-hydroxyfluorene), phenanthrene (2,3-hydroxyphenanthrene, 1-hydroxyphenanthrene, 4-hydroxyphenanthrene), and pyrene (1-hydroxypyrene) were analyzed. The analyzed biomarkers related to oxidative damage were: 4-hydroxynonenal mercapturic acid (4-HNE-MA) reflecting lipid peroxidation [118], 8-oxo-2'-deoxyguanosine (8-oxodG) reflecting DNA oxidative damage [119], and 3-hydroxypropyl mercapturic acid (3-HPMA)

which is a metabolite of acrolein (both from exposure and endogenously formed) reflecting oxidative stress and acrolein related diseases [120].

Ethical considerations

The human exposure study presented in Paper 4 was approved by the Swedish Ethical Review Authority (registration no. 2019-03320). The biomonitoring (collection of urine samples) in Paper 3 was approved by the Regional Ethical Review Committee at Lund University (registration no. 2009-0568). Both studies were performed in accordance with the Declaration of Helsinki, including obtaining informed written consent from all subjects. Details of inclusion criteria are included in Papers 3 and 4.

For the human exposure paper 4 study, the aim was to investigate the physiological reactions in lung function during and immediately after the exposure. It was important to know beforehand that the proposed exposure concentration would not harm the study participants with unproportionally severe acute or long-term effects. The levels were designed to be below the current OELs of NO (30 mg m^{-3}) and NO_2 (2 mg m^{-3}), and below the future OELs of EC (50 µg m^{-3}). These levels are considered acceptable by Swedish legislation. Hence, the exposure was considered to add a negligible addition to the volunteer's cumulative dose of traffic exhaust. In addition, the used PM exposure levels were around a third of previous studies on diesel exhaust studies where up to 300 µg m^{-3} have been accepted. Previous diesel studies have also included people with underlying lung and cardiovascular diseases without any complications. The participants were informed that they were allowed to stop their participation in the study at any time.

For the biomonitoring in the Paper 3 study, no invasive measurements were performed, and no alterations of their exposures were performed. The participants in both studies consented to the storage of their anonymized samples in biobanks.

The participants' identity has not and will not be revealed at any stage of the research project. Data protection, privacy and confidentiality have been handled in accordance with EU legislation.

Results and Discussion

Exhaust emissions

Exhaust emissions depending on EGR and fuels

Regulated emissions and eBC

In the Paper 1 study, the exhaust gas recirculation (EGR) was varied to change the in-cylinder O_2 availability. This was done to investigate fundamental exhaust emission characteristics at different combustion settings for diesel, HVO and RME. The O_2 availability was varied stepwise from 9% to 21% intake O_2 (high to low EGR). This changed the combustion conditions fundamentally which had an immense impact on the eBC and NO_x concentrations for all the fuels (Fig. 9a). At no or low EGR, that is at high intake O_2, the NO_x emissions were high and the eBC emissions low (<4 mg kWh^{-1}) for all fuels. As we increased the EGR, the intake O_2 decreased, and the NO_x emissions decreased for all fuels while eBC increased. This is similar to previous studies on fossil diesel [47] and RME [48]. At around 15-17% intake O_2, NO_x and eBC emissions were both relatively low. As we increased the EGR further, the NO_x emissions were reduced to a minimum, while the eBC emissions significantly increased. This is known as the PM-NO_x trade-off due to the decrease in flame temperature caused by the EGR [121]. While the decreased temperature efficiently reduces the NO_x formation, the lowered temperature also decreases the soot oxidation (removal) rate during late cycle combustion leading to increased soot emissions [122,123]. At very high EGR levels (i.e., very low intake O_2, <approx.10%), we simulated low temperature combustion (LTC, Fig. 9a). During these conditions both eBC and NO_x were simultaneously reduced, but in this engine setup the combustion became less complete, with high HC and CO emissions as a result (shown in Paper 1). In addition, the highest fraction of organic aerosol (including PAHs) compared to eBC was found at a very high EGR.

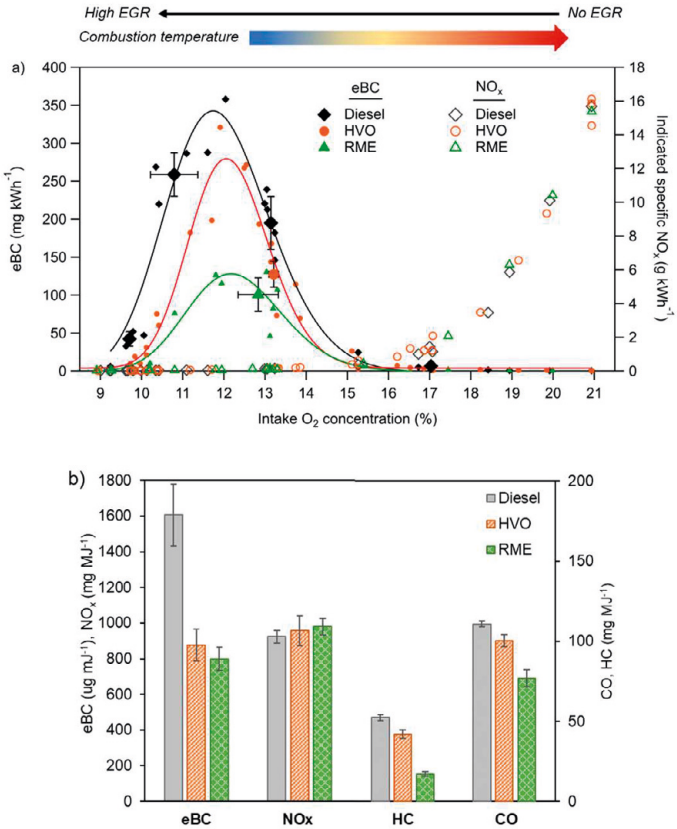

Figure 9. a) The eBC and NO_x emissions as a function of intake O_2 concentration (Paper 1). **b)** The exhaust emissions at 18% intake O_2 concentration of eBC, NO_x, CO and HC (Paper 2). The error bars in b) represent ±1 standard deviation (std. dev.) of repeated measurements (n=2-6).

Effect of fuel

Even though the eBC-NO_x trend is similar for all fuels, we found a considerable influence of the fuels on eBC emissions. In Paper 1, this was clearly seen at 11-14% intake O_2 (Fig. 9a) and further evaluated under longer samplings periods (hours) at 13% intake O_2. In comparison to diesel, the eBC emission (mg kWh^{-1}) was reduced by 30% and 54% for HVO and RME, respectively, at 13% intake O_2. In the Paper 2 study, the effects of the fuels were further evaluated at 18% intake O_2 (Fig. 9b). The eBC emissions (mg MJ^{-1}) were significantly reduced by 42% and 48% for HVO and RME compared to diesel, respectively (Fig. 9b). This was similar to the reductions at 13% intake O_2 in the Paper 1 study. Similar mass reductions for HVO and RME have been found in other studies, with combustion variables other than EGR [124,125]. In addition, multiple reviews have concluded that the use of biodiesel and renewable diesel in general reduces the soot and PM, based on many studies with different engines and engine operations [126–129]. This indicates that the use

of renewable diesel fuels in comparison to fossil diesel, has the potential to reduce eBC in most vehicles under normal operation.

No significant differences in NO_x emissions at low levels of EGR (>17% intake O_2) were observed for RME or HVO compared to diesel in either Paper 1 or 2. This is not in line with previous studies, for which RME generally causes an increase in NO_x emissions (up to around 20% [19,126,127]). For HVO, the potential NO_x reduction or increase has been found to vary and depends on the operation conditions such as load, etc. [128,130,131]. In general, the effect of fuel on eBC emissions is larger than on NO_x emissions.

In the Paper 2 study, RME reduced the HC and CO emissions on average by 67% and 31%, respectively, relative to diesel (Fig. 9b). HVO had a smaller effect but reduced the HC emissions by 20%, and the CO emissions by 9% compared to diesel.

The eBC (and consequently the PM) reductions of HVO and RME exhaust emissions compared to diesel are attributed to their different chemical compositions. The oxygen content of RME can increase combustion completeness, as it increases the oxygen entrainment in the premixing phase [5], thus decreasing the eBC, HC and CO (Fig. 9a-b and Paper 1). However, the trade-off is a higher combustion temperature and thus potentially increased NO_x emissions as seen in other studies [132]. The increased oxygen entrainment is also hypothesized to increase the oxidation rate during late cycle combustion [5]. HVO does not have an oxygen content (like diesel) but a more homogenous composition and lower boiling point compared to diesel which would improve the spray characteristics and mixture formation that reduce the soot formation [133]. On the other hand, HVO has a higher cetane number than diesel, which would decrease the premixing time, followed by increased soot emissions [134]. However, the ignition delay and premixing time were kept similar for all tested fuels, which excludes these parameters as causalities. Instead, similar to previous publications, we attribute the reduction in eBC to the lack of aromatic content, which acts as a soot precursor in HVO compared to diesel [131,135,136].

Non-regulated emissions

Particle samples were collected at 10%, 13% and 17% intake O_2 for diesel, and at 13% intake O_2 for HVO and RME for further analysis (Paper 1). At low temperature combustion (10% intake O_2), the diesel exhaust particles had a high mass fraction of particulate PAHs, refractory organic carbon, and non-refractory organic carbon, indicating immature soot (details in Paper 1). At 13% O_2, the exhaust particles were dominated by EC for all fuels. At 17% intake O_2, the diesel exhaust particles were dominated by non-refractory organic carbon (from the lubricating oil) but had low relative mass fractions of PAHs and refractory organic carbon (contrary to the low temperature combustion particles).

While the mass fraction of carbon composition and PAHs varied depending on combustion conditions, the normalized metal emissions per kWh were similar and independent of combustion conditions (details in Paper 1). However, as the mass emissions were the absolute lowest at 17% O_2, this sample became enriched with metals compared to the others and had the highest metal fraction per particle mass.

The estimated specific surface area (SSA) of the soot particles increased with increasing O_2 availability, from 152 to 191 $m^2\ g^{-1}$ for diesel at 10% to 17% intake O_2, respectively (Paper 1). Of the three fuels, RME had the largest SSA (222 $m^2\ g^{-1}$) and HVO the smallest (160 $m^2\ g^{-1}$). The surface area has been suggested to be the biologically most important dose metric for inhalation toxicity evaluation [7]. The surface areas in our study were in the lower range of different soot particles, (30-800 in [137]), but the difference may potentially be enough to evaluate if there was a surface area dose response.

Particle induced reactive oxygen species (ROS) formation

The ROS formation potential was found to strongly correlate (R^2=0.89) with the intake O_2% (determined by the amount of EGR), shown in Fig. 10a. This indicates that the in-cylinder O_2 availability (and followingly the flame temperature) is a fundamental combustion parameter that may affect the ROS formation potential of diesel soot particles. Metals, PAHs, organic content, and specific surface areas have been suggested as drivers of ROS, but we did not find any correlations with these parameters (Paper 1). However, the exhaust particles, especially the 13% and 17% intake O_2 samples, had a similarly strong ROS formation potential per surface area as a well-known ROS-generating carbon black material (Printex90 [138], Fig 10b, left axis).

It has been shown that combustion conditions affect the soot structure, and that a higher oxygen availability increases the maturity and the soot oxidation [37]. For diesel soot particles, we therefore hypothesize that the ROS generation is a function of increasing soot maturity and soot oxidation (represented by increasing intake O_2). In the first step, the ROS formation depends on the soot formation and the degree of maturity. In the second step, the soot oxidation (O_2 >13%) can further increase the ROS formation ability. During this step, primary soot particles, as well as agglomerated soot particles, shrink or are removed by complete oxidation. This phase will also change the soot surface and depending on the O_2 availability, create different oxygenated functional groups on the surface [139]. This has been found to increase both the particle bound ROS production (DTT assay [140]) and the cellular ROS production ($DCFH_2$-DA assay [141]).

At low temperature conditions (10% intake O_2), immature soot was formed that contained large fractions of refractory OC and non-refractory PAHs (Paper 1). This soot had by far the lowest ROS formation potential in-vitro, compared to the more mature soot generated at 13% and 17% intake O_2. The ROS production potential

was lower both per SSA (Fig. 10b) and per mass unit (Fig. 10a). However, in-vivo the immature soot yielded similar inflammatory response per surface area as the other soot samples (analyzed by Bendtsen et al. 2020 [97]), possibly driven by the OC and PAH components. Stoeger et al. describe a similar observation for soot with higher OC content. The particle-induced oxidative potential (based on the consumption of ascorbate) for diesel exhaust particles and soot with high organic fractions (≈20%) was lower than predicted by the surface area, compared to pure carbon black particles or flame soot with low organic fractions [142]. However, the high OC soot samples showed a higher inflammatory potential in-vivo, similar to the other soot samples and proportional to the BET surface area [142]. The authors suggest that the particle-related inflammatory reaction in-vivo due to ROS has two pathways: For pure soot samples, the ROS process is driven by surface reactivity during particle-cell interaction, while for samples with higher organic content (such as PAHs) these compounds initiate an enzymatic driven process resulting in oxidative stress. This emphasizes the importance of understanding both the impact of the soot formation processes on surface reactivity, and the chemical composition of PM for toxicological studies and risk assessments.

Considering the ROS potential normalized to per kWh (Fig. 10b), the 17% intake O_2 setting yielded the lowest exhaust ROS potential followed by the low temperature exhaust particles (10% intake O_2). However, the PAH concentration was the highest at the low temperature combustion. PAHs are known carcinogens and may therefore have other hazardous biological effects that are not distinguished by the particle-induced ROS formation (or inflammation).

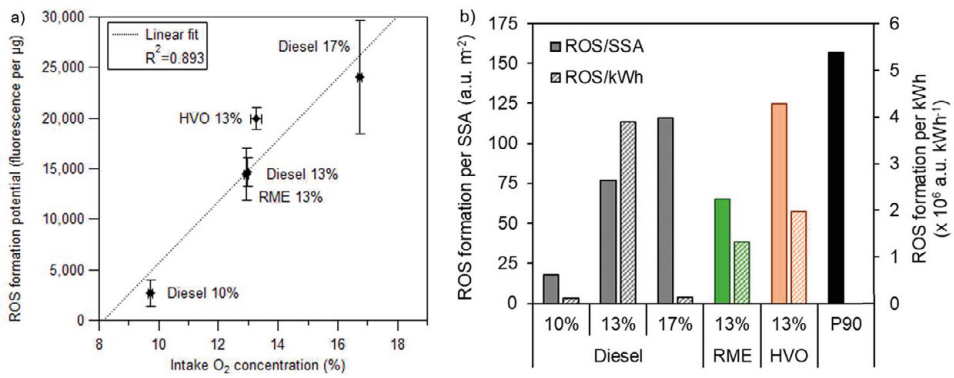

Figure 10. The ROS formation potential of the diesel fuel samples generated at 10, 13 and 17% intake O_2, and for HVO and RME generated at 13% intake O_2. **a)** The ROS formation potential (per µg) as a function of intake O_2 concentration. **b)** The ROS formation potential normalized to SSA and to per kWh, and in comparison to the high ROS generating carbon black material Printex90 (P90, per SSA). P90 was analyzed simultaneously as the exhaust particles samples with the same assay, and are hence directly comparable. The error bars in a) show the standard error of the mean for the ROS formation potential and ±1 std. dev. for the O_2 concentration.

ROS potential depending on fuel

The difference in ROS formation potential per particle mass (µg) was more dependent on combustion conditions than on the type of fuel used (Fig. 10a). However, when normalized to the specific surface area, HVO had a higher ROS formation potential per surface area (Fig. 10b, solid bars) compared to diesel and RME generated at the same combustion conditions (13% O_2). This was because the potential was higher per mass at the same time as the specific surface area was lower for HVO compared to diesel and RME. RME and diesel had similar ROS formation potentials per specific surface area.

Considering the ROS potential per kWh instead (Fig. 10b, dashed bars), the renewable fuels reduced the ROS potential by half at the same combustion conditions. This means that even though the exhaust particles from diesel and renewable diesel fuels share the same strong ROS forming capabilities in-vitro, the potential ROS forming output from the engine is lower for RME and HVO. This indicates that replacing fossil diesel with HVO or RME in engines without aftertreatment systems may reduce the oxidative stress and related health effects originating from the soot surface area.

Exhaust emissions depending on aftertreatment systems and fuels

Regulated emissions and equivalent black carbon (eBC)

In the Paper 2 study, the effects of a diesel oxidation catalyst (DOC) alone, and in combination with a diesel particulate filter (DPF) on the eBC emissions were evaluated for diesel, HVO and RME (Fig. 11a). The DOC (operated at 215±6 °C) did not remove any significant amount of eBC for any of the fuels (Fig. 11a) compared to engine-out emissions (no aftertreatment system). Instead, the DOC on average decreased the HC and CO emissions for diesel (Fig. 11b) by 73% and 80%, respectively. The decreases in HC and CO emissions were similar to the reductions that occurred by replacing diesel with RME without using the DOC (Fig. 9b). The DOC in combination with the DPF were efficient in removing eBC, with an average removal efficiency of 99.4±0.5% for all fuels compared to engine-out emissions. This corresponds to a high removal efficiency and is in line with previous studies that generally show a removal efficiency of over 95% [55].

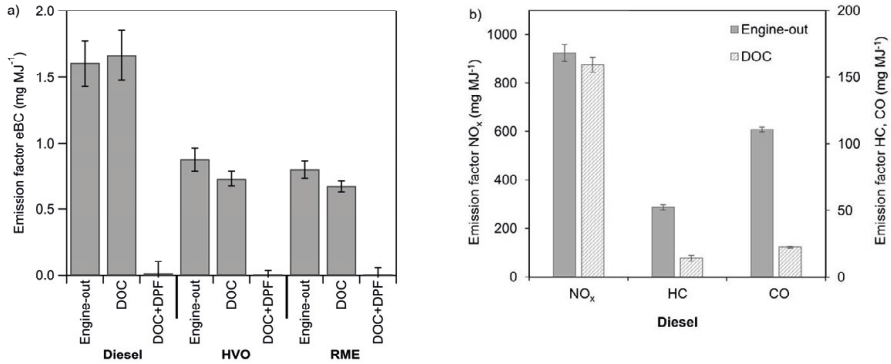

Figure 11. a) eBC emissions for diesel, HVO, and RME at different measurement points: engine-out (i.e., without aftertreatment), after the DOC, and after the DOC+DPF. The exhaust gas emissions of NO_x, HC and CO were measured engine-out and after the DOC for diesel and compared in **b)**. The engine was operated at constant low load (≈25%), at 18% intake O_2. The error bars in b) represent ±1 std. dev. of repeated measurements (n=2-6).

Particle size distributions

The particle number size distributions from the fuels at 18% intake O_2, engine-out, after the DOC, and after the DOC+DPF are shown in Fig. 12 (a-c) together with the particle emissions during motoring (i.e., when simulating engine braking with no combustion). Particle size distributions are clearly seen engine-out (Fig. 12a) and after the DOC (Fig. 12b), but not resolved over the PN background concentration after the DOC in combination with the DPF. This indicates that the DPF in addition to a high eBC removal efficiency (Fig. 11a), also had a high PN removal efficiency of both nucleation and soot mode particles.

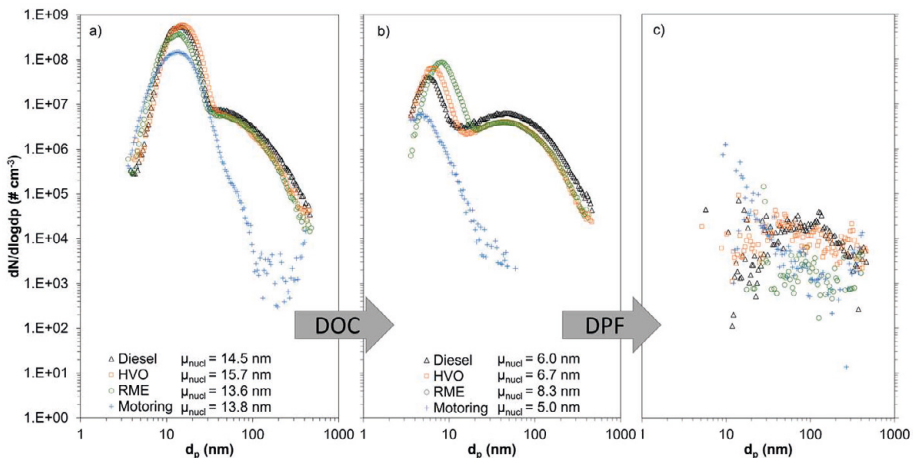

Figure 12. The particle number size distribution for the fuels: diesel, HVO and RME, and under motoring (no combustion). **a)** The engine-out emissions (before any aftertreatment), **b)** after the DOC, and **c)** after the DOC+DPF. The nucleation mode decreases in size and concentration after the DOC, while the soot mote is less affected. The DPF removes both modes effectively. The nucleation mode geometric diameter is denoted μ_{nucl}.

Engine-out and after the DOC, we observed a distinct nucleation mode that dominated the number concentration for all three fuels as well as during motoring. There is also a soot mode present during combustion, but not during motoring. The nucleation mode number concentration and geometric mean diameter (μ_{nucl}) are both strongly reduced after the DOC (Fig. 11b), as well as the mass concentration (shown in Paper 2). The DOC oxidizes organic compounds, which likely contribute to the reduced nucleation mode, as this is often comprised of semi-volatile particles, with or without a non-volatile core [31,143]. The soot mode was found to be less affected after the DOC, which is consistent with the eBC emissions seen in Fig. 11a.

The strong nucleation mode present during motoring indicates that there is a non-combustion particle source present (the particles which are partly removed by the DOC). The source most likely originates from the lubricating oil. This oil evaporates and can exit the combustion cylinder [144], and during cooling and dilution, the evaporated lubricant compounds will nucleate and condense on the existing particulate surfaces.

Secondary emissions

Estimations of the secondary emissions are of great importance in determining the total atmospheric impact of renewable fuels or aftertreatment systems. The potential secondary aerosol formations of diesel, HVO, and RME engine-out and after the DOC are shown in Fig. 13a-b. The aged (and fresh) mass emissions factors (mg MJ^{-1}) were estimated from mass weighted size distributions (PM1, shown in Paper 2). Compared to the respective primary emissions, the total aged engine-out PM1 mass emissions were about 5 times higher for diesel, 4 times higher for HVO, and 3 times higher for RME. After the DOC, the aged mass formation was significantly reduced for all fuels compared to engine-out, which is similar to previous results from studies on diesel exhaust with similar aftertreatment systems [70,145]. Compared to the primary emissions after the DOC, the total aged PM1 mass after the DOC increased less than a factor 2 for all fuels.

In the limited literature on secondary aerosol formation of HVO and RME, the lack of aromatic content has been hypothesized to be one reason for the decreased SOA formation [68]. In addition, the gas-phase HC concentration has been identified as a strong SOA indicator [70,146,147], and from vehicle exhaust, SOA is preferably formed from alkanes and aromatics compounds [148]. The HC emission factor was significantly lower compared to diesel for RME (67% reduction), and slightly reduced for HVO (20% reduction) (Fig. 9b). The DOC was found to reduce HC emissions by 73% for the diesel combustion (Fig. 11b). In Paper 2 (illustrated in Paper 2 Fig. S6a) we show that the HC emissions correlated with aged PM1 mass emissions (R=0.96), supporting the hypothesis that the reduced HC emissions likely explain the lower aged PM emissions. The reduced SOA emissions of RME and HVO compared to diesel may therefore potentially be understood as a combination of reduced HC emissions and the lack of aromatics in the fuel.

The lubricating oil has also been found to influence the secondary aerosol formation independent of the fuel in diesel engines [70,149,150]. The DOC was efficient at removing the nucleation mode mass (primary organic aerosol) and hence the lubricant-derived and organic components of the engine-out emissions. This could further have contributed to the reduced secondary PM emission factors (illustrated in Paper 2 Fig. S6b). However, the effect was most likely small in comparison to the fuel-induced effect of altered HC emissions.

It should be noted that the emission factors may be more biased (giving a higher total mass) after the DOC compared to engine-out. This is because the OFR background may have contributed to up to 60% of the total aged PM mass after the DOC (estimated from mass size distributions), but relatively less for engine out (20%) (Fig. 13).

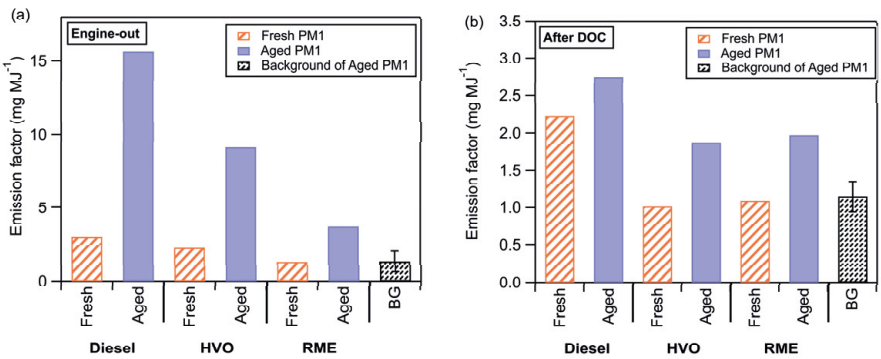

Figure 13. The mass emission factors of fresh and aged PM: **a)** engine-out, and **b)** after the DOC. The mass was estimated from the mass weighted size distributions (PM1) measured by the SMPS + APM. The total mass of aged PM1 represents the upper limit of the possible aged mass estimated from the aged mass size distribution because the background PM1 formed from impurities may contribute. The mean background contribution of PM1 is shown as a separate bar with error bars of ±1 std. dev. For engine-out, the maximum background of aged mass was 20%, and after the DOC the maximum background contribution was 60%.

Exhaust emissions from in-use vehicles

Exhaust emissions from non-road vehicles

For the chamber exposure study in Paper 4, two modern (2019) non-road vehicles with different emission legislation were chosen to generate the two different HVO exposures. Vehicle 1 was a smaller wheel loader complying with Stage IIIA emission legislation, and vehicle 2 was a larger wheel loader complying with Stage V emission legislation. Vehicle 1 did not have any external aftertreatment systems and emitted both PM and NO_x (hereafter denoted as HVO_{PM+NOx}). Vehicle 2 had an aftertreatment system composed of a DOC and a DPF (no more details disclosed by the manufacturer), but no specific NO_x removal unit (hereafter denoted as HVO_{NOx}). The particle number size distribution in the chamber during the two HVO exposures,

and the filtered air exposure for comparison, are shown in Fig. 14a. A clear soot mode, GMD 71 nm (GSD: 1.64, PN: 3.0±0.3 × 10^5 particles cm^{-3}), is resolved for the HVO_{PM+NOx} exposures. Similar soot modes GMDs have also been reported for other small non-road vehicles without aftertreatment systems (46-48 kW, GMD:45-70 nm, [151,152]). A particle number size distribution could be resolved during the HVO_{NOx} and filtered air exposure, however, the number concentration was <100 particles cm^{-3} and the exposures were both considered "particle free". The HVO_{NOx} exposure yielded a 330 times lower particle number exposure compared to HVO_{PM+NOx} which highlights the reduced potential exposure from vehicles with DPFs.

No nucleation mode was resolved in any of the exposures. The dilution system was not optimized for simulating a potential nucleation mode (long residence time, long sampling lines, no rapid cooling, etc.). This may have eliminated a potential nucleation mode due to coagulation. Even though the nucleation mode may be of health relevance, these particles are not conveyed in vehicle emission standards, as only solid PN >23 nm are included in the PN standards (in EU Stage V engines from 2019). No occupational exposure limit of particle number exists.

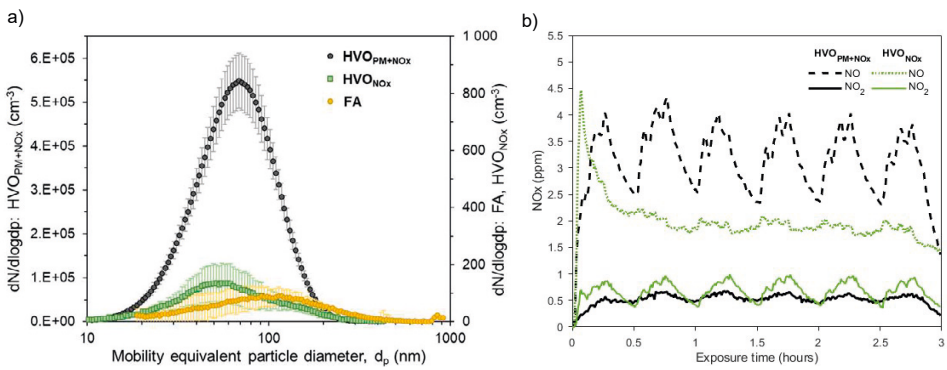

Figure 14. a) The average particle number size distributions (note the different scale on the y-axes), and **b)** the NO and NO_2 concentrations in the chamber during the exposure scenarios. The error bars in a) represent ±1 std. dev. of the repeated exposure scenarios (n=5-6).

Both vehicles emitted NO and NO_2, and the following exposure concentrations during the duration of the exposures are shown in Fig. 14b. Both vehicles were operated by switching from idle to load every 15 minutes in order to simulate a more realistic real-world operation than just staying in the idle mode, as well as to generate similar NO_x exposures. During load, the buckets were lifted to their upper position and gas was applied to keep an rpm of around 1800. During idle, the engine was kept idling at around 800 rpm. The events were seen as increasing NO emissions for HVO_{PM+NOx} during load and as decreasing NO emission during idle. A similar pattern was seen for NO_2 instead during the HVO_{NOx} exposure. In addition

during the cold start, the NO was seen to rapidly increase before decreasing to a steady state level for HVO_{NOx}, probably as an effect of the warm-up period of the DOC. NO_x is known to increase during cold-start [153], and our result indicates that this is mainly from an increase in NO emissions. A DOC partially oxidizes NO to NO_2, and some DPFs use NO_2 in the oxidation of the soot particles [154].

Particle size distributions

The particle number size distribution during the HVO_{PM+NOx} exposure (Paper 4) is compared to real-world particle size distributions measured in the mine (Paper 3) in Fig. 15. The particle size distributions in the mine were measured underground in drifts where the production loading takes place, and at the underground roadside where all types of vehicles but mainly light-duty vehicles passed by. A clear nucleation mode was detected in the drifts in the mine, but not as clearly at the roadside, and not at all during the generated HVO_{PM+NOx} exposure (Paper 4). At the underground roadside, the larger soot mode particles dominated the number concentration (nucleation mode <10% of total concentration). In the drifts, the nucleation mode particles instead contributed to around 40-55% of the total number concentration (PM1). Pirjola et al. found that the nucleation mode particle emissions from a non-road engine (Stage IIIB) were around one order of magnitude higher in real-world conditions compared to when measured in the laboratory [155]. The nucleation mode particles formed when the vehicle accelerated uphill and during engine braking from driving downhill [155]. Similar acceleration, and deceleration might have been present in the drifts as the loaders drive back and forth with the iron ore, however the drift had no considerable elevation shift.

The soot modes at the different locations in the mine had larger GMDs than the exposure in Paper 4 (HVO_{PM+NOx}). The vehicle in Paper 4 had a smaller engine (23 kW) and was operated under low load, while the loaders in the mine were much larger (300kW) and likely operated at high loads. The soot particle size generally increase with increasing load [156,157]. For example, Bugarski et al. found that an increase from 50% to 100% load at intermediate speed yielded an increase in GMD from 50 nm to 95 nm for a smaller diesel loader (48 kW) [152]. In addition, the difference in soot mode GMD between the laboratory exposure study (Paper 4) and the real-world particle size distributions in the underground mine (Paper 3) may also be affected by the fuel, as HVO for example yielded a smaller GMD than diesel in the laboratory study in Paper 1.

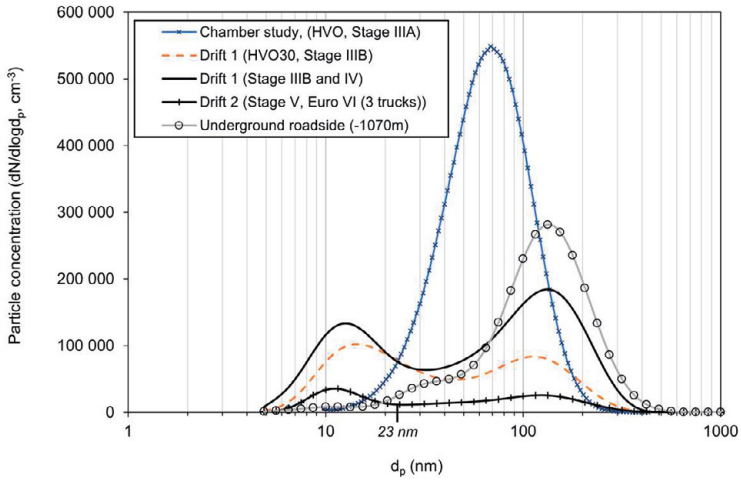

Figure 15. Particle number size distributions of diesel and HVO30 exhaust in the mine compared to the pure HVO chamber exposure in Paper 4 (HVO_{PM+NOx}). The particle size distributions in the mine were measured in the underground ambient air in the same area as the vehicles were operated. The fuel used in the vehicles was diesel if not otherwise stated.

In the Paper 4 study, a second vehicle with a DOC+DPF was used to generate the particle-free exposure scenario (HVO_{NOx}). From this, a particle size distribution was just barely resolved (PN<100 particles cm^{-3}, Fig. 14a) while a particle size distribution was not resolved over the background concentrations after the DOC+DPF tested in Paper 2 (Fig. 12c). In contrast, in the area of the mine where only vehicles with DOC and DPFs were used full-time (drift 2, Fig. 15), both a nucleation mode and soot mode were resolved even though the total concentration was around 3-6 times lower here than in drift 1 where older vehicles without DOC+DPFs were used. This indicates that the actual removal efficiency of the DPFs might be smaller than measured in lab studies. However, this particle size distribution might also be influenced by other sources that are not present in the lab studies (Papers 2 and 4), such as non-exhaust vehicle emissions caused by road wear or wear of tires and brakes. In addition, some other heavy equipment may have been in operation during shorter times in the same area (road gravels, etc.) with unknown emission classification.

In addition, the size distribution may have been influenced by the degree of dilution. In general, the soot mode GMDs were larger in the mine compared to the lab studies, which indicates that there may be a difference depending on the type of vehicle, but also that the conditions in the mine might cause more agglomeration than under normal ambient dilutions. However, as the concentrations were fairly low in the mine (30,000-180,000 particles cm^{-3}), agglomeration will have a negligible effect (rule of thumb is below 10^6 particles cm^{-3} in occupational settings [158]). The

dilution systems for the exposure study in Paper 4 or particle characterization in Paper 1 were not optimized to preserve the nucleation mode, which makes absolute comparisons of the studies limited. From the occupational study in the mine (Paper 3), we see a clear contribution of both modes, and studies of the nucleation and soot mode are both important.

Real-world emission factors in the mine and EU vehicle emission standards

The real-world emission factors (per estimated kWh) from the vehicle fleet in each location in the mine are shown in comparison to EU emission standards (i.e., legislated limits) in Fig. 16a-c. The emission factors of soot mode PN and EC are higher in drift 1 than in drift 2. PN emission is not regulated for the Stage IIIB and IV loaders used in drift 1, and followingly the vehicles did not have any DPFs. In drift 2, where a Stage V loader and Euro VI diesel trucks with DPFs were used, the PN emission factor was noticeably higher than the EU regulations (Fig. 16a). However, the EC emission factor in the same drift was lower than the PM regulation (even though PM and EC are not entirely comparable, Fig.16b). This potentially indicates that the vehicles with DPFs are more efficient in removing particulate mass than particle number. However, the PN concentration can also originate from non-exhaust vehicle sources. The total dust concentration in drift 2 was almost 3 times higher than in drift 1. Even if this mass mainly originated from PM>1, the soot mode PN in drift 2 could be influenced from dust or wear sources. Similarly, part of the EC concentration might have originated from wear of the tires, even if the majority of the wear would generate PM>1. In the emission test facility above ground, the EC emission factor was similar to that of drift 2, but the soot mode PN emission factor was significantly higher. The light-duty and heavy-duty vehicles tested in the emission test facility mainly followed the later emission legislation (Euro 5-6) and should have DPFs.

The NO_x emission factors in both drifts were similar, but slightly lower in drift 2 (Fig. 16c). Noticeably, the NO_x emission factor in the emission test facility was much higher, with a high variability during the day. Compared to the EC emissions that were lower than the corresponding emission standards, the real-world NO_x emission factor in the emission test facility was higher than the EU emission standards. In the emission test facility above ground, light-duty vehicles and heavy-duty trucks (mostly Euro 5-6 and Euro VI, respectively) were tested in idle mode one at a time. The idling can reduce the aftertreatment system temperature which may cause the NO_x reduction units (SCR) to operate with lower removal efficiency [159].

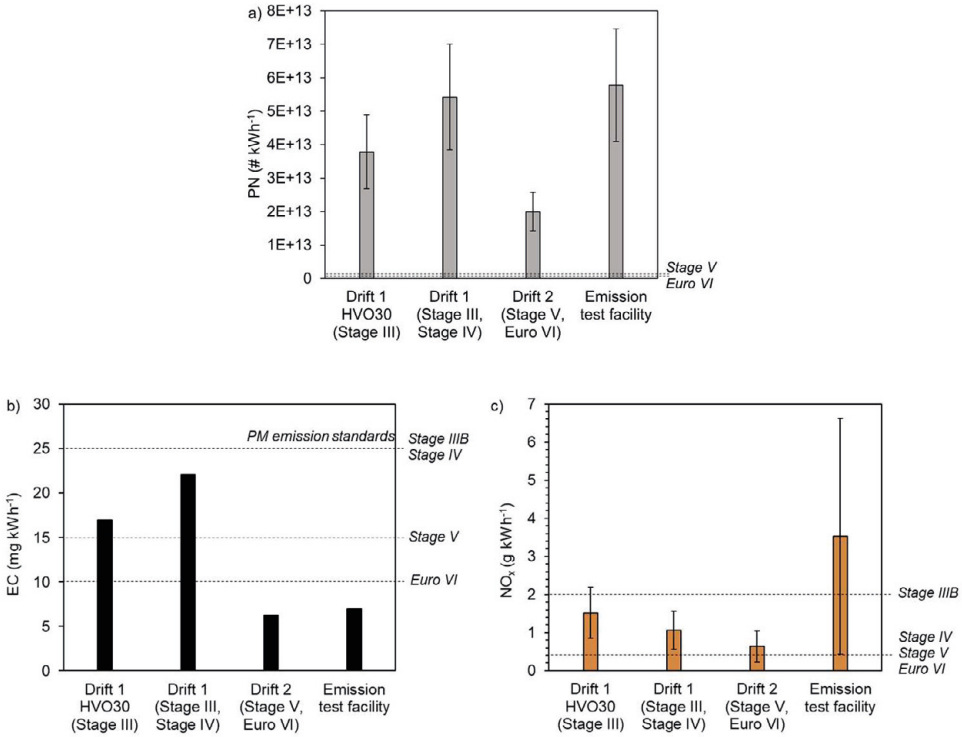

Figure 16. Average real-world emission factors (per kWh) in the drifts and at the emission test facility of **a)** PN (measured as the soot mode concentration, which approximates the solid fraction of PN>23nm), **b)** EC, and **c)** NO_x. The error bars represent ±1 std. dev. of the variation throughout the measurement day (not available for EC). The dashed lines represent the EU vehicle emission standards of the respective compounds, which are the legislated values using steady-state and transient test cycles (Stage IIIB-V) and steady state test cycles (Euro VI). In b) the emission standards for PM are shown as there are no standards for EC, but EC is generally the major fraction of the PM mass. The real-world emission factors are calculated by a number of assumptions. We assume that: 1) all background-corrected aerosols originate from the vehicle combustion, 2) all background adjusted CO_2 originates from complete combustion in the vehicles, and 3) the values are converted from mg kg $fuel^{-1}$ to per kWh by using the standard energy content of diesel and an average energy conversion efficiency of 35%.

In comparison with on-road emission factors of heavy-duty vehicles in an urban area [160], the PN emission factors in the mine were around 100-200 times lower (number and units compared in Paper 3). However, the emission factors in drift 1 (Stage IIIB & IV vehicles, Fig. 16) were very similar to on-road emission factors of a Stage IIIB non-road vehicle (tractor, 99kW, [155]). The NO_x emission in drift 1 was around 1.1±0.5 g kWh^{-1} compared to 2.03±0.24 g kWh^{-1} for the tractor. The soot mode PN emission factor in the mine was 5.4±1.6 × 10^{13} particles kWh^{-1}, comparable to the nonvolatile PN emission factor for the tractor of 7.48±1.44 × 10^{13} particles kWh^{-1} [155]. This indicate that our emission factor estimations may yield a realistic approximation even though it is based on several assumptions. Firstly, all background-corrected aerosols are assumed to originate from the combustion. The background-corrected CO_2 is assumed to originate from complete combustion in the

engines to calculate emissions per kg fuel. In order to convert the emission factors from per kg fuel to per kWh, the energy conversion efficiency is assumed to be 35% for all the vehicles. The legislation compliance tests are performed with standardized test cycles (in the test laboratory, but also on-road in later legislation), and the emissions may therefore vary when the vehicle is used under real-world conditions compared to the emission standards. In addition, the PM and PN legislation are measured with different methods than were used in this study. We approximated the soot mode concentration in the ambient air as the solid PN, while in the legislation, the exhaust is sampled from the exhaust pipe, diluted and led through a heated evaporator (300-400 °C) that removes the volatile PM [161]. For the legislation, the cut-off is 23 nm, but as less than 5% of the soot mode concentration came from sub-23 nm particles in Paper 3, this error is minor.

Occupational exposure and health effects

Occupational exposure

Underground occupational exposure to EC and NO_2

The personal breathing zone EC exposure of the investigated workers in the mine ranged from <0.5 to 94 µg m^{-3}, with a GM of 7 µg m^{-3} (GSD 3.7). The NO_2 exposure correlated well with the EC exposure (R=0.66, p=0.002, Fig. 17a), and ranged from 60 to 1200 µg m^{-3}, with GM: 152 µg m^{-3} (GSD 2.2). Even though no strong conclusions can be drawn from the personal exposure depending on the emission standard of the individual miner's vehicle due to the low number of miners in each group, we saw trends that a higher degree of emission control technology reduced the EC exposure (Paper 1). For example, the operator of the loader following Stage V emission standards had the lowest EC and NO_2 exposures, while the operator of a Stage IIIB loader had the second highest exposure. A miner working in the tunnels with service operations had the highest EC and NO_2 exposures (94 µg EC m^{-3} and 1200 µg NO_2 m^{-3}).

The ratios between the personal exposures and the ambient concentrations of EC and NO_2 measured in the near vicinity were close to 1. This indicates that the stationary area monitoring gave a good estimation of the exposures. Compared to an earlier study from 2006 in a Swedish iron mine, the average EC exposure has decreased by 74% (GM: 27 vs. 7 µg m^{-3}), and the NO_2 exposure by 46% (GM: 280 vs. 152 µg m^{-3}) [162]. This is likely an effect of the improved emission aftertreatment systems, as the vehicles used in the mine were from 2012 or newer. However, the highest exposed miner (id. 3) in the underground tunnels was exposed to levels exceeding the measured range in the previous study. The miner's exposure

was twice as high as the underground ambient concentration measured at a busy roadside in another part of the tunnel system. This indicates that a large source is likely from the miner's vehicle which was idling during maintenance operations, even though it should be following a newer emission standard (light-duty vehicles, Euro 6).

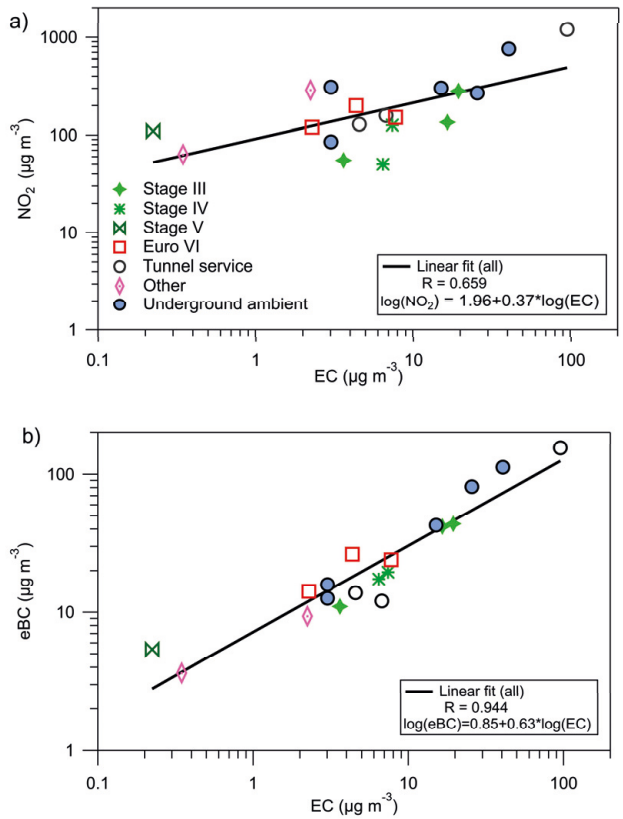

Figure 17. The daily average personal exposure (breathing zones) and ambient background concentrations of **a)** NO_2 and **b)** of eBC, vs. EC. The measurements in personal breathing zones are divided into several subgroups denoting the emission standard regulation of the mining vehicle the workers operated in the drift (Stage III, IV, V or Euro VI). The "Tunnel service" group worked with tunnel maintenance and drove light-duty vehicles (Euro 5-6). The data were log transformed, and the lines show the linear regression model. The correlation was statistically significant for NO_2 ($R=0.659$, $p=0.002$) and for eBC ($R=0.944$, $p<0.001$). NO_2 was measured with a passive sampling technique. EC was measured with an offline filter-based method, and eBC with 1 second (underground ambient zones, AE33) or 30 seconds resolution (breathing zones, AE51).

Compared to recent studies of Canadian underground mines, the average EC exposure in the Swedish mine was significantly lower (7 µg EC m^{-3} compared to 67-110 µg EC m^{-3} [163,164]). However, the Canadian studies also found a difference between operators of different types of vehicles, but detailed information on the

vehicles (e.g., age, emission abatement techniques) was not disclosed. In addition, as no emission factors were presented (such as those presented in Paper 3 and Fig. 16), it is not possible to conclude if the elevated exposure in the Canadian mines was due to poorer ventilation, air volume in the mine, or to older, more high-emitting vehicles.

Evaluation of occupational monitoring measures of eBC versus EC

In the Paper 3 study, parallel eBC and EC measurements were performed both in the breathing zone (AE51) and in a stationary measurement zone (AE33). EC and eBC showed a strong positive correlation ($R=0.94$ $p<0.001$) (Fig. 17b). However, the eBC concentration was consistently higher than EC, similar to the results of the intercomparison (Table 4). The average ratio (GM) of eBC/EC was 3.0 (low EC exposed miners were excluded). The AE33 had a higher offset compared to EC (GM: 3.5) than AE51 (GM: 2.9).

The eBC/EC offset of AE33 during the laboratory intercomparison was 2.75 (Table 4) and was also similar in Paper 2 (2.8±0.6), and in semi-urban areas according to literature: 2.7-3.3 [114]. The eBC_{AE51}/EC factor during the laboratory intercomparison was 2.0±0.2, which was slightly lower than in the mine (GM: 2.9). Similar offsets between eBC_{AE51} and EC have been reported in previous studies of waste workers (1.99 [115]) and toll both workers (2.2 [165]). The discrepancy between the eBC and EC is most likely due to the particles' varying light absorption and scattering efficiency, which is dependent on chemical composition (organic carbon, brown carbon) and structure (size, intermixing state, degree of graphitization) [166,167].

The comparisons show that using real-time monitoring of eBC is a good proxy for EC, which is useful in occupational assessments for identifying work tasks or areas with elevated risks of EC exposure, for example. However, eBCs from AE51 or AE33 generally show a factor 2-3 higher values than EC.

Underground occupational exposure to PAHs

The miners' personal exposure to airborne PAHs (sum of 16 EPA PAHs, measured by a passive sampler) in the Paper 3 study ranged from around 500 to 6000 ng m^{-3}, with a GM of 1660 (GSD: 1.9, Table 5). Urinary PAH metabolites were also analyzed in 27 miners. Samples were only collected after the work shift. Therefore, the levels can only be discussed compared to other studies and to the general population, but not in relation to the study subjects' pre-exposure baselines. The urinary metabolite concentrations of phenanthrene and pyrene were a factor 1.6 and 3.5, respectively, higher compared to the general levels found in the non-occupationally exposed Swedish population (healthy teenagers [168]). This indicates that the miners have an occupational exposure to PAHs. However, for the 10 miners for whom we monitored the airborne PAH exposure on the same day as

the urine samples were collected, no correlation was found between PAH metabolites and airborne exposure of PAHs (or airborne exposure of EC or NO_2). The discrepancy may be due to the limited number of subjects studied, the additional dermal uptake [169], or the non-occupational activities. However, previous publications have indicated that the correlation between airborne PAHs and metabolites is low or lacking in low-exposure scenarios (as in the range of this study) [170,171]. Correlations between airborne PAHs and metabolites have instead been found for higher exposures (around 10 times higher metabolite concentrations), such as in asphalt workers [172].

The ratio between personal exposure to airborne PAHs and ambient concentrations in the near vicinity was significantly higher than 1 (Paper 3). This indicates that the ambient measurements of PAH were not a good approximation of the PAH exposure (contrary to what was found for EC and NO_2). Additionally, the PAHs were neither correlated with EC nor NO_2, nor were they lower in areas with, or for workers in, vehicles with more advanced aftertreatment systems (Paper 3).

The higher PAH exposure may originate from secondary sources. The majority of the measured PAHs were small and in the gas phase (around 60% were naphthalene). The gas-phase PAHs condense and accumulate onto surfaces in the mines and vehicles (walls, cabin filter, clothes, etc.) and reevaporate causing secondary emissions of the smaller PAHs (3-4 rings PAHs) [173]. In addition, the miners' average PAH exposures were at least 2 times higher than during the HVO_{PM+NOx} exposure scenario in Paper 4 despite the much lower EC exposure (6 vs. 54 µg m^{-3}, Table 5). The difference may be due to the buildup of PAHs on surfaces over a longer time in the mine compared to in the chamber.

Comparison of occupational exposure, chamber exposure study and OELs

The average occupational exposures to NO_2 and EC in the underground mine (Paper 3) and the exposure concentrations during the HVO exposure study (Paper 4) are compared to the Swedish OELs in Table 5.

Compared to the chamber exposure study (Paper 4), the average occupational exposure (Paper 3) was lower for both EC and NO_2. However, if the exposure scenario (3-hours) concentrations were normalized to a full working shift (8-hours), the exposure concentrations would be closer to the occupational exposures (Table 5). For HVO_{PM+NOx}, the 8-hours normalized concentration was ≈20 µg m^{-3} for EC, and ≈400 µg m^{-3} for NO_2. For HVO_{NOx}, the 8-hour normalized NO_2 concentration was ≈492 µg m^{-3}. These levels are close to the Tunnel service workers' average exposure, and to the highest exposed individuals (Tunnel service, Table 5, and some Stage IIIB and Stage IV operators in Paper 3). This indicates that the exposure scenarios may represent one-day exposures for workers in the mine that are

unsatisfactorily close (i.e., a third of the OEL or higher [174]) to the future Swedish OELs of EC and NO_2 underground. It should be noted that the loader and truck operators in the mine spend most of their time inside vehicle cabins, which according to the company had particle and gas filters with up to 97% efficiency for PM (>0.1 µm) and 75% for gases (such as NO_x, CO, ammonia, etc.). However, the ambient concentrations of NO_2 in the drifts were similar to the average personal exposure concentrations in the same drifts, which indicates that the real-world filtration efficiencies are lower or that there is additional infiltration in the vehicle cabins.

Table 5. The average personal exposure (geometric mean) in the mine and the average exposure concentration in the chamber study (arithmetic mean of all exposure, n=5-6) of EC, NO_2, PAHs. The exposure concentrations in the chamber study are also presented as 8-hour normalized concentrations. The Swedish current and future 8h OELs of EC and NO_2 are included. The chamber exposure concentrations have been normalized to the 8-hour related exposure level (exposure concentration*3 hour/8 hours). NO_2 and PAHs were measured with a passive sampler in the mine (Paper 3), but with active sampling (PAHs) and a direct reading instrument (NO_2) in Paper 4. The PAHs were dominated by gas-phase PAHs in both studies.

	Work group/exposure scenario	Emission source			Average exposure concentrations		
		Type of vehicle(s)	Emission standard	Fuel	EC (µg/m³)	NO_2 (µg/m³)	PAHs (ng/m³)
Paper 3	All underground personnel			Diesel	7 [3.7]	152 [2.2]	1660 [1.9]
	Tunnel service (n=3)	Light-/heavy-duty vehicles	Euro 5-6	Diesel	15	292	2920
	Production loading (n=5)	Loaders	Stage IIIB & IV (300 kW)	Diesel	11	110	1700
	Production loading (n=4)	Loader and trucks (3)	Stage V & Euro VI	Diesel	4	141	1320
Paper 4	HVO_{PM+Nox}	Wheel loader	Stage IIIA (23 kW)	HVO	54 ± 6	1068 ± 75	68 ± 22
			8-hour normalized concentration		20	400	26
	HVO_{NOx}	Wheel loader	Stage V (55.4 kW)	HVO	<1	1312 ± 75	794 ± 60
			8-hour normalized concentration		<1	492	298
Swedish OELs	Above ground	-	-	-	50 from 2023	960	-
	Underground and tunnel work	-	-	-	50 from 2026	2000/ 960 from 2023	-

Relation to OELs and health effects

The underground workers average EC exposure (GM: 7 μg m^{-3}) was below the future Swedish and EU OELs (Table 5). Compared to the newly implemented OEL of EC in Denmark and the Netherlands (2020-2021, 10 μg m^{-3}), 5 out of 12 workers in the Paper 3 study were exposed to higher concentrations, and all but one exceeding one third (>3 μg EC m^{-3}) of this more stringent OEL. One third of the OELs is generally considered as the precautionary level during occasional monitoring, limiting the risk for exposure above the OEL [174]. Furthermore, all workers except two were exposed to EC levels well above 1 μg m^{-3} (Paper 3), which poses a substantial excess lifetime risk of lung cancer for exposures during a full working life [15,16].

Excess lifetime risk of lung cancer from EC exposure

Recent epidemiological estimates of the mortality risk of lung cancer from a working life (45 years) exposure show an increasing risk with increasing EC exposure [15,16]. Both the Dutch Expert Committee on Occupational Safety (DECOS) and the Danish National Research Centre for the Working Environment (NFA) have calculated health-based occupational cancer risk values for diesel exposure [175]. DECOS concluded in 2019 that the health-based occupational exposure limit (8-hour average, 40 years) of EC should be 0.011 μg m^{-3} in order to reach their target risk level of 4 excess deaths in lung cancer per 100,000 workers. In order to not exceed their prohibition risk level of 4 excess lung cancer deaths per 1,000 workers, the OELs should be limited to 1.03 μg m^{-3} [176]. NFA also recommended to base the OELs on the epidemiological data. For the Danish population they proposed an OEL of 0.45 μg m^{-3} for a 1/1000 risk, and 0.0045 μg m^{-3} for a 1/100,000 risk. These calculations were based on the meta-analysis of three large epidemiological studies and occupational exposure data [16]. Following the same method and including a more recent publication of 14 pooled case-control studies (EC exposure quantified from job-exposure matrix, [15]), I estimated occupational cancer risk values for Swedish workers. The exposure at different relative risk (RR) levels is derived by the following equation from [16]:

$$\ln RR = \text{intercept} + \text{dose response slope} * \text{exposure} \qquad (6)$$

where the intercept is set at zero, the slope is 0.000982 [16] or 0.000034 [15], and the exposure is the cumulative exposure concentration of EC after 45 years of exposure (DECOS used 40 years of exposure). The relative risk (RR) is calculated from the lung cancer incidence risk for the non-exposed population, which in Sweden is 2.3% in males [177]. The average of the two studies (average of the dose-response slope) is also given in Table 6 as the studies are not directly comparable (the occupational exposures were quantified differently).

Based on this estimation, the Swedish health-based exposure limit becomes 1.4 µg EC m^{-3} to limit the risk to 1/1000, and 0.15 µg EC m^{-3} to decrease the risk to 1/10,000.

Following the same estimations the excess lifetime risk for lung cancer at the future OEL for EC (50 µg m^{-3}, 45 years) for the Swedish population varies from 26 based on [15] to 187 based on [16] per 1000 workers. However, the uncertainty at such high exposure levels is high in the epidemiological models [16,176]. An occupational exposure of 7 µg m^{-3} as the miners in Paper 3 had, would with the same estimations (45 years exposure), yield between 2.6 and 8.3 excess lung cancer incidences per 1000 workers, based on [15] and [16] respectively.

These estimates indicate that the health-based limit should be limited to 1 µg m^{-3} rather than 50 µg m^{-3}, and that the workers in the mine still are at considerable risk of lung cancer because of their exposure.

Table 6. Estimated EC exposure concentrations corresponding to different excess lifetime risk levels for lung cancer for the Swedish population. The exposure concentrations are estimated from the meta-analysis of epidemiological studies in Vermeulen et al. [16] and from pooled case-control studies in Ge et al. [15].

Ecxess lifetime risk estimates for lung cancer (EC)	Based on Vermeulen et al.	Based on Ge et al.	Average
1/100	8.2 µg m^{-3}	23.6 µg m^{-3}	12.1 µg m^{-3}
1/1000	0.96 µg m^{-3}	2.78 µg m^{-3}	1.43 µg m^{-3}
1/10,000	0.10 µg m^{-3}	0.28 µg m^{-3}	0.15 µg m^{-3}
1/100,000	0.01 µg m^{-3}	0.03 µg m^{-3}	0.01 µg m^{-3}

The epidemiological models may have a high uncertainty and several limitations, however, they have been evaluated and endorsed by several occupational exposure expert groups [175]. Even if the estimated risk values would be the worst-case estimates, they are still far higher than what is generally accepted for occupational exposure to carcinogens.

Genotoxicity/mutagenicity

Long-term risk of excess death or cancer is not possible to assess from a 3-hour long exposure during 1 day (as performed in Paper 4), where only the effects of short-term exposure are potentially measurable. Acute genotoxicity was assessed after the HVO exposures presented in Paper 4 in a separate publication by Scholten et al. [178]. They did so by measuring biomarkers of DNA damage after the exposures but did not find any indications of increased biomarkers related to genotoxicity. Nor was there any evidence of oxidative DNA damage in urine (by 8-oxodG biomarker) found in the miners (Paper 3) or after the HVO exposures in Paper 4 [117]. Combustion particle exposure is consistently associated with oxidatively damaged DNA [119]; however, the exposure levels and times in the Paper 3 and 4 studies might have yielded a dose which is too low to have biologically measurable effects. The risk assessment based on epidemiological studies, however, suggest that there is an excess lung cancer risk even from lower exposures. In addition, mutagenicity

or cancer from diesel exhaust is considered to occur by a non-threshold mechanism, which means that there is no safe concentration limit [175].

Implications of oxidative stress

Urinary biomarkers for acute phase oxidative stress were analyzed in Paper 3. Similar analyses were performed after the HVO exposure in Paper 4 in a separate publication by Krais et. al. [117]. The oxidative stress was assessed by measuring a biomarker for lipid peroxidation. ROS oxidize fatty acids, which increases 4-HNE-MA as it is a by-product of lipid peroxidation. The HVO chamber exposure (Paper 4) yielded increased lipid peroxidation after the HVO_{PM+NOx} exposure ($p<0.001$), but not after the HVO_{NOx} exposure [117]. This indicates that there might be some particle effect on the lipid peroxidation after exposure correlating to levels below the future EC OEL (3 h, 54±6 μg m^{-3}). Similarly, urinary 4-HNE-MA was analyzed in 27 miners after their work shift in the Paper 3 study. Similar levels, as those after the HVO_{PM+NOx} exposure in Paper 4 [117], were found in the miners (Paper 3). No correlation between the PAH exposure and lipid peroxidation was found for the miners in Paper 4, nor after diesel or HVO exposure in the separate publication by Krais et al. [117]. In addition in Paper 1, we found that acellular ROS production was not correlated with PAHs, organic carbon content, or metal (but in-vivo inflammation correlated with OC and PAHs [97]). This indicates that the solid soot fraction from fresh exhaust emissions plays an important role in causing oxidative stress.

ROS may also cause DNA damage, which at least in the Paper 4 exposure study [178] and in the miners in the Paper 3 study was not possible to detect (measured as 8-oxodG). However, in Paper 1 we found that the acellular ROS production increased with increasing combustion temperature. The same particles were used for a mice instillation study at NFA by Bendtsen et al. [97]. They found that the ROS formation potential of our exhaust samples correlated with in-vivo genotoxicity in lung and liver tissue 28 and 90 days after instillation, respectively [97]. In addition, the HVO and diesel samples generated a dose-dependent inflammation and acute phase response (measured as neutrophil influx), but the response from RME exposure was limited. The acute inflammation response correlated with the surface area and EC, but the organic compounds and PAH fraction also had a major impact. The toxicity in relation to the combustion conditions and specific particle-induced mechanisms are hence of interest to investigate in future studies.

Respiratory effects

The acute effect on the respiratory system was assessed in the Paper 4 study, but no clinically significant change was indicated in any of the pulmonary function tests (spirometry, peak expiratory flow, forced oscillation technique). Instead, a decrement in nasal patency was found during the exposure to HVO_{NOx}

(-18.1, 95%CI: -27.3 to -8.8 L min-1, p<0.001), and for the HVO_{PM+NOx} (-7.4 (-15.6 to 0.8) L min-1, p=0.08). As the effects were more evident for the particle-free exposure (HVO_{NOx}), we attributed the effect mainly to the NO and NO_2 exposure. However, the uptake of NO and NO_2 generally occur in the distal areas in the lung and there are no studies of the effect of these gases on the nasal patency. NO_2 may cause asthma-related effects (reviewed in [179]), while NO has a pulmonary vasodilative effect. How the uptake occurs in the nasal regions, and the effect on nasal obstruction needs to be further evaluated in future studies. A temporarily reduced nasal patency does not affect the respiratory function, but clinically, a long-term nasal obstruction caused by occupational exposure could be considered indicative for the development of irritation asthma [180].

Self-rated symptoms

Compared to the filtered air exposure (control exposure), the exposures to HVO_{PM+NOx} and HVO_{NOx} caused a higher incidence of self-reported irritation symptoms (78% and 63%, respectively, vs. 28% for filtered air, p<0.03). Especially, exposure to HVO_{PM+NOx} showed 40-50% higher eye and throat irritation symptoms (all details in Paper 4). This exposure also contained organic gases (in addition to PM and NO_x), such as formaldehyde, which is known to cause eye and respiratory tract irritation [181]. The formaldehyde concentration was relatively low (51±6 µg m^{-3}) in comparison to other exposure studies reporting irritation symptoms (>200 µg m^{-3}, [106,182]). Self-rated irritation symptoms were also reported after the particle-free HVO_{NOx} exposure, which indicates that there might also be an effect of NO and NO_2, but to a lower extent than when combined with a particle and organic gas fraction. Similar symptoms have been reported after whole diesel exhaust exposures at similar concentrations as HVO_{PM+NOx}, which indicates that the HVO fuels are not causing more irritative symptoms than fossil diesel [183].

Lung deposited dose

The particle deposition in the lungs depends on the size and shape of the particles. Fig. 18 (Paper 4) shows the results of a comparison made between the estimated lung depositions for soot particles generated with i) a modern diesel vehicle (2019) operating on HVO, and ii) generated with an older diesel vehicle (1998) running on fossil diesel (used in a previous human chamber study [106]). In addition, the lung deposition for the diesel soot particles was estimated with the original diesel exhaust concentration as reported in the previous study (performed in the same chamber as the Paper 4 study) [106], and with a reduced concentration to match the mass concentration of the HVO exhaust presented in Paper 4. It is clearly seen that the deposited doses were larger for the diesel exhaust at the higher mass concentration (276 µg m^{-3}). However, when reducing the mass to match the HVO exposure mass, the mass deposition of diesel exhaust ("Diesel 93 µg m^{-3}" in Fig. 18) becomes lower

than that of the HVO exhaust. The deposited fraction (deposited mass versus inhaled mass) was higher for the HVO exhaust in the tracheobronchial and alveolar regions (Fig. 18) compared to diesel. This caused the higher deposited dose when the same mass concentration was available.

The differences in the deposited fractions come from the different size distributions for diesel and the HVO exhaust. The diesel exhaust particles had a mass median diameter of 195 nm (number GMD: 89 nm) while the HVO particles were 108 nm (number GMD: 71 nm). The smaller particles can penetrate and deposit in the distal parts of the lungs due to diffusion. In addition, the particle number concentrations were similar for both the HVO exposure and the diesel exposure, even though the HVO mass concentration in the chamber was 3 times lower (Paper 4). The comparison highlights that mass regulations may not be the most efficient for reducing the soot exposure from modern engines or renewable diesel fuels (which tend to yield smaller soot particles). In order to reduce the emissions, particle number regulations (PN<23 nm) are being implemented in newer vehicle emission standards. Implementing a similar particle number concentration limit in workplaces is welcomed to further reduce the occupational exposure of soot particle (EC).

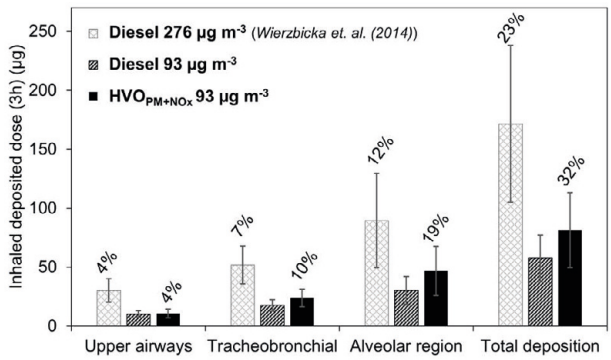

Figure 18. The average accumulated deposited particle doses (PM1, µg) in the upper airways, tracheobronchial region, alveolar region, as well as the total deposited dose. HVO_{PM+NOx} are compared to the estimated deposition of fossil diesel exhaust particles generated in a previous [106] study with its original exposure concentration (276 µg m^{-3}) and with a reduced mass (93 µg m^{-3}) to directly compare to the HVO_{PM+NOx} PM1 exposure concentration. The number on top of each bar represents the fraction of the deposited mass compared to the total exposure concentration. The deposited fraction (%) is the same for both fossil diesel exposures, regardless of exposure concentration, as the fraction depends on individual particle characteristics (size, density) and lung parameters. The error bars represent the groups' individual variability of ±1 std. dev.

Sustainability

Even though the renewable diesel fuels discussed in this thesis are produced from non-fossil sources, the production is not free of sustainability challenges. The challenges involve the sustainability of production and distribution, and the availability of feedstock (edible or nonedible). This is an increasing challenge as there are global initiatives to increase the use of renewable fuels in an effort to reduce the climate impact from fossil fuels [184].

In Sweden, the use of renewable fuels will continue to increase due to the Swedish greenhouse gas reduction mandate [17]. The mandate requires fuel suppliers to use add-ins of biofuels in their fossil fuels to reduce the greenhouse gas emission from diesel (and gasoline). In 2020, the reduction mandate stipulated that the greenhouse gas emissions of fossil diesel should be decreased by 21% by using renewable diesel blends. This number will increase yearly, to reach 66% reduction in 2030 [17]. The renewable fraction in the Swedish standard diesel fuel (MK1) in 2020 originated from HVO (24.4 vol.%) and FAME (5.5 vol.%) [22].

HVO is a diesel fuel that can be made from used oils or different oil waste products. This is beneficial in the aim for a waste-free economy. However, this can give waste products a large economical value and incentive to produce the waste product (i.e., no longer waste). This happened to one of the main feedstocks of HVO in Sweden, palm fatty acid distillate (PFAD), which recently was reclassified to not be a waste product any longer due to its large economical value (since Jan. 7, 2019 [185]). As a result, the cost of pure HVO fuel (HVO100) increased and the quantities in Sweden have decreased from 4.2 TW in 2017 to 2.9 TW in 2019 [22], and 2.8 TW in 2020 (which represent 3.2% of the total amount of vehicle fuels in Sweden [23], Fig. 1b). However, the use of HVO as an add-in to fossil diesel has increased by 2.9% (volume) over the same years [22]. In addition, the production of and demand for HVO are deemed to increase globally in the coming year [186].

The PFAD reclassification highlights the problem with developing a system where we are dependent on waste products. A similar challenge is found in the type of feedstocks that are replacing PFAD, and how sustainable they are in the long run. In 2019, 36% of the HVO used in Sweden originated from PFAD but in 2020 this had decreased to 4% [22,23]. Instead, slaughterhouse waste is the dominating feedstock for HVO, as it increased from 42% in 2019, to 72% in 2020. Animal products cause majority of the greenhouse gas emissions related to food production [187]. Palm oil and PFAD production is also related to several sustainability issues such as the exploitation of tropical forests and peat swamps, which causes high surface emissions of greenhouse gases [188]. Neither the palm oil industry nor the live feedstock industry is sustainable in their current states. Nor is it sustainable for us to increase our dependence on these industries. A smaller fraction of the HVO (12%) is made from Swedish tall oil, which is a by-product from the kraft process

for producing wood pulp, and potentially a more sustainable feedstock for the HVO used in Sweden.

FAME type biodiesels instead, are commonly made from vegetable oil derived from edible crops such as soy, rapeseed, etc. In Sweden, 85-90% of the FAME fuels are made from rapeseed; 63% of the Swedish feedstock is produced in the EU, but only 7% originates from Sweden [22]. The EU is limiting the amount of biofuels that are allowed to be produced from edible crops, which will drive the production towards second generation biofuels (such as HVO) compared to FAME fuels [184]. In addition, to provide food for an increasing population, we cannot reduce the amount of agricultural land used for producing food, and food production also needs to become more efficient without resulting in further negative impacts on biodiversity.

In conclusion, many challenges lie ahead for renewable diesel fuels, yet they still play an important role in the transition to a sustainable transport system.

The transport system today is dependent on combustion engines. Even though the transition to electrical vehicles with confirmed zero exhaust pipe emissions (although the sustainability issues throughout the production can be discussed) is moving rapidly, the accessibility to a sufficient number of vehicles and charging stations are problematic. For heavy transport, there is no sufficient commercial electrical alternative yet, and we will be dependent on combustion engines for years to come. Moreover, in developing parts of the world, the transition to a transportation system with vehicles other than ones with combustion engines is lagging. In the EU, discussions are in progress to stop selling combustion engines/fossil fuels beyond 2030. However, at that point in time, many combustion vehicles will still be operational, and it would be a tremendous environmental and economical waste to scrap them while they are still operational. In these situations, renewable fuels play an important role. Renewable fuels can enable us to fuel combustion vehicles with a fraction of the greenhouse gas emissions from fossil fuels, and to ensure a smoother transition into a fully sustainable transportation system.

Conclusions

With the studies presented in this thesis, I have shown that replacing fossil diesel with HVO and RME reduced the primary PM mass emissions by 30-50%. Both renewable fuels also reduced the HC and CO emissions compared to diesel, for RME about 70% and 30%, respectively, and for HVO about 20% and 10%, respectively. The significantly reduced HC emissions from RME also reduced the secondary aerosol formation, and thus potentially reducing the atmospheric particle burden. As long as a large portion of the vehicle fleet does not have any PM aftertreatment systems (in Sweden only 22% of the heavy-duty vehicles had a DPF in 2019), the use of HVO and RME will have a positive impact on overall PM reductions.

The DOC+DPF tested in the laboratory studies reduced the particle emissions to being barely distinguishable above the background concentrations. In the underground mine, however, there was a considerable particle concentration in the areas where only vehicles with such aftertreatment systems where used. But, the particle number and EC emission factors here were around half compared to those in the drift where vehicles without DPFs were used. Part of the emissions may have originated from non-exhaust sources, such as road, tire, or brake wear particles. The contribution of such sources needs to be further evaluated in occupational exposure studies where vehicles with advanced exhaust emission control strategies are used.

The miners' personal exposure to EC was reduced by more stringent emission standard legislation, but not for NO_2 or PAHs. The average EC and NO_2 exposure were significantly lower than in an older study in the same mine, and the EC exposure was much lower compared to recent studies in Canadian mines. The lower EC exposure reduce the lung cancer risk, but the risk is still high based on epidemiological models.

The method evaluation of eBC and EC in the mine and during the intercomparison had a strong correlation and validated that using the real-time monitoring of eBC was a good proxy of EC from diesel and HVO exhaust. This is useful for identifying work tasks or areas with elevated risks of EC exposure, for example. However, eBC measured with the aethalometers generally showed a factor 2-3 higher values than the EC measured with the NIOSH 5040 method for diesel exhaust. The comparison also confirmed the importance of performing the filter loading correction for the

portable aethalometer (AE51), and that the stationary aethalometer (AE33) generally yielded slightly higher eBC values.

The exhaust particles' ability to induce oxidative stress (per mass unit), evaluated as their ROS forming potential, was similar for fossil diesel and HVO and RME. However, the ROS formation potential was found to depend strongly on the combustion conditions and increased at higher oxygen availability (i.e., at higher degrees of soot maturity and particle oxidation). This indicates that the renewable fuels generate particles with similarly high ROS forming surface characteristics, and that the soot maturity and soot surfaces generated by late-cycle oxidation further increase their reactivity. However, considering the ROS formation potential per generated kWh, HVO and RME reduced the potential by around half as the particle mass emissions were reduced.

The short-term health effects from HVO exposure, with and without the particle fraction (from vehicles without or with a DOC+DPF), were evaluated in a chamber study. No severe effects on self-rated irritation symptoms or lung function were found. However, minor self-rated irritation symptoms were found, with a higher incidence after the HVO exhaust exposure with particles. A minor nasal obstruction (compared to filtered air exposure) was found after the HVO particle-free exposure, and a trend towards the same pattern after the HVO particle exposure. This indicates that even at low concentrations during a short time, the HVO exhaust causes measurable responses. In addition, the HVO exhaust particles from the modern non-road engine were smaller than those from past studies on diesel exhaust which caused a higher calculated deposited mass fraction in the lungs. Although the HVO fuel is more sustainable from a climate perspective, our study indicates that from a health perspective, the exposure levels need to be as carefully controlled as they are for fossil diesel.

Outlook

Renewable diesel fuels are one potential solution during the transition away from a transportation system dependent on fossil fuels. The health effect of the renewable diesel fuels' exhaust particles should be considered to be similarly potent as diesel exhaust. However, the net effect would be lower for the renewable fuels considering the reduced PM emissions, which is beneficial in vehicles without aftertreatment systems. While the soot particles are known to cause adverse health effects, the effects of nucleation mode particles are less known. The nucleation mode concentration was found to be significant in the underground mine, and the potential health effects of these should be addressed in future studies.

The research presented in this thesis only studied the combustion exhaust emissions from the vehicles involved. However, there are other vehicle emission sources that should be considered in future studies, namely the non-exhaust vehicle wear sources. These emissions are mainly from wear on roads, tires, and brakes and can often contain metals (from the brakes and tire studs). Wear emissions from roads and tires are still present in all electrical vehicles and may even increase since the battery electric vehicles are generally heavier, and thus increase the amount of wear on roads and tires. Even though the metal content of the exhaust particles studied in this thesis did not correlate with the in-vitro ROS forming potential, metals are potent ROS producers which could be a potential health hazard from future vehicles. In addition, the mechanistic effects of non-exhaust wear particles need to be studied in order to make risk assessments based on exposure levels.

Air pollution from combustion sources (not only from vehicles) is a global problem that will be present for years to come. Due to the many adverse effects linked to aerosol air pollution, measures need to be taken to reduce the particle exposure in environmental and occupational settings. The future occupational exposure limit of 50 μg EC m^{-3} (from 2023) is still much higher than the proposed health-based limit. For combustion vehicles, the most efficient way of reducing the EC emissions is using aftertreatment systems focused on removing the PM, such as DPFs. Resources need to be focused to ensure such systems are in place and are working efficiently in all combustion vehicles in use, especially in highly exposed areas such as cities and enclosed work environments.

Acknowledgements

First, I would like to thank my main supervisor, *Joakim Pagels*. I have learned a lot from you, and I am ever so grateful for your time, enthusiasm, and encouragement. Big thanks also to my co-supervisors *Maria Hedmer* and *Aneta Wierzbicka* for your support and for contributing with a wider perspective.

To the participants in the exposure study and volunteering miners, thank you for your effort in participating and lending us your time. You were the most important persons in the studies.

My deepest thanks to all my co-authors and colleagues who have generously contributed with their time and expertise. I have very much enjoyed the scientific discussions with you and the opportunity to learn from your many different expert areas and perspectives. It has been both challenging and exciting to work in interdisciplinary projects, and I am grateful to bring this experience with me.

Thanks to all the senior researchers in the Aerosol group who have created a very nice and collaborative working environment. It has been a great asset to be able to talk and discuss with so many skilled researchers not directly involved in my projects.

A big thanks to the technical and administrative personnel at the engine lab and IKDC who have provided various kinds of support which has been essential for conducting our research.

To all the present and previous PhD students in the Aerosol group, thanks for creating such a generous and kind atmosphere. Thanks for all the fun times at the office and at conferences, and for always taking the time to discuss and give input. To *Ville* and *Malin* for staying in academia so I could continue having you as colleagues. Thanks for all the advice (on everything) and always making my day better.

Finally, thanks to friends and family for the love and support. To *Mandy* and *Frida,* I am grateful for your encouragement and believing more in me than I do myself. To *Sara*, it has been great to have a friend doing a PhD in another department, to be able to share all the ups and downs with. To my (human) friends in the stable, it has truly been a blessing having your company every day and I would have gone insane without you during COVID lockdown. To my lovely cats for being outstanding work colleagues when working from home and to my horse for limiting my working

hours in a healthy manner (and taking my mind off everything else). And finally to *Elias*, I cannot imagine a better person to spend my life with and thanks for always making everything possible.

Funding: AFA Insurance Sweden (project no. 160323) and Swedish Research Council FORMAS (project no. 2016–00697 and 2016-00824).

References

1. IPCC Climate Change 2021: The Physical Science Basis. Contribution of Working Group I to the Sixth Assessment Report of the Intergovernmental Panel on Climate Change; Masson-Delmotte, V., P. Zhai, A. Pirani, S.L., Connors, C. Péan, S. Berger, N. Caud, Y. Chen, L. Goldfarb, M.I. Gomis, M. Huang, K. Leitzell, E. Lonnoy, J.B.R., Matthews, T.K. Maycock, T. Waterfield, O. Yelekçi, R. Yu, Zhou, B., Eds.; Cambridge University Press., 2021;
2. Andersson, C.; Ekman, A.; Forsberg, B.; Grennfelt, P.; Gruzieva, O.; Hansson, H.-C.; Karlsson, P.E.; Langner, J.; Moldan, F.; Munthe, J.; et al. Achievements and experiences from science – policy interaction in the field of air pollution; 2021;
3. World Health Organization (WHO) WHO global air quality guidelines: particulate matter (PM2.5 and PM10), ozone, nitrogen dioxide, sulfur dioxide and carbon monoxide.; 2021;
4. Gustafsson, M.; Lindén, J.; Tang, L.; Forsberg, B.; Orru, H.; Åström, S.; Sjöberg, K. Quantification of population exposure to NO2, PM2.5 and PM10 and estimated health impacts; 2018;
5. Lapuerta, M.; Armas, O.; Rodríguez-Fernández, J. Effect of biodiesel fuels on diesel engine emissions. Prog. Energy Combust. Sci. **2008**, 34, 198–223, doi:10.1016/j.pecs.2007.07.001.
6. Murtonen, T.; Aakko-Saksa, P.; Kuronen, M.; Mikkonen, S.; Lehtoranta, K. Emissions with heavy-duty diesel engines and vehicles using FAME, HVO and GTL fuels with and without DOC+ POC aftertreatment. SAE Int. J. Fuels Lubr. **2010**, 2, 147–166.
7. Schmid, O.; Stoeger, T. Surface area is the biologically most effective dose metric for acute nanoparticle toxicity in the lung. J. Aerosol Sci. **2016**, 99, 133–143, doi:10.1016/j.jaerosci.2015.12.006.
8. Matti Maricq, M. Chemical characterization of particulate emissions from diesel engines: A review. J. Aerosol Sci. **2007**, 38, 1079–1118, doi:10.1016/j.jaerosci.2007.08.001.
9. Burtscher, H. Physical characterization of particulate emissions from diesel engines: A review. J. Aerosol Sci. **2005**, 36, 896–932, doi:10.1016/j.jaerosci.2004.12.001.
10. Reuter, S.; Gupta, S.C.; Chaturvedi, M.M.; Aggarwal, B.B. Oxidative stress, inflammation, and cancer: How are they linked? Free Radic. Biol. Med. **2010**, 49, 1603–1616, doi:10.1016/j.freeradbiomed.2010.09.006.
11. Mazzoli-Rocha, F.; Fernandes, S.; Einicker-Lamas, M.; Zin, W.A. Roles of oxidative stress in signaling and inflammation induced by particulate matter. Cell Biol. Toxicol. **2010**, 26, 481–498, doi:10.1007/s10565-010-9158-2.

12. Bendtsen, K.M.; Brostrøm, A.; Koivisto, A.J.; Koponen, I.; Berthing, T.; Bertram, N.; Kling, K.I.; Dal Maso, M.; Kangasniemi, O.; Poikkimäki, M.; et al. Airport emission particles: Exposure characterization and toxicity following intratracheal instillation in mice. Part. Fibre Toxicol. **2019**, 16, 1–23, doi:10.1186/s12989-019-0305-5.
13. IARC Diesel and Gasoline Engine Exhausts and Some Nitroarenes.; 2014; Vol. 105;.
14. Pronk, A.; Coble, J.; Stewart, P.A. Occupational exposure to diesel engine exhaust : A literature review. **2009**, 443–457, doi:10.1038/jes.2009.21.
15. Ge, C.; Peters, S.; Olsson, A.; Portengen, L.; Schüz, J.; Almansa, J.; Ahrens, W.; Bencko, V.; Benhamou, S.; Boffetta, P.; et al. Diesel engine exhaust exposure, smoking, and lung cancer subtype risks: A pooled exposure-response analysis of 14 case-control studies. Am. J. Respir. Crit. Care Med. **2020**, 202, 402–411, doi:10.1164/rccm.201911-2101OC.
16. Vermeulen, R.; Silverman, D.T.; Garshick, E.; Vlaanderen, J.; Portengen, L.; Steenland, K. Exposure-response estimates for diesel engine exhaust and lung cancer mortality based on data from three occupational cohorts. Environ. Health Perspect. **2014**, 122, 172–177, doi:10.1289/ehp.1306880.
17. SFS 2017:1201 Lag om reduktion av växthusgasutsläpp från vissa fossila drivmedel; Stockholm: Infrastrukturdepartementet;
18. Energimyndigheten Drivmedel 2017: Redovisning av uppgifter enligt drivmedelslagen och hållbarhetslagen; 2018;
19. Lapuerta, M.; Octavio, A.; Rodriguez-Fernandez, J. Effect of biodiesel on diesel engine emissions. Prog. energy Combust. Sci. **2008**, 34, 198–223, doi:10.2298/TSCI18S5483N.
20. Wan Ghazali, W.N.M.; Mamat, R.; Masjuki, H.H.; Najafi, G. Effects of biodiesel from different feedstocks on engine performance and emissions: A review. Renew. Sustain. Energy Rev. **2015**, 51, 585–602, doi:10.1016/j.rser.2015.06.031.
21. Bjørgen, K.O.P.; Emberson, D.R.; Løvås, T. Combustion and soot characteristics of hydrotreated vegetable oil compression-ignited spray flames. Fuel **2020**, 266, 116942, doi:10.1016/j.fuel.2019.116942.
22. Statens Energimyndighet Drivmedel 2019 - Redovisning av rapporterade uppgifter enligt drivmedelslagen, hållbarhetslagen och reduktionsplikten; 2020;
23. Statens Energimyndighet Drivmedel 2020 - Redovisning av rapporterade uppgifter enligt drivmedelslagen, hållbarhetslagen och reduktionsplikten; 2021;
24. Knothe, G. Biodiesel and renewable diesel: A comparison. Prog. Energy Combust. Sci. **2010**, 36, 364–373, doi:10.1016/j.pecs.2009.11.004.
25. Aatola, H.; Larmi, M.; Sarjovaara, T. Hydrotreated Vegetable Oil (HVO) as a Renewable Diesel Fuel: Trade-off between NOx, Particulate Emission, and Fuel Consumption of a Heavy Duty Engine. SAE **2008**.
26. Kittelson, D.; Watts, W.; Johnson, J. Diesel Aerosol Sampling Methodology - CRC E-43: Executive Summary. Crc **2002**.

27. Ntziachristos, L.; Giechaskiel, B.; Pistikopoulos, P.; Samaras, Z.; Mathis, U.; Mohr, M.; Ristimäki, J.; Keskinen, J.; Mikkanen, P.; Casati, R.; et al. Performance evaluation of a novel sampling and measurement system for exhaust particle characterization. SAE Tech. Pap. **2004**, 2004, doi:10.4271/2004-01-1439.
28. Rönkkö, T.; Virtanen, A.; Vaaraslahti, K.; Keskinen, J.; Pirjola, L.; Lappi, M. Effect of dilution conditions and driving parameters on nucleation mode particles in diesel exhaust: Laboratory and on-road study. Atmos. Environ. **2006**, 40, 2893–2901, doi:10.1016/j.atmosenv.2006.01.002.
29. de Filippo, A.; Maricq, M.M. Diesel Nucleation Mode Particles : Semivolatile or Solid ? **2008**, 42, 7957–7962, doi:10.1021/es8010332.
30. Tobias, H.J.; Beving, D.E.; Ziemann, P.J.; Sakurai, H.; Zuk, M.; McMurry, P.H.; Zarling, D.; Waytulonis, R.; Kittelson, D.B. Chemical analysis of diesel engine nanoparticles using a nano-DMA/thermal desorption particle beam mass spectrometer. Environ. Sci. Technol. **2001**, 35, 2233–2243, doi:10.1021/es0016654.
31. Karjalainen, P.; Ntziachristos, L.; Murtonen, T.; Wihersaari, H.; Simonen, P.; Mylläri, F.; Nylund, N.O.; Keskinen, J.; Rönkkö, T. Heavy Duty Diesel Exhaust Particles during Engine Motoring Formed by Lube Oil Consumption. Environ. Sci. Technol. **2016**, 50, 12504–12511, doi:10.1021/acs.est.6b03284.
32. Giechaskiel, B.; Manfredi, U.; Martini, G. Engine Exhaust Solid Sub-23 nm Particles: I. Literature Survey. SAE Int. J. Fuels Lubr. **2014**, 7, 950–964, doi:10.4271/2014-01-2834.
33. Johansson, K.O.; Head-Gordon, M.P.; Schrader, P.E.; Wilson, K.R.; Michelsen, H.A. Resonance-stabilized hydrocarbon-radical chain reactions may explain soot inception and growth. Science (80-.). **2018**, 361, 997–1000, doi:10.1126/science.aat3417.
34. Frenklach, M.; Mebel, A.M. On the mechanism of soot nucleation. Phys. Chem. Chem. Phys. **2020**, 22, 5314–5331, doi:10.1039/d0cp00116c.
35. Michelsen, H.A.; Colket, M.B.; Bengtsson, P.E.; D'Anna, A.; Desgroux, P.; Haynes, B.S.; Miller, J.H.; Nathan, G.J.; Pitsch, H.; Wang, H. A review of terminology used to describe soot formation and evolution under combustion and pyrolytic conditions. ACS Nano **2020**, 14, 12470–12490, doi:10.1021/acsnano.0c06226.
36. Kholghy, M.R.; Veshkini, A.; Thomson, M.J. The core-shell internal nanostructure of soot - A criterion to model soot maturity. Carbon N. Y. **2016**, 100, 508–536, doi:10.1016/j.carbon.2016.01.022.
37. Khosousi, A.; Dworkin, S.B. Detailed modelling of soot oxidation by O2and OH in laminar diffusion flames. Proc. Combust. Inst. **2015**, 35, 1903–1910, doi:10.1016/j.proci.2014.05.152.
38. Lack, D.A.; Moosmüller, H.; McMeeking, G.R.; Chakrabarty, R.K.; Baumgardner, D. Characterizing elemental, equivalent black, and refractory black carbon aerosol particles: A review of techniques, their limitations and uncertainties. Anal. Bioanal. Chem. **2014**, 406, 99–122, doi:10.1007/s00216-013-7402-3.
39. Birch, M.E.; Noll, J.D. Submicrometer elemental carbon as a selective measure of diesel particulate matter in coal mines. J. Environ. Monit. **2004**, 6, 799–806, doi:10.1039/b407507b.

40. Nicole, J. Manuscript XIX — The first missionary text in a polynesian language. J. Pacific Hist. Folders/Downloads/scholar (3).ris **1987**, 22, 94–101, doi:10.1080/00223348708572555.
41. Cavalli, F.; Viana, M.; Yttri, K.E.; Genberg, J.; Putaud, J.-P. Toward a standardised thermal-optical protocol for measuring atmospheric organic and elemental carbon: the EUSAAR protocol. Atmos. Meas. Tech. **2010**, 3, 79–89.
42. Mofijur, M.; Atabani, A.E.; Masjuki, H.H.; Kalam, M.A.; Masum, B.M. A study on the effects of promising edible and non-edible biodiesel feedstocks on engine performance and emissions production: A comparative evaluation. Renew. Sustain. Energy Rev. **2013**, 23, 391–404, doi:10.1016/j.rser.2013.03.009.
43. Kim, D.S.; Hanifzadeh, M.; Kumar, A. Trend of biodiesel feedstock and its impact on biodiesel emission characteristics. Environ. Prog. Sustain. Energy **2018**, 37, 7–19, doi:10.1002/ep.12800.
44. Savic, N.; Rahman, M.M.; Miljevic, B.; Saathoff, H.; Naumann, K.H.; Leisner, T.; Riches, J.; Gupta, B.; Motta, N.; Ristovski, Z.D. Influence of biodiesel fuel composition on the morphology and microstructure of particles emitted from diesel engines. Carbon N. Y. **2016**, doi:10.1016/j.carbon.2016.03.061.
45. Qu, L.; Wang, Z.; Zhang, J. Influence of waste cooking oil biodiesel on oxidation reactivity and nanostructure of particulate matter from diesel engine. Fuel **2016**, 181, 389–395, doi:10.1016/j.fuel.2016.04.113.
46. Happonen, M.; L??hde, T.; Messing, M.E.; Sarjovaara, T.; Larmi, M.; Wallenberg, L.R.; Virtanen, A.; Keskinen, J. The comparison of particle oxidation and surface structure of diesel soot particles between fossil fuel and novel renewable diesel fuel. Fuel **2010**, 89, 4008–4013, doi:10.1016/j.fuel.2010.06.006.
47. Zheng, M.; Reader, G.T.; Hawley, J.G. Diesel engine exhaust gas recirculation - A review on advanced and novel concepts. Energy Convers. Manag. **2004**, 45, 883–900, doi:10.1016/S0196-8904(03)00194-8.
48. Tsolakis, A.; Megaritis, A.; Wyszynski, M.L.; Theinnoi, K. Engine performance and emissions of a diesel engine operating on diesel-RME (rapeseed methyl ester) blends with EGR (exhaust gas recirculation). Energy **2007**, 32, 2072–2080, doi:10.1016/j.energy.2007.05.016.
49. Maiboom, A.; Tauzia, X.; Hétet, J.F. Experimental study of various effects of exhaust gas recirculation (EGR) on combustion and emissions of an automotive direct injection diesel engine. Energy **2008**, 33, 22–34, doi:10.1016/j.energy.2007.08.010.
50. Imtenan, S.; Varman, M.; Masjuki, H.H.; Kalam, M.A.; Sajjad, H.; Arbab, M.I.; Rizwanul Fattah, I.M. Impact of low temperature combustion attaining strategies on diesel engine emissions for diesel and biodiesels: A review. Energy Convers. Manag. **2014**, 80, 329–356, doi:10.1016/j.enconman.2014.01.020.
51. Török, S.; Malmborg, V.B.; Simonsson, J.; Eriksson, A.; Martinsson, J.; Mannazhi, M.; Pagels, J.; Bengtsson, P.E. Investigation of the absorption Ångström exponent and its relation to physicochemical properties for mini-CAST soot. Aerosol Sci. Technol. **2018**, 52, 757–767, doi:10.1080/02786826.2018.1457767.

52. Malmborg, V.B.; Eriksson, A.C.; Török, S.; Zhang, Y.; Kling, K.; Martinsson, J.; Fortner, E.C.; Gren, L.; Kook, S.; Onasch, T.B.; et al. Relating aerosol mass spectra to composition and nanostructure of soot particles. Carbon N. Y. **2019**, 142, 535–546, doi:10.1016/j.carbon.2018.10.072.
53. Jung, Y.; Bae, C. Immaturity of soot particles in exhaust gas for low temperature diesel combustion in a direct injection compression ignition engine. Fuel **2015**, 161, 312–322, doi:10.1016/j.fuel.2015.08.068.
54. Malmborg, V.; Eriksson, A.; Gren, L.; Török, S.; Shamun, S.; Novakovic, M.; Zhang, Y.; Kook, S.; Tunér, M.; Bengtsson, P.-E.; et al. Characteristics of BrC and BC emissions from controlled diffusion flame and diesel engine combustion. Aerosol Sci. Technol. **2021**, 0, 1–19, doi:10.1080/02786826.2021.1896674.
55. Olabi, A.G.; Maizak, D.; Wilberforce, T. Review of the regulations and techniques to eliminate toxic emissions from diesel engine cars. Sci. Total Environ. **2020**, 748, 141249, doi:10.1016/j.scitotenv.2020.141249.
56. Reşitoğlu, I.A.; Altinişik, K.; Keskin, A. The pollutant emissions from diesel-engine vehicles and exhaust aftertreatment systems. Clean Technol. Environ. Policy **2015**, 17, 15–27, doi:10.1007/s10098-014-0793-9.
57. Neyertz, C.A.; Miró, E.E.; Querini, C.A. K/CeO 2 catalysts supported on cordierite monoliths: Diesel soot combustion study. Chem. Eng. J. **2012**, 181–182, 93–102, doi:10.1016/j.cej.2011.11.010.
58. Tan, P.; Duan, L.; Li, E.; Hu, Z.; Lou, D. Experimental study on the temperature characteristics of a diesel particulate filter during a drop to idle active regeneration process. Appl. Therm. Eng. **2020**, 178, 115628, doi:10.1016/j.applthermaleng.2020.115628.
59. Akihama, K.; Takatori, Y.; Inagaki, K.; Sasaki, S.; Dean, A.M. Mechanism of the smokeless rich diesel combustion by reducing temperature. SAE Tech. Pap. **2001**, 110, 648–662, doi:10.4271/2001-01-0655.
60. Mohan, S.; Dinesha, P.; Kumar, S. NOx reduction behaviour in copper zeolite catalysts for ammonia SCR systems: A review. Chem. Eng. J. **2020**, 384, 123253, doi:10.1016/j.cej.2019.123253.
61. Resitoglu, I.A. The effect of biodiesel on activity of diesel oxidation catalyst and selective catalytic reduction catalysts in diesel engine. Renew. Sustain. Energy Rev. **2021**, 148, 111286, doi:10.1016/j.rser.2021.111286.
62. Merelli, L.; Fridell, E. SMED rapport Nr 23 2020: Emissioner från vägtrafikfordon med HVO; 2020;
63. Hallquist, M.; Wenger, J.C.; Baltensperger, U.; Rudich, Y.; Simpson, D.; Claeys, M.; Dommen, J.; Donahue, N.M.; George, C.; Goldstein, A.H.; et al. The formation, properties and impact of secondary organic aerosol: Current and emerging issues. Atmos. Chem. Phys. **2009**, 9, 5155–5236, doi:10.5194/acp-9-5155-2009.
64. Saha, P.K.; Reece, S.M.; Grieshop, A.P. Seasonally Varying Secondary Organic Aerosol Formation from In-Situ Oxidation of Near-Highway Air. Environ. Sci. Technol. **2018**, 52, 7192–7202, doi:10.1021/acs.est.8b01134.

65. Robinson, A.L.; Donahue, N.M.; Shrivastava, M.K.; Weitkamp, E.A.; Sage, A.M.; Grieshop, A.P.; Lane, T.E.; Pierce, J.R.; Pandis, S.N. Rethinking Organic Aerosols: Semivolatile Emissions and Photochemical Aging. **2007**, 315, 1259–1263.
66. Popovicheva, O.B.; Irimiea, C.; Carpentier, Y.; Ortega, I.K.; Kireeva, E.D.; Shonija, N.K.; Schwarz, J.; Vojtíšek-Lom, M.; Focsa, C. Chemical composition of diesel/biodiesel particulate exhaust by FTIR spectroscopy and mass spectrometry: Impact of fuel and driving cycle. Aerosol Air Qual. Res. **2017**, 17, 1717–1734, doi:10.4209/aaqr.2017.04.0127.
67. Surawski, N.; Miljevic, B.; Ayoko, G.A.; Eltahir, S.; Stevanovic, S.; Fairfull-Smith, K.E.; Bottle, S.E.; Ristovski, Z.D. A physico-chemical characterisation of particulate emissions from a compression ignition engine: the influence of biodiesel feedstock. Environ. Sci. Technol. **2011**, 45, 10337–10343, doi:10.1021/es2018797.
68. Gentner, D.R.; Jathar, S.H.; Gordon, T.D.; Bahreini, R.; Day, D.A.; El Haddad, I.; Hayes, P.L.; Pieber, S.M.; Platt, S.M.; De Gouw, J.; et al. Review of Urban Secondary Organic Aerosol Formation from Gasoline and Diesel Motor Vehicle Emissions. Environ. Sci. Technol. **2017**, 51, 1074–1093, doi:10.1021/acs.est.6b04509.
69. Jathar, S.H.; Friedman, B.; Galang, A.A.; Link, M.F.; Brophy, P.; Volckens, J.; Eluri, S.; Farmer, D.K. Linking Load , Fuel , and Emission Controls to Photochemical Production of Secondary Organic Aerosol from a Diesel Engine. **2017**, doi:10.1021/acs.est.6b04602.
70. Karjalainen, P.; Rönkkö, T.; Simonen, P.; Ntziachristos, L.; Juuti, P.; Timonen, H.; Teinilä, K.; Saarikoski, S.; Saveljeff, H.; Lauren, M.; et al. Strategies to Diminish the Emissions of Particles and Secondary Aerosol Formation from Diesel Engines. Environ. Sci. Technol. **2019**, 53, 10408–10416, doi:10.1021/acs.est.9b04073.
71. Heyder, J.; Gebhart, J.; Rudolf, G.; Schiller, C.F.; Stahlhofen, W. Deposition of particles in the human respiratory tract in the size range 0.005-15 μm. J. Aerosol Sci. **1986**, 17, 811–825, doi:10.1016/0021-8502(86)90035-2.
72. Lippman, M.; Yates, D.B.; Albert, R.E. Deposition, retention, and clearance of inhaled particles. Bristish J. Ind. Med. **1980**, VOL. 37, 337–362, doi:10.1289/ehp.8455369.
73. West, J.B.; Luks, A.M. Respiratory physiology: the essentials; Tenth.; Lippincott Williams & Wilkins, 2012;
74. Steiner, S.; Bisig, C.; Petri, A.; Barbara, F.; Rutishauser, R. Diesel exhaust : current knowledge of adverse effects and underlying cellular mechanisms. Arch. Toxicol. **2016**, 90, 1541–1553, doi:10.1007/s00204-016-1736-5.
75. Nel, A.E.; Diaz-Sanchez, D.; Ng, D.; Hiura, T.; Saxon, A. Enhancement of allergic inflammation by the interaction between diesel exhaust particles and the immune system. J. Allergy Clin. Immunol. **1998**, 102, 539–554, doi:10.1016/s0091-6749(98)70269-6.
76. Bates, J.T.; Fang, T.; Verma, V.; Zeng, L.; Weber, R.J.; Tolbert, P.E.; Abrams, J.Y.; Sarnat, S.E.; Klein, M.; Mulholland, J.A.; et al. Review of Acellular Assays of Ambient Particulate Matter Oxidative Potential: Methods and Relationships with Composition, Sources, and Health Effects. Environ. Sci. Technol. **2019**, 53, 4003–4019, doi:10.1021/acs.est.8b03430.

77. Hedayat, F.; Stevanovic, S.; Miljevic, B.; Bottle, S.; Ristovski, Z.D. Review – Evaluating the molecular assays for measuring the oxidative potential of particulate matter. Chem. Ind. Chem. Eng. Q. **2015**, 21, 201–210, doi:10.2298/CICEQ140228031H.
78. Jalava, P.I.; Aakko-Saksa, P.; Murtonen, T.; Happo, M.S.; Markkanen, A.; Yli-Pirilä, P.; Hakulinen, P.; Hillamo, R.; Mäki-Paakkanen, J.; Salonen, R.O.; et al. Toxicological properties of emission particles from heavy duty engines powered by conventional and bio-based diesel fuels and compressed natural gas. Part. Fibre Toxicol. **2012**, 9, 37, doi:10.1186/1743-8977-9-37.
79. Cheung, K.L.; Polidori, A.; Ntziachristos, L.; Cassee, F.R.; Gerlofs, M. Chemical Characteristics and Oxidative Potential of Particulate Matter Emissions from Gasoline , Diesel , and Biodiesel Cars. **2009**, 43, 6334–6340.
80. Gerlofs-Nijland, M.E.; Totlandsdal, A.I.; Tzamkiozis, T.; Leseman, D.L.A.C.; Samaras, Z.; Låg, M.; Schwarze, P.; Ntziachristos, L.; Cassee, F.R. Cell toxicity and oxidative potential of engine exhaust particles: Impact of using particulate filter or biodiesel fuel blend. Environ. Sci. Technol. **2013**, 47, 5931–5938, doi:10.1021/es305330y.
81. Unosson, J.; Kabele, M.; Boman, C.; Nyström, R.; Sadiktsis, I.; Westerholm, R.; Mudway, I.; Purdie, E.; Raftis, J.; Miller, M.; et al. Acute Cardiovascular Effects of Controlled Exposure to Dilute Petrodiesel and Biodiesel Exhaust in Healthy Volunteers: A Crossover Study. Part. Fibre Toxicol. **2021**, 18:22, 1–14, doi:10.21203/rs.3.rs-34684/v1.
82. Pandya, R.J.; Solomon, G.; Kinner, A.; Balmes, J.R. Diesel Exhaust and Asthma : Hypotheses and Molecular Mechanisms of Action. **2002**, 110, 103–112.
83. Miller, M.R.; Newby, D.E. Air pollution and cardiovascular disease: Car sick. Cardiovasc. Res. **2020**, 116, 279–294, doi:10.1093/cvr/cvz228.
84. Health Council of the Netherlands Guidelines for the calculation of occupational cancer risk values.; 2012;
85. Federal Institute for Occupational safety and Health (BAuA), Dortmund, Germany The risk-based concept for carcinogenic substances developed by the Committee for Hazardous Substances.; 2013;
86. Plato, N.; Lewné, M.; Gustavsson, P. A historical job-exposure matrix for occupational exposure to diesel exhaust using elemental carbon as an indicator of exposure. Arch. Environ. Occup. Heal. **2020**, 75, 321–332, doi:10.1080/19338244.2019.1644277.
87. Arbetsmiljöverket Hygieniska gränsvärden 2018, AFS 2018:01; 2018; ISBN 9789179306496.
88. Directive (EU) 2019/130 The protection of workers from the risks related to exposure to carcinogens or mutagens at work. European Parliament, Council of the European Union; 2019;
89. Swedish Work Environment Authority AFS 2020:6, Occupational exposure limits; 2020;
90. Arbejdstilsynet Arbejdstilsynets bekendtgørelse nr. 1426: Bilag 2 - Grænseværdier for luftforureninger m.v.; 2021;

91. Health Council of the Netherlands Diesel Engine Exhaust Health-based recommended occupational exposure limit; 2020;
92. Landwehr, K.R.; Larcombe, A.N.; Reid, A.; Mullins, B.J. Critical Review of Diesel Exhaust Exposure Health Impact Research Relevant to Occupational Settings: Are We Controlling the Wrong Pollutants? Expo. Heal. **2020**, doi:10.1007/s12403-020-00379-0.
93. Weitekamp, C.A.; Kerr, L.B.; Dishaw, L.; Nichols, J.; Lein, M.; Stewart, M.J. A systematic review of the health effects associated with the inhalation of particle-filtered and whole diesel exhaust. Inhal. Toxicol. **2020**, 32, 1–13, doi:10.1080/08958378.2020.1725187.
94. Lucking, A.J.; Lundbäck, M.; Barath, S.L.; Mills, N.L.; Sidhu, M.K.; Langrish, J.P.; Boon, N.A.; Pourazar, J.; Badimon, J.J.; Gerlofs-Nijland, M.E.; et al. Particle traps prevent adverse vascular and prothrombotic effects of diesel engine exhaust inhalation in men. Circulation **2011**, 123, 1721–1728, doi:10.1161/CIRCULATIONAHA.110.987263.
95. Madden, M.C. A paler shade of green? The toxicology of biodiesel emissions: Recent findings from studies with this alternative fuel. Biochim. Biophys. Acta - Gen. Subj. **2016**, 1860, 2856–2862, doi:10.1016/j.bbagen.2016.05.035.
96. Møller, P.; Scholten, R.H.; Roursgaard, M.; Krais, A.M. Inflammation, oxidative stress and genotoxicity responses to biodiesel emissions in cultured mammalian cells and animals. Crit. Rev. Toxicol. 2020, 50, 383–401.
97. Bendtsen, K.; Gren, L.; Malmborg, V.; Shukla, P.; Tunér, M.; Essig, Y.; Krais, A.; Clausen, P.; Berthing, T.; Loeschner, K.; et al. Particle characterization and toxicity in C57BL/6 mice following instillation of five different diesel exhaust particles designed to differ in physicochemical properties. Part. Fibre Toxicol. **2020**, doi:10.21203/rs.3.rs-18458/v1.
98. Mao, J.; Ren, X.; Brune, W.H.; Olson, J.R.; Crawford, J.H.; Fried, A.; Huey, L.G.; Cohen, R.C.; Heikes, B.; Singh, H.B.; et al. Airborne measurement of OH reactivity during INTEX-B. Atmos. Chem. Phys. **2009**, 9, 163–173, doi:10.5194/acp-9-163-2009.
99. Drinovec, L.; Močnik, G.; Zotter, P.; Prévôt, A.S.H.; Ruckstuhl, C.; Coz, E.; Rupakheti, M.; Sciare, J.; Müller, T.; Wiedensohler, A.; et al. The "dual-spot" Aethalometer: An improved measurement of aerosol black carbon with real-time loading compensation. Atmos. Meas. Tech. **2015**, 8, 1965–1979, doi:10.5194/amt-8-1965-2015.
100. Good, N.; Mölter, A.; Peel, J.L.; Volckens, J. An accurate filter loading correction is essential for assessing personal exposure to black carbon using an Aethalometer. J. Expo. Sci. Environ. Epidemiol. **2017**, 27, 409–416, doi:10.1038/jes.2016.71.
101. Kirchstetter, T.W.; Novakov, T. Controlled generation of black carbon particles from a diffusion flame and applications in evaluating black carbon measurement methods. Atmos. Environ. **2007**, 41, 1874–1888, doi:10.1016/j.atmosenv.2006.10.067.
102. NIOSH Diesel particulate matter (as Elemental Carbon): Method 5040. NIOSH Man. Occup. Saf. Heal. **2003**, 4, 1–5.
103. McMurry, P.H.; Wang, X.; Park, K.; Ehara, K. The relationship between mass and mobility for atmospheric particles: A new technique for measuring particle density. Aerosol Sci. Technol. **2002**, 36, 227–238, doi:10.1080/027868202753504083.

104. Park, K.; Cao, F.; Kittelson, D.B.; McMurry, P.H. Relationship between particle mass and mobility for diesel exhaust particles. Environ. Sci. Technol. **2003**, 37, 577–583, doi:10.1021/es025960v.

105. Rissler, J.; Swietlicki, E.; Bengtsson, A.; Boman, C.; Pagels, J.; Sandström, T.; Blomberg, A.; Löndahl, J. Experimental determination of deposition of diesel exhaust particles in the human respiratory tract. J. Aerosol Sci. **2012**, 48, 18–33, doi:10.1016/j.jaerosci.2012.01.005.

106. Wierzbicka, A.; Nilsson, P.T.; Rissler, J.; Sallsten, G.; Xu, Y.; Pagels, J.H.; Albin, M.; Österberg, K.; Strandberg, B.; Eriksson, A.; et al. Detailed diesel exhaust characteristics including particle surface area and lung deposited dose for better understanding of health effects in human chamber exposure studies. Atmos. Environ. **2014**, 86, 212–219, doi:10.1016/j.atmosenv.2013.11.025.

107. Ferm, M.; Svanberg, P.A. Cost-efficient techniques for urban- and background measurements of SO2 and NO2. Atmos. Environ. **1998**, 32, 1377–1381, doi:10.1016/S1352-2310(97)00170-2.

108. Ferm, M.; Rodhe, H. Measurements of air concentrations of SO2, NO2 and NH3 at rural and remote sites in Asia. J. Atmos. Chem. **1997**, 27, 17–29, doi:10.1023/A:1005816621522.

109. Strandberg, B.O. Field evaluation of PUF passive air samplers to assess airborne PAHs in occupational environments_2010.pdf. **2010**, 44, 749–754.

110. Strandberg, B.; Julander, A.; Sjöström, M.; Lewné, M.; Koca Akdeva, H.; Bigert, C. Evaluation of polyurethane foam passive air sampler (PUF) as a tool for occupational PAH measurements. Chemosphere **2018**, 190, 35–42, doi:10.1016/j.chemosphere.2017.09.106.

111. Kirchstetter, T.W.; Harley, R.A.; Kreisberg, N.M.; Stolzenburg, M.R.; Hering, S. V. On-road measurement of fine particle and nitrogen oxide emissions from light- and heavy-duty motor vehicles. Atmos. Environ. **1999**, 33, 2955–2968, doi:10.1016/S1352-2310(99)00089-8.

112. Engman, A.; Hartikka, T.; Honkanen, M.; Kiiski, U.; Kuronen, M.; Lehto, K.; Mikkonen, S.; Nortio, J.; Nuottimäki, J.; Saikkonen, P. (Eds) Neste Renewable Diesel Handbook; 2015; ISBN 2119450077420.

113. Thuijl, E. Van; Roos, C.; Beurskens, L. An overview of biofuel technologies, markets and policies in Europe. **2003**, 1–64.

114. Jeong, C.-H.; Hopke, P.K.; Kim, E.; Lee, D.-W. The comparison between thermal-optical transmittance elemental carbon and Aethalometer black carbon measured at multiple monitoring sites. Atmos. Environ. **2004**, 38, 5193–5204, doi:10.1016/j.atmosenv.2004.02.065.

115. Lee, K.-H.; Jung, H.-J.; Park, D.-U.; Ryu, S.-H.; Kim, B.; Ha, K.-C.; Kim, S.; Yi, G.; Yoon, C. Occupational exposure to diesel particulate matter in municipal household waste workers. PLoS One **2015**, 10, 1–17, doi:10.1371/journal.pone.0135229.

116. Mo, S.; Gupta, S.S.; Stroud, A.; Strazdins, E.; Hamizan, A.W.; Rimmer, J.; Alvarado, R.; Kalish, L.; Harvey, R.J. Nasal Peak Inspiratory Flow in Healthy and Obstructed Patients: Systematic Review and Meta-Analysis. Laryngoscope **2021**, 131, 260–267, doi:10.1002/lary.28682.

117. Krais, A.M.; Essig, J.Y.; Gren, L.; Vogs, C.; Assarsson, E.; Dierschke, K.; Nielsen, J.; Strandberg, B.; Pagels, J.; Broberg, K.; et al. Biomarkers after controlled inhalation exposure to exhaust from hydrogenated vegetable oil (HVO). Int. J. Environ. Res. Public Health **2021**, 18, 6492, doi:10.3390/ijerph18126492.

118. Dalleau, S.; Baradat, M.; Guéraud, F.; Huc, L. Cell death and diseases related to oxidative stress:4-hydroxynonenal (HNE) in the balance. Cell Death Differ. **2013**, 20, 1615–1630, doi:10.1038/cdd.2013.138.

119. Møller, P.; Loft, S. Oxidative damage to DNA and lipids as biomarkers of exposure to air pollution. Environ. Health Perspect. **2010**, 118, 1126–1136, doi:10.1289/ehp.0901725.

120. Higashi, K.; Igarashi, K.; Toida, T. Recent progress in analytical methods for determination of urinary 3-Hydroxypropylmercapturic acid, a major metabolite of acrolein. Biol. Pharm. Bull. **2016**, 39, 915–919, doi:10.1248/bpb.b15-01022.

121. Bittle, J.A.; Knight, B.M.; Jacobs, T.J. Investigation into the use of ignition delay as an indicator of low-temperature diesel combustion attainment. Combust. Sci. Technol. **2011**, 183, 138–153, doi:10.1080/00102202.2010.496380.

122. Gallo, Y.; Svensson, E.; Shen, M.Q.; Tunér, M.; Andersson, Ö.; Malmborg, V.B.; Pagels, J.; Simonsson, J.; Bengtsson, P.E.; Garcia, A. Investigation of late-cycle soot oxidation using laser extinction and in-cylinder gas sampling at varying inlet oxygen concentrations in diesel engines. Fuel **2017**, 193, 308–314, doi:10.1016/j.fuel.2016.12.013.

123. Aronsson, U.; Chartier, C.; Andersson, Ö.; Johansson, B.; Sjöholm, J.; Wellander, R.; Richter, M.; Alden, M.; Miles, P. Analysis of EGR Effects on the Soot Distribution in a Heavy Duty Diesel Engine using Time-Resolved Laser Induced Incandescence. SAE Int. J. Engines **2010**, Vol. 3.

124. Pflaum, H.; Hofmann, P.; Geringer, B.; Weissel, W. Potential of Hydrogenated Vegetable Oil (HVO) in a modern diesel engine. SAE Tech. Pap. **2010**, doi:10.4271/2010-32-0081.

125. Zubel, M.; Bhardwaj, O.P.; Heuser, B.; Holderbaum, B.; Doerr, S.; Nuottimäki, J. Advanced Fuel Formulation Approach using Blends of Paraffinic and Oxygenated Biofuels: Analysis of Emission Reduction Potential in a High Efficiency Diesel Combustion System. SAE Int. J. Fuels Lubr. **2016**, 9, 481–492, doi:10.4271/2016-01-2179.

126. Tamilselvan, P.; Nallusamy, N.; Rajkumar, S. A comprehensive review on performance, combustion and emission characteristics of biodiesel fuelled diesel engines. Renew. Sustain. Energy Rev. **2017**, 79, 1134–1159, doi:10.1016/j.rser.2017.05.176.

127. Shahir, V.K.; Jawahar, C.P.; Suresh, P.R. Comparative study of diesel and biodiesel on CI engine with emphasis to emissions - A review. Renew. Sustain. Energy Rev. **2015**, 45, 686–697, doi:10.1016/j.rser.2015.02.042.

128. Singh, D.; Subramanian, K.A.; Garg, M.O. Comprehensive review of combustion, performance and emissions characteristics of a compression ignition engine fueled with hydroprocessed renewable diesel. Renew. Sustain. Energy Rev. **2018**, 81, 2947–2954, doi:10.1016/j.rser.2017.06.104.

129. Mohamed Shameer, P.; Ramesh, K.; Sakthivel, R.; Purnachandran, R. Effects of fuel injection parameters on emission characteristics of diesel engines operating on various biodiesel: A review. Renew. Sustain. Energy Rev. **2017**, 67, 1267–1281, doi:10.1016/j.rser.2016.09.117.
130. Karavalakis, G.; Jiang, Y.; Yang, J.; Durbin, T.; Nuottimäki, J.; Lehto, K. Emissions and Fuel Economy Evaluation from Two Current Technology Heavy-Duty Trucks Operated on HVO and FAME Blends. SAE Int. J. Fuels Lubr. **2016**, 9, 177–190, doi:10.4271/2016-01-0876.
131. McCaffery, C.; Karavalakis, G.; Durbin, T.; Jung, H.; Johnson, K. Engine-Out Emissions Characteristics of a Light Duty Vehicle Operating on a Hydrogenated Vegetable Oil Renewable Diesel. SAE Tech. Pap. **2020**, 2020-April, 1–11, doi:10.4271/2020-01-0337.
132. Mueller, C.J.; Boehman, A.L.; Martin, G.C. An experimental investigation of the origin of increased NOx emissions when fueling a heavy-duty compression-ignition engine with soy biodiesel. SAE Int. J. Fuels Lubr. **2009**, 2, 789–816, doi:10.4271/2009-01-1792.
133. Bhardwaj, O.P.; Lüers, B.; Holderbaum, B.; Koerfer, T.; Pischinger, S.; Honkanen, M. Utilization of HVO Fuel Properties in a High Efficiency Combustion System: Part 2: Relationship of Soot Characteristics with its Oxidation Behavior in DPF. SAE Int. J. Fuels Lubr. **2014**, 7, 979–994, doi:10.4271/2014-01-2846.
134. Tree, D.R.; Svensson, K.I. Soot processes in compression ignition engines. Prog. Energy Combust. Sci. **2007**, 33, 272–309, doi:10.1016/j.pecs.2006.03.002.
135. Singh, D.; Subramanian, K.A.; Singal, S.K. Emissions and fuel consumption characteristics of a heavy duty diesel engine fueled with Hydroprocessed Renewable Diesel and Biodiesel. Appl. Energy **2015**, 155, 440–446, doi:10.1016/j.apenergy.2015.06.020.
136. Tan, C.; Xu, H.; Shuai, S.J.; Ghafourian, A.; Liu, D.; Tian, J. Investigation on transient emissions of a turbocharged diesel engine fuelled by HVO blends. SAE Int. J. Engines **2013**, 6, 1046–1058, doi:10.4271/2013-01-1307.
137. Stoeger, T.; Reinhard, C.; Takenaka, S.; Schroeppel, A.; Karg, E.; Ritter, B.; Heyder, J.; Schulz, H. Instillation of six different ultrafine carbon particles indicates a surface area threshold dose for acute lung inflammation in mice. Environ. Health Perspect. **2006**, 114, 328–333, doi:10.1289/ehp.8266.
138. Jacobsen, N.R.; Pojana, G.; White, P.; Möller, P.; Cohn, C.A.; Korsholm, K.S.; Vogel, U.; Marcomini, A.; Loft, S.; Wallin, H. Genotoxicity, Cytotoxicity, and Reactive Oxygen Species Induced by Single-Walled Carbon Nanotubes and C60 Fullerenes in the FE1-MutaTM Mouse Lung Epithelial Cells. Environ. Mol. Mutagen. **2008**, 49, 249–255, doi:10.1002/em.20406.
139. Johansson, K.O.; El Gabaly, F.; Schrader, P.E.; Campbell, M.F.; Michelsen, H.A. Evolution of maturity levels of the particle surface and bulk during soot growth and oxidation in a flame. Aerosol Sci. Technol. **2017**, 51, 1333–1344, doi:10.1080/02786826.2017.1355047.

140. Holder, A.L.; Carter, B.J.; Goth-Goldstein, R.; Lucas, D.; Koshland, C.P. Increased cytotoxicity of oxidized flame soot. Atmos. Pollut. Res. **2012**, 3, 25–31, doi:10.5094/APR.2012.001.
141. Le, Y.T.H.; Youn, J.S.; Moon, H.G.; Chen, X.Y.; Kim, D.I.; Cho, H.W.; Lee, K.H.; Jeon, K.J. Relationship between cytotoxicity and surface oxidation of artificial black carbon. Nanomaterials **2021**, 11, doi:10.3390/nano11061455.
142. Stoeger, T.; Takenaka, S.; Frankenberger, B.; Ritter, B.; Karg, E.; Maier, K.; Schulz, H.; Schmid, O. Deducing in vivo toxicity of combustion-derived nanoparticles from a cell-Free oxidative potency assay and Metabolic activation of organic compounds. Environ. Health Perspect. **2009**, 117, 54–60, doi:10.1289/ehp.11370.
143. Kuuluvainen, H.; Karjalainen, P.; Saukko, E.; Ovaska, T.; Sirviö, K.; Honkanen, M.; Olin, M.; Niemi, S.; Keskinen, J.; Rönkkö, T. Nonvolatile ultrafine particles observed to form trimodal size distributions in non-road diesel engine exhaust. Aerosol Sci. Technol. **2020**, 3–6, doi:10.1080/02786826.2020.1783432.
144. Tornehed, P.; Olofsson, U. Towards a model for engine oil hydrocarbon particulate matter. SAE Tech. Pap. **2010**, 3, 543–558, doi:10.4271/2010-01-2098.
145. Chirico, R.; Decarlo, P.F.; Heringa, M.F.; Tritscher, T.; Richter, R.; Prévôt, A.S.H.; Dommen, J.; Weingartner, E.; Wehrle, G.; Gysel, M.; et al. Impact of aftertreatment devices on primary emissions and secondary organic aerosol formation potential from in-use diesel vehicles: Results from smog chamber experiments. Atmos. Chem. Phys. **2010**, 10, 11545–11563, doi:10.5194/acp-10-11545-2010.
146. Karjalainen, P.; Timonen, H.; Saukko, E.; Kuuluvainen, H.; Saarikoski, S.; Aakko-Saksa, P.; Murtonen, T.; Bloss, M.; Dal Maso, M.; Simonen, P.; et al. Time-resolved characterization of primary particle emissions and secondary particle formation from a modern gasoline passenger car. Atmos. Chem. Phys. **2016**, 16, 8559–8570, doi:10.5194/acp-16-8559-2016.
147. Roth, P.; Yang, J.; Peng, W.; Cocker, D.R.; Durbin, T.D.; Asa-Awuku, A.; Karavalakis, G. Intermediate and high ethanol blends reduce secondary organic aerosol formation from gasoline direct injection vehicles. Atmos. Environ. **2020**, 220, 117064, doi:10.1016/j.atmosenv.2019.117064.
148. Liu, S.; Ahlm, L.; Day, D.A.; Russell, L.M.; Zhao, Y.; Gentner, D.R.; Weber, R.J.; Goldstein, A.H.; Jaoui, M.; Offenberg, J.H.; et al. Secondary organic aerosol formation from fossil fuel sources contribute majority of summertime organic mass at Bakersfield. J. Geophys. Res. Atmos. **2012**, 117, 1–21, doi:10.1029/2012JD018170.
149. Le Breton, M.; Psichoudaki, M.; Hallquist, M.; Watne, K.; Lutz, A.; Hallquist, M. Application of a FIGAERO ToF CIMS for on-line characterization of real-world fresh and aged particle emissions from buses. Aerosol Sci. Technol. **2019**, 53, 244–259, doi:10.1080/02786826.2019.1566592.
150. Watne, Å.K.; Psichoudaki, M.; Ljungström, E.; Le Breton, M.; Hallquist, M.; Jerksjö, M.; Fallgren, H.; Jutterström, S.; Hallquist, Å.M. Fresh and Oxidized Emissions from In-Use Transit Buses Running on Diesel, Biodiesel, and CNG. Environ. Sci. Technol. **2018**, 52, 7720–7728, doi:10.1021/acs.est.8b01394.

151. Bugarski, A.D.; Cauda, E.G.; Janisko, S.J.; Hummer, J.A.; Patts, L.D. Aerosols emitted in underground mine air by diesel engine fueled with biodiesel. J. Air Waste Manag. Assoc. **2010**, 60, 237–244, doi:10.3155/1047-3289.60.2.237.

152. Bugarski, A.D.; Schnakenberg, G.H.; Hummer, J.A.; Cauda, E.; Janisko, S.J.; Patts, L.D. Effects of diesel exhaust aftertreatment devices on concentrations and size distribution of aerosols in underground mine air. Environ. Sci. Technol. **2009**, 43, 6737–6743, doi:10.1021/es9006355.

153. Zare, A.; Bodisco, T.A.; Jafari, M.; Verma, P.; Yang, L.; Babaie, M.; Rahman, M.M.; Banks, A.; Ristovski, Z.D.; Brown, R.J. Cold-start NOx emissions : Diesel and waste lubricating oil as a fuel additive. **2021**, 286.

154. Jiao, P.; Li, Z.; Shen, B.; Zhang, W.; Kong, X.; Jiang, R. Research of DPF regeneration with NOx-PM coupled chemical reaction. Appl. Therm. Eng. **2017**, 110, 737–745, doi:10.1016/j.applthermaleng.2016.08.184.

155. Pirjola, L.; Rönkkö, T.; Saukko, E.; Parviainen, H.; Malinen, A.; Alanen, J.; Saveljeff, H. Exhaust emissions of non-road mobile machine: Real-world and laboratory studies with diesel and HVO fuels. Fuel **2017**, 202, 154–164, doi:10.1016/j.fuel.2017.04.029.

156. Ovaska, T.; Niemi, S.; Sirviö, K.; Heikkilä, S.; Portin, K.; Asplund, T. Effect of alternative liquid fuels on the exhaust particle size distributions of a medium-speed diesel engine. Energies **2019**, 12, doi:10.3390/en12112050.

157. Shukla, P.C.; Shamun, S.; Gren, L.; Malmborg, V.; Pagels, J.; Tuner, M. Investigation of Particle Number Emission Characteristics in a Heavy-Duty Compression Ignition Engine Fueled with Hydrotreated Vegetable Oil (HVO). SAE Tech. Pap. Ser. **2018**, 1, 495–505, doi:10.4271/2018-01-0909.

158. Hinds, W.C. Aerosol technology: properties, behavior, and measurement of airborne particles.; Second Edi.; John Wiley & Sons, 1999;

159. Mera, Z.; Matzer, C.; Hausberger, S.; Fonseca, N. Performance of selective catalytic reduction (SCR) system in a diesel passenger car under real-world conditions. Appl. Therm. Eng. **2020**, 181, 115983, doi:10.1016/j.applthermaleng.2020.115983.

160. Larson, T.; Gould, T.; Riley, E.A.; Austin, E.; Fintzi, J.; Sheppard, L.; Yost, M.; Simpson, C. Ambient air quality measurements from a continuously moving mobile platform: Estimation of area-wide, fuel-based, mobile source emission factors using absolute principal component scores. Atmos. Environ. **2017**, 152, 201–211, doi:10.1016/j.atmosenv.2016.12.037.

161. UNECE 2013 Addendum 48: Regulation No. 49. Concerning the Adoption of Uniform Technical Prescriptions for Wheeled Vehicles, Equipment and Parts which can be fitted and/or be used on Wheeled Vehicles and the Conditions for Reciprocal Recognition of Approvals Granted . **2013**.

162. Ädelroth, E.; Hedlund, U.; Blomberg, A.; Helleday, R.; Ledin, M.C.; Levin, J.O.; Pourazar, J.; Sandström, T.; Järvholm, B. Airway inflammation in iron ore miners exposed to dust and diesel exhaust. Eur. Respir. J. **2006**, 27, 714–719, doi:10.1183/09031936.06.00034705.

163. Debia, M.; Couture, C.; Njanga, P.E.; Neesham-Grenon, E.; Lachapelle, G.; Coulombe, H.; Hallé, S.; Aubin, S. Diesel engine exhaust exposures in two underground mines. Int. J. Min. Sci. Technol. **2017**, 27, 641–645, doi:10.1016/j.ijmst.2017.05.011.

164. da Silveira Fleck, A.; Couture, C.; Sauvé, J.F.; Njanga, P.E.; Neesham-Grenon, E.; Lachapelle, G.; Coulombe, H.; Hallé, S.; Aubin, S.; Lavoué, J.; et al. Diesel engine exhaust exposure in underground mines: Comparison between different surrogates of particulate exposure. J. Occup. Environ. Hyg. **2018**, 15, 549–558, doi:10.1080/15459624.2018.1459044.

165. Shin, J.; Kim, B.; Lee, J.; Jung, J.S.; Shin, Y.C.; Lee, K. Exposure assessment of elemental carbon, ultrafine particles, and crystalline silica at highway toll booths. Environ. Eng. Res. **2020**, 26, 200380–0, doi:10.4491/eer.2020.380.

166. Watson, J.G.; Chow, J.C.; Chen, L.-W.A. Summary of Organic and Elemental Carbon/Black Carbon Analysis Methods and Intercomparisons; 2005; Vol. 5; ISBN 7756747046.

167. Kirchstetter, T.W.; Novakov, T.; Hobbs, P. V. Evidence that the spectral dependence of light absorption by aerosols is affected by organic carbon. J. Geophys. Res. D Atmos. **2004**, 109, 1–12, doi:10.1029/2004JD004999.

168. Alhamdow, A.; Zettergren, A.; Kull, I.; Hallberg, J.; Andersson, N.; Berglund, M.; Wheelock, C.E.; Essig, Y.J.; Krais, A.M.; Ekstr, S.; et al. Low-level exposure to polycyclic aromatic hydrocarbons is associated with reduced lung function among Swedish young adults. Environ. Res. **2021**, 197, 111169, doi:https://doi.org/10.1016/j.envres.2021.111169.

169. Wahlberg, K.; Liljedahl, E.R.; Alhamdow, A.; Lindh, C.; Lidén, C.; Albin, M.; Tinnerberg, H.; Broberg, K. Filaggrin variations are associated with PAH metabolites in urine and DNA alterations in blood. Environ. Res. **2019**, 177, 108600, doi:10.1016/j.envres.2019.108600.

170. Kuusimäki, L.; Peltonen, Y.; Mutanen, P.; Peltonen, K.; Savela, K. Urinary hydroxy-metabolites of naphthalene, phenanthrene and pyrene as markers of exposure to diesel exhaust. Int. Arch. Occup. Environ. Health **2004**, 77, 23–30, doi:10.1007/s00420-003-0477-y.

171. Schoket, B.; Poirier, M.C.; Mayer, G.; Török, G.; Kolozsi-Ringelhann, Á.; Bognár, G.; Bigbee, W.L.; Vincze, I. Biomonitoring of human genotoxicity induced by complex occupational exposures. Mutat. Res. - Genet. Toxicol. Environ. Mutagen. **1999**, 445, 193–203, doi:10.1016/S1383-5718(99)00126-6.

172. Sobus, J.R.; McClean, M.D.; Herrick, R.F.; Waidyanatha, S.; Nylander-French, L.A.; Kupper, L.L.; Rappaport, S.M. Comparing urinary biomarkers of airborne and dermal exposure to polycyclic aromatic compounds in asphalt-exposed workers. Ann. Occup. Hyg. **2009**, 53, 561–571, doi:10.1093/annhyg/mep042.

173. Bohlin, P.; Jones, K.C.; Tovalin, H.; Strandberg, B. Observations on persistent organic pollutants in indoor and outdoor air using passive polyurethane foam samplers. Atmos. Environ. **2008**, 42, 7234–7241, doi:10.1016/j.atmosenv.2008.07.012.

174. Health & Safety Executive Exposure measurement: Air sampling. **2002**, 9–11.

175. Saber, A.T.; Hadrup, N.; Poulsen, S.S.; Jacobsen, N.R.; Vogel, U. Diesel exhaust particles : Scientific basis for setting a health-based occupational exposure limit; 2018;

176. Vermeulen, R.; Portengen, L. Is diesel equipment in the workplace safe or not? Occup. Environ. Med. **2016**, 73, 846–848, doi:10.1136/oemed-2016-103977.

177. Nordcan project - Cancer statistics for the nordic countries Available online: https://www-dep.iarc.fr/NORDCAN/SW/StatsFact.asp?cancer=180&country=752 (accessed on Nov 22, 2021).
178. Scholten, R.H.; Essig, Y.J.; Roursgaard, M.; Jensen, A.; Krais, A.M.; Gren, L.; Dierschke, K.; Gudmundsson, A.; Wierzbicka, A.; Møller, P. Inhalation of hydrogenated vegetable oil combustion exhaust and genotoxicity responses in humans. Arch. Toxicol. **2021**, doi:10.1007/s00204-021-03143-8.
179. Berglund, M.; Boström, C.-E.; Bylin, G.; Ewetz, L.; Gustafsson, L.; Moldéus, P.; Norberg, S.; Pershagen, G.; Victorin, K. Health risk evaluation of nitrogen oxides. Genotoxicity. Scand. J. Work. Environ. Health **1993**, 19 Suppl 2, 50–56.
180. Shusterman, D. Occupational irritant and allergic rhinitis. Curr. Allergy Asthma Rep. **2014**, 14, doi:10.1007/s11882-014-0425-9.
181. Arts, J.H.E.; Rennen, M.A.J.; De Heer, C. Inhaled formaldehyde: Evaluation of sensory irritation in relation to carcinogenicity. Regul. Toxicol. Pharmacol. **2006**, 44, 144–160, doi:10.1016/j.yrtph.2005.11.006.
182. Lang, I.; Bruckner, T.; Triebig, G. Formaldehyde and chemosensory irritation in humans: A controlled human exposure study. Regul. Toxicol. Pharmacol. **2008**, 50, 23–36, doi:10.1016/j.yrtph.2007.08.012.
183. Mudway, I.S.; Stenfors, N.; Duggan, S.T.; Roxborough, H.; Zielinski, H.; Marklund, S.L.; Blomberg, A.; Frew, A.J.; Sandström, T.; Kelly, F.J. An in vitro and in vivo investigation of the effects of diesel exhaust on human airway lining fluid antioxidants. Arch. Biochem. Biophys. **2004**, 423, 200–212, doi:10.1016/j.abb.2003.12.018.
184. European Parliament Directive (EU) 2018/2001 of the European Parliament and of the Council on the promotion of the use of energy from renewable sources; 2018; Vol. 2018;.
185. Regeringskansliet Ökade hållbarhetskrav för biodrivmedel och flytande biobränslen Available online: https://www.regeringen.se/pressmeddelanden/2018/11/okade-hallbarhetskrav-for-biodrivmedel-och-flytande-biobranslen/?fbclid=IwAR2cXusOUNDQ7pZnk40FAcqsilu53wzKaXScU1vTM6Bg4DS4plDnFQVIdEY (accessed on Nov 2, 2021).
186. IAE Renewable Energy Market Update; Paris, 2021;
187. Springmann, M.; Clark, M.; Mason-D'Croz, D.; Wiebe, K.; Bodirsky, B.L.; Lassaletta, L.; de Vries, W.; Vermeulen, S.J.; Herrero, M.; Carlson, K.M.; et al. Options for keeping the food system within environmental limits. Nature **2018**, 562, 519–525, doi:10.1038/s41586-018-0594-0.
188. International Council of Clean Transportation (ICCT) Review of Peat Surface Greenhouse Gas Emissions From Oil Palm Plantations in; 2011;